BACTERIAL MUTATION BY LOW-ENERGY PLASMA FOR DAIRY CATTLE FEED

NITIPOL POLSA

A Dissertation Submitted to University of Phayao

in Partial Fulfillment of the Requirements

for the Doctor of Philosophy Degree in Applied Sciences

February 2022

การกลายพันธุ์แบคทีเรียด้วยเทคนิคพลาสมาพลังงานต่ำ เพื่อผลิตอาหารหมักในโคนม

นิติพล พลสา

วิทยานิพนธ์เสนอมหาวิทยาลัยพะเยา เพื่อเป็นส่วนหนึ่งของการศึกษา
หลักสูตรปริญญาปรัชญาดุษฎีบัณฑิต
สาขาวิชาวิทยาศาสตร์ประยุกต์
กุมภาพันธ์ 2565

BACTERIAL MUTATION BY LOW-ENERGY PLASMA FOR DAIRY CATTLE FEED

NITIPOL POLSA

A Dissertation Submitted to University of Phayao

in Partial Fulfillment of the Requirements

for the Doctor of Philosophy Degree in Applied Sciences

February 2022

Dissertation

Title

Bacterial Mutation by Low–Energy Plasma for Dairy Cattle Feed

Submitted by NITIPOL POLSA

Approved in partial fulfillment of the requriements for the

Doctor of Philosophy Degree in Applied Sciences

University of Phayao

Approved by

..... Chairman

(Professor Emeritus Dr. Thiraphat Vilaithong)

..... Advisor

(Associate Professor Dr. Somboon Anuntalabhochai)

..... Examiner

(Associate Professor Dr. Sarot Cheenpracha)

..... Examiner

(Assistant Professor Dr. Lucksagoon Ganranoo)

..... Examiner

(Assistant Professor Dr. Sugunya Suebsan)

..... Dean of School of Science

(Associate Professor Dr. Chayan Boonyarak)

Title: BACTERIAL MUTATION BY LOW-ENERGY PLASMA FOR DAIRY CATTLE FEED

Author: Nitipol Polsa, Dissertation: Ph.D. (Applied Sciences), University of Phayao, 2021

Advisor: Associate Professor Dr. Somboon Anuntalabhochai

Keywords: Low-energy plasma, Agricultural wastes, Fermented feed, Microorganism, Dairy cattle

ABSTRACT

The aim of this work was to induce three bacterial species, including *Bacillus amyloliquefaciens* (cellulase-producing bacteria), *Bacillus subtilis* (xylanase-producing bacteria) and *Enterococcus faecium* (lactic acid bacteria), by using a low-energy plasma technique. The mutant bacteria were screened by hydrolysis capacity (H.C.) on carboxymethyl cellulose substrate. Then, the investigation of molecular changes, enzyme mechanisms, and fermentation processing from agricultural wastes, such as durian peel, corn cob, pineapple peel, and pineapple cork, was observed. The results showed that lactic acid bacteria, *E. faecium*, showed a mutant with higher lactic acid activity than control, approximately 12% under argon plasma treatment at 1.5/1.5 min on MRS broth. *B. amyloliquefaciens*, a cellulase-producing bacteria, was treated by low-energy plasma immersion ion implantation (PIII) to enhance their cellulase activity. According to a protein modeling analysis, replacing K370 with glutamic acid was proposed to form a hydrogen bond to Y436 a shorter distance (2.6 Å) than the control (5.4 Å), which may allow the structure to be more compact and stable, contributing to higher catalytic efficiency. Moreover, xylanase-producing bacteria, *B. subtilis*, were bombarded by an atmospheric pressure plasma jet (APPJ) and higher catalytic activity was screened. Sequence analysis revealed only a single amino acid substitution from threonine to serine at position 162 (T162S) to be in the glycosyl hydrolase family (GH11). To reduce feed costs, agricultural wastes were an optional choice as raw material to feed under fermentation processing, which required bacteria. The quality of fermented feed after fermented by mutant bacteria showed that the mutant bacteria produced protein at a higher level than the control, increasing 20–30%. The pH was decreased by 10–20%, indicating the quality of fermentation associated with lactic acid content increased by 10–20%. After that, the dairy cattle were fed for a month. The amount of milk and milk composition (fat, protein, lactose, and ash) were not different from the control, although the feed cost was decreased by 40%.

ACKNOWLEDGEMENT

I would like to express my heartfelt thanks and appreciation to my advisor, Associate Professor Dr. Somboon Anuntalabhochai, for their supervision, guidance, encouragement, and kindness throughout this research project.

I am particularly grateful to Professor Emeritus Dr. Thiraphat Vilaithong, Associate Professor Dr. Sarot Cheenpracha, Assistant Professor Dr. Sugunya Suebsan, and Assistant Professor Dr. Lucksagoon Ganranoo, for their kindness, valuable suggestions, and discussions. I am grateful to Dr. Kanta Sangwijit for her valuable suggestion.

I am indebted to Miss Somsri Taisanthia, farm manager of PPO farm, for allowing me to use cattle throughout this research.

Thank you, Miss Chananbhorn Thongrote, Hathairat Laksuk, and all the friends at the Plasma Bioengineering Unit for every bit of assistance and for being good friends.

I am very grateful to my parents as well as Mr. and Mrs. Polsa. The countless times you took care of your child during our hectic schedules will not be forgotten. Finally, to my supportive project, Thailand Center of Excellence in Physics (THEP): supporting research projects that can be extended to me. and help farmers reduce costs as well.

Nitipol Polsa

LIST OF CONTENTS

LIST OF TABLES

Pages

LIST OF FIGURES

Page

LIST OF FIGURES (CONT.)

Page

LIST OF FIGURES (CONT.)

Page

LIST OF FIGURES (CONT.)

Page

LIST OF FIGURES (CONT.)

Page

ABBREVIATIONS

%	=	Percent
~	=	Around
±	=	Plus–minus sign
16S rDNA	=	16S ribosomal deoxyribonucleic acid
Å	=	Angstrom
a.m.	=	Ante meridiem (before noon)
ADP	=	Adenosine diphosphate
ANOVA	=	Analysis of variance
APPJ	=	Atmospheric pressure plasma jet
Ar	=	Argon gas
ATP	=	Adenosine triphosphate
B. circulans	=	*Bacillus circulans*
B. subtilis	=	*Bacillus subtilis*
BB	=	Preserved bamboo shoots
BglC–M	=	Mutant of BglC gene
BglC–W	=	Wild type of BglC gene
Bp	=	base pair
C	=	Control
C	=	Fresh grass + Concentrated feed
C+F	=	Concentrated feed 50% + Fermented feed 50%
Ca	=	Calcium
$CaCO_3$	=	Calcium carbonate
CAPS buffer	=	*N*–Cyclohexyl–3–aminopropanesulfonic acid
CBM	=	Carbohydrate–binding module
CBMs	=	Carbohydrate–binding modules
CD	=	Catalytic domain
CFUs	=	Colony forming units
Cm	=	Centimeter
CMC	=	Carboxymethyl cellulose

Co	=	Cobalt
CxynA	=	Control of XynA gene
DMRT	=	Duncan's multiple range test
DNA	=	Deoxyribonucleic acid
DNS method	=	Dinitrosalicylic acid method
DSBs	=	Double-strand breaks
E	=	Glutamate
E. coli	=	*Escherichia coli*
E. faecium	=	*Enterococcus faecium*
EDTA	=	Ethylenediaminetetra-acetic acid
EM	=	Bio-fermented water
EMP pathway	=	Emden-meyerhof-parnas pathway
EPF	=	Pickled eastern fish (Pra-ra)
F	=	Phenylalanine
FCM	=	Fat-corrected milk
FDA	=	Food and drug administration
Fe	=	Ferrous
$FeCl_3$	=	Ferric chloride
Fig.	=	Figure
G	=	Glycine
g/L	=	Grams per liter
GH	=	Glycoside hydrolase
GRAS	=	Generally recognized as safe
H	=	Histidine
h	=	hour
H.C.	=	Hydrolysis capacity
HAT-RAPD	=	High annealing temperature-random amplified polymorphic DNA
HCl	=	Hydrochloric acid
He	=	Helium gas

HV Electrode	=	High voltage electrode
I	=	Isoleucine
IPTG	=	Isopropyl β–D–1–thiogalactopyranoside
IU/mg	=	International unit per milligrams
K	=	Lysine
k_{cat}	=	Kinetic parameter: The turnover number
k_{cat}/K_m	=	Catalytic efficiency
keV	=	Kilo electron volt
kg	=	Kilogram
Km	=	Constant of enzyme/substrate
L	=	Leucine
L	=	Liter
LB medium	=	Luria–bertani medium
LET	=	Linear energy transfer
M	=	Methionine
M	=	Molar
MeV	=	Mega electron volt
mg/ml	=	milligram per milliliter
min	=	Minute
ML	=	Marinated lettuce
ml	=	Milliliter
mM	=	Millimolar
MRS medium	=	de Man, rogosa and sharpe medium
MT	=	Mutant
MxynA	=	Mutant of XynA gene
N	=	Asparagine
NAD	=	Nicotinamide adenie dinucleotide
NADH	=	Nicotinamide adenine dinucleotide (NAD) + hydrogen (H)
NCBI	=	The national center for biotechnology information

nm	=	Nanometer
NPF	=	Pickled northern fish (Plasom)
^{o}C	=	Degree celsius
OD_{600}	=	The optical density at 600 nm
p value	=	Probability value
P	=	Proline
p.m.	=	Post meridiem (after midday)
PCR	=	Polymerase chain reaction
pH	=	Potential of hydrogen
p*Ka*	=	Ionization constant (chemistry, kinetics)
PM	=	Pickled mussel
ppm	=	Parts per million
rDNA	=	ribosomal deoxyribonucleic acid
rpm	=	Revolutions per minute
s^{-1}	=	per second
SB	=	Fermented soybean
SCCM	=	Standard cubic centimeters per minute
SmF	=	Submerged fermentation
SNF	=	Solids-not-fat
SP	=	Sour pork
sp.	=	Species
spp.	=	Multiple species
SSF	=	Solid state fermentation
TBE buffer	=	Tris-borate-EDTA buffer
USA	=	United states of america
UV	=	Ultraviolet
V	=	Volt
W	=	Tryptophan
W	=	Watt
w/v	=	Weight per volume

Y	=	Tyrosine
α	=	Alfa/Alpha (First letter from Greek alphabet)
β	=	Beta (Second letter from Greek alphabet)
μ	=	Micro: a factor of 10^{-6} (one millionth)
μg/ ml	=	Microgram per milliliter
μl	=	Microliter
ρ	=	Mass density

CHAPTER I

Introduction

Background and significance of the research

The human population was expected to reach 9.15 billion in 2050, up 15% from 2020 (United Nations, 2019). During the next few decades, human population growth, urbanization, and increasing incomes will result in significant increases in demand for animal products. The number of dairy farmers in Thailand increased by 14.06% between 2016 and 2017, reaching 1,865 in 2017 (Information and Statistical Data Group, 2017). In addition, the cost of production in the agricultural animal industry had increased across the board. Feed was the most important factor (accounting for 60–70%) of total livestock production costs (Greenwood, 2021). Dairy cattle required nutrients to survive, grow, develop fetuses, and produce milk. Normally, forages were the main feed for ruminants, lack sufficient nutrients and minerals to fulfill the basic requirements of dairy animals, particularly those with high milk production. Concentrates were abundant in nutrients that forages lack, assist in balancing the diet. However, the concentrates were expensive, and as arable agriculture expands, the availability of conventional grazing areas for fodder quickly reducing, forcing the utilization of alternative feed sources. Furthermore, roughage was limited during the dry season (Velho, et al., 2018). As a result, microorganism–fermented feed or drying will be necessary. In small–scale agriculture, feeding cattle with a variety of feed types was based on seasonal changes in feed supplies (Ajila, et al., 2012).

Furthermore, a large amount of agricultural waste in Thailand might be used to create an alternative feed. Agricultural wastes used as livestock feed vary depending on the season. Corn was harvested during August to November, as well as March to April. Durian was harvested twice a year, during May and October, while pineapple was harvested all year. Corn production provides for 60% of total country production, whereas durian production amounts for 10% and pineapple production provides for 25% (Office of Agricultural Economics, 2017). Agricultural wastes such as corn husks, corncobs, durian

peel, pineapple peel, pineapple cork, and other unnecessary components were left behind during harvest. Corncobs were about 1.2 million tons of annual production, whereas corn husks were about 3.1 million tons, or around 25% of total production (Tengkaew and Wiwattanadate, 2014). In Thailand, durian peels were wasted at a rate of 1,992 tons per day, or around 730,000 tons per year (Jirapornvaree, et al., 2017). Furthermore, a total of 2.8 million tons of pineapple peels was wasted each year at factories all around country. A total of 4 million tons of pineapples were wasted each year, and approximately 370,000 tons of cork were wasted each year. (Office of Agricultural Economics, 2017). The burning in agricultural waste mentioned about caused pollution and dust particles smaller than 10 microns, affecting the respiratory system, or fertilizer would be created in landfills. However, this is costly and require up a lot of space. Increasing feed production efficiency using agricultural wastes was another strategy. Agricultural feed must be fermented to aid animal digestion and preservation. In terms of quantity, fiber feed (high lignocellulose content) had the best availability. Fermented feeds were usually simpler to degradable and contain more nutrients than the original materials. (Tengkaew and Wiwattanadate, 2014). Fermentation may also be used to preserve materials and to minimize or even eliminate toxic compounds included in the components, as well as the presence of various microorganisms capable of carbohydrates conversion. Microorganisms in the rumen then utilized carbohydrates to synthesize protein.

Atmospheric pressure plasma technology was useful due of its appropriate cost. Simple components can be constructed in the laboratory. To treat metals, plastics, glass, or polymers, the technique must be applied to material sciences especially plasma. At present time, medical research had used atmospheric pressure plasma technologies, such as using atmospheric pressure plasma to sterilize surfaces. (Laroussi, 2015). Plasma was used to repair surgical wounds. Investigation of the impact of atmospheric pressure plasma on DNA damage was reported as well. (Connell 'O, et al., 2011; Lee, et al., 2014). Yaopromsiri, et al. (2015) investigated DNA mutations induced by low-energy plasma technology. Bacterial mutations enhancing cellulase activity was reported (Sangwijit, et al., 2016). Moreover, *Streptomyces albulus* was mutated by room temperature and atmospheric pressure plasma (Hong, et al., 2011). On a small farm, the availability of feed

was dependent on seasonal changes. Most farmers attempt to maintain forage, but they were disappointing due to long-term preservation, which contributes microorganisms to growth from natural sources. As a result, low-energy plasma technologies were already being used to induce bacterial mutations to increase lignocellulose degrading enzymes and lactic acid activity, which allowed a rapid fermentation process. Therefore, low-energy plasma technology was used to produce fermented feed.

Fermented feed was the anaerobic preservation of animal feed for the fermentation process. Fermented feed provides the benefit of maintaining the nutritional content of raw ingredients while allowing for long-term storage. However, the fermented feed had several disadvantages, including the loss of vitamin D, minerals, and the degradability of the feed when exposed to air. As a result, it required the application of professional knowledge (Dai, et al., 2020). Cellulase and xylanase were enzymes that break down agricultural waste into water-soluble carbohydrates. To prevent spoilage, the lactic acid was converted by adjusting the lower pH value (4.0) (Kim, et al., 2021; Puntillo, et al., 2020). *Bacillus amyloliquefaciens* (Ye, et al., 2017), *Bacillus macernas* SM (Ali, 2003) and *Bacillus megaterium* MYB3 (Bai, et al., 2017) produced cellulase and xylanase. Lactic acid bacteria found in fermented feed include *Lactobacillus plantarum*, *Lactobacillus casei* (Li, et al., 2016), and *Enterococcus faecium* NCIMB 11181 (Jatkauskas, et al., 2013).

In this research, low-energy plasma technology was used to induce mutation in three types of bacteria groups (cellulase-producing bacteria, xylanase-producing bacteria, and lactic acid bacteria) for fermented feed production. The mechanism for enhancing hydrolysis efficiency at the molecular level was investigated. Then, instead of concentrated feed, fermented agricultural waste feed was used. As a result of the community's contribution, this research could help for the cost of feed for farmers and reducing 2.5 PM dust from agricultural waste burning.

Objectives

1. To apply a low-energy plasma technique for enhance cellulase, xylanase activity and lactic acid production in bacteria

2. To formulate fermented feed from agricultural wastes after fermentation with bacterial mutants

3. To analyze the mechanism of increasing the efficiency of molecular enzymes

4. To monitor the quality of milk after provided the designed farming

5. To train and disseminate fermented feed to the animal farmers

The scope of research

This research integrates scientific knowledge from physics, biology, and agriculture fields to produce feed for dairy cattle from a wide range of agricultural wastes. Mutated bacteria, such as cellulase-producing bacteria, xylanase-producing bacteria, and lactic acid bacteria, were treated with low-energy plasma techniques. The effectiveness of cellulase (*BglC*) and xylanase (*XynA*) genes at the molecular level, as well as their protein conformation changes, were examined. To identify lactic acid bacteria, the HAT-RAPD technique was chosen. The bacterial mutants were then used in feed fermentation with agricultural wastes such as corncobs, corn husks, pineapple peels, and durian peels as raw materials. The protein contents, pH, and lactic acid concentration of the feed were then determined. Following, dairy cattles were fed with fermented feed produced from agricultural waste, and milk quality was evaluated as shown in **Figure 1**.

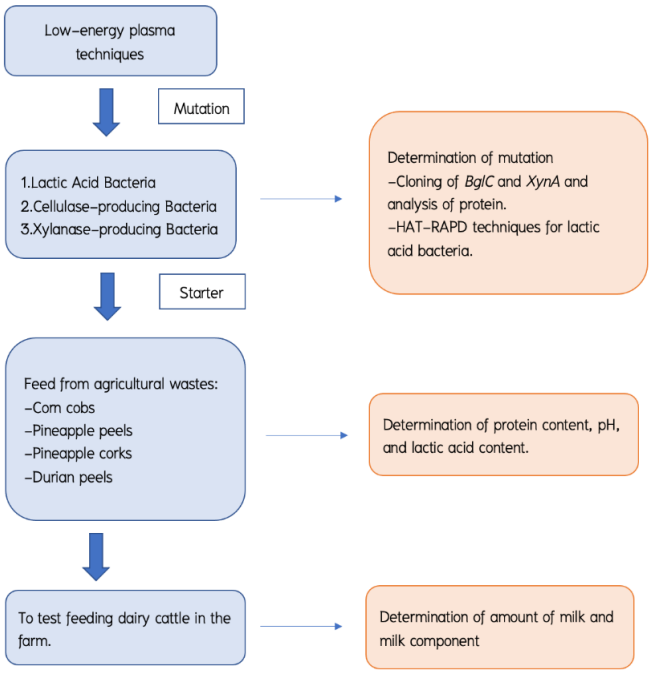

Figure 1 The scope of research

Expected benefits

1. To obtain bacterial mutants with higher efficiency for agricultural waste hydrolysis
2. To obtain microbes for the fermentation of animal feed
3. To reduce the feed costs for dairy cattle farmers
4. To decrease 2.5 PM dust from the burning by using agricultural waste as feed
5. To be capable of supplying fermented feed for dairy cattle all year
6. To disseminate fermentation knowledge to farmers

CHAPTER II

Lactic acid bacteria

Literature Review

Lactic acid bacteria characteristics

Gram–positive bacteria were categorized as lactic acid bacteria. It produced no immobile spores, no catalase enzyme, and survives in anaerobic conditions. They were cocci and rods. The yield was the lactic acid produced by the carbohydrate fermentation process (Axelsson, 2004). There were also two types of lactic acid bacteria. Homofermentative and heterofermentative glucose fermentations were the two types of glucose fermentation it uses. Lactic acid bacteria could grow in milk, cheese, meat, vegetables, soils, lakes, animals' digestive, and humans' digestive tracts (Chen, et al., 2005; Suree, et al., 2016; Tserovska, 2002).

Lactic acid fermentation

Homofermentative

The fermentation of glucose or galactose by the Emden–Meyerhof–Parnas (EMP) or glycolytic pathway produces approximately 95% of the lactic acid. When one molecule of glucose enters the EMP, two molecules of pyruvate were produced. The pyruvate is then converted into lactic acid (**Figure 2**). As a result, lactic acid may be discovered in D– and L–lactic acid (Burgé, et al., 2015). Lactic acid bacteria appear in a range of shapes, including rod–shaped types such as *Lactobacillus* and spherical–shaped species such as *Streptococcus*, *Lactococcus*, and *Enterococcus*.

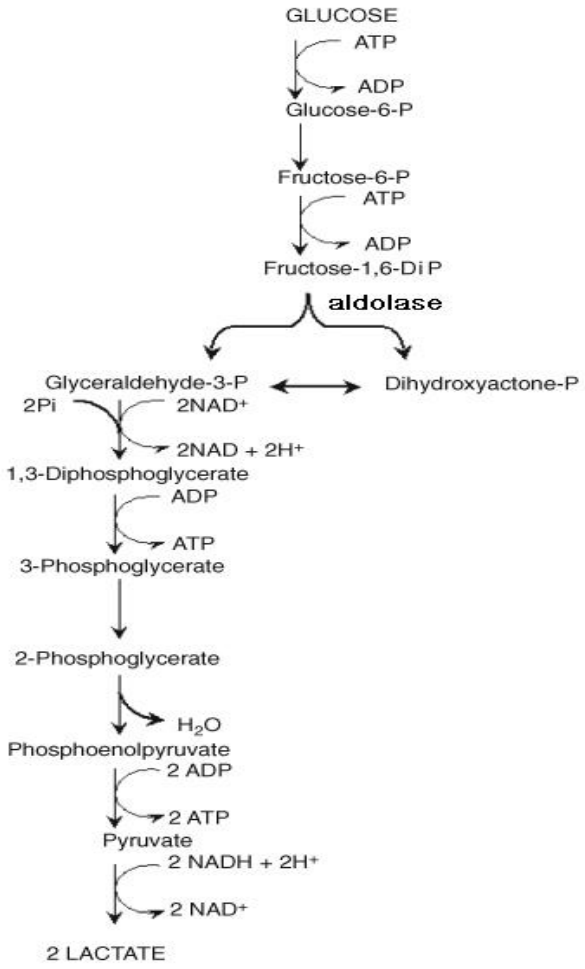

Figure 2 Lactic acid production pathway representative in homofermentative

Source: Axelsson (2004)

Heterofermentative

The fermentation of lactic acid bacteria was known as heterofermentation. The 6–phosphogluconate/phosphoketolase pathway produces lactic acid, acetic acid, carbon dioxide, and ethanol in producing energy. Since these bacteria lacked the aldolase enzyme (a component of the EMP pathway), bacteria did not convert fructose–1,6–diphosphate to triose–phosphate. As a result, glucose–6–phosphate will be oxidized to 6–phosphogluconate via the phosphogluconate fermentation pathway. The decarboxylation of pentose phosphate and the production of carbon dioxide followed. Phosphoketolase breaks

down the pentose–phosphate into triose–phosphate and acetyl–phosphate, with the triose–phosphate subsequently converted to lactic acid. As shown in **Figure 3**, the acetyl–phosphate is eventually converted to ethanol. Lactic acid bacteria can also produce formic acid and glycerol through various mechanisms. Lactic acid bacteria with heterofermentative *Leuconostoc* bacteria and *Lactobacillus* bacteria (Wagner, et al., 2005) had both fermentation pathways and products. Some species can also ferment hexose and pentose sugars, as well as lactic acid and acetic acid. These lactic acid bacteria were known as facultative heterofermentative because they use aldolase and phosphoketolase (Hammes and Vogel, 1995).

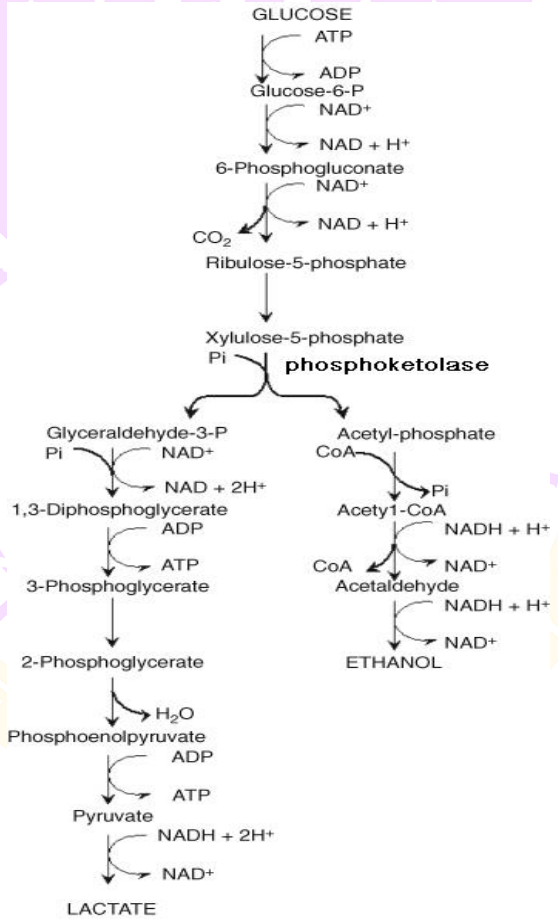

Figure 3 Lactic acid production pathway representative in heterofermentative

Source: Axelsson (2004)

Pathogen inhibition

The accumulation of organic acids (lactic acid, acetic acid, ethanol, and carbon dioxide) and a decrease in pH inhibit pathogen development (Rakhmanova, et al., 2018). As a result, lactic acid increased the shelf life of fermented feed. Bacteria depend on sugar fermentation to produce organic acids, that lower the pH of the feed and reduce nutrients (Lee, et al., 2009). Organic acids from lactic acid bacteria were found to be antibacterial agents, comparable to hydrogen peroxide (H_2O_2), diacetyl, and carbon dioxide (CO_2) (Reis, et al., 2012).

Moreover, lactic acid bacteria could be consumed to prevent spoiling (Wagner, et al., 2005) and can produce a variety of inhibitory chemicals to inhibit pathogen infection

1. Organic acid: lactic acid, lower the pH, of the feed inhibited pathogen growth. Furthermore, the cytoplasm was strongly acidic due to hydrogen ions (H^+) penetrating the cell membrane and entering cellular bacteria, causing damage to the proton electrochemical gradient within the cell (Chalantom, et al., 2008). Acetic acid is the major metabolite generated by heterofermentative bacteria, with a small amount of propionic acid. The electrochemical proton gradient was affected by both molecules and showed a higher p*K*a value than lactic acid.

2. Bacteriocin: Bacteriocins were peptides or small proteins that inhibit pathogens from growing. Bacteriocins were toxic to bacteria that had a similar affinity (Wagner, et al., 2005) and were bacteriocin sensitive (Chalantom, et al., 2008). Bacteriocins produced by lactic acid bacteria such as *Bacillus cereus*, *Clostridium botulinum*, *Clostridium perfringens*, *Staphylococcus aureus*, *Listeria monocytogenes* (Yang, et al., 2014).

3. Hydrogen peroxide (H_2O_2): Even with its hydroxyl group, hydrogen peroxide (H_2O_2) was another strong oxidizer that can inhibit the growth of bacteria. In addition, it can oxidize cell protein molecules and the lipid layer of the cell membranes. The structure of nucleic acids and proteins in oxidized cells will change until they can no longer function correctly. In addition, the hydrogen peroxide process transports oxygen, resulting in a lack of oxygen and preventing other bacteria from growing (Chalantom, et al., 2008).

Lactobacilli, *Pediococcus*, and *Leuconostoc* were among the microorganisms that can be produced (Mokoena, 2017).

4. Acetaldehyde: Acetaldehyde was produced by lactic acid bacteria when carbohydrates were fermented. The difficulty, however, was a lack of hydrogen alcohol enzymes. According to research, the concentration of acetaldehyde 10–100 ppm can inhibit *Escherichia coli* and *Staphylococcus aureus* (Chalantom, et al., 2008).

5. Reuterin : Under anaerobic conditions, the breakdown of glycerol and glyceraldehyde *Lactobacillus reuterin* produce reuterin, which was a broad-spectrum pathogen inhibitor (Mokoena, 2017). Reuterin can inhibit intracellular activity by resisting the inhibitory effect of ribonucleotide oxidoreductase from a variety of bacteria, yeast, and fungi (Mokoena, 2017). Furthermore, the addition of reuterin to meat had been shown to suppress bacteria such as *E. coli* (Walsham, et al., 2016).

Application of lactic acid bacteria for fermented feed production

Fermented livestock feed had become increasingly popular these days. It had a significant effect on crops and reduced the amount of agricultural waste that was burned. Agricultural waste feed will also assist in reducing the dry season's inadequate and insufficient feed supplies. To maintain the quality of the grass, fermentation must be done in accordance with naturally occurring microbes in various parts of the plant (Bureenok, et al., 2011). To produce lactic acid, the fermentation process, such as microorganisms found in nature, must be supplemented with pure starter. Lactic acid bacteria, a valuable nutrient for product storage, were the most commonly used microbes in fermented feed preservation (Hwanhlem, et al., 2011). Lactic acid bacteria were frequently used to improve nutrition and inhibit mold or yeast growth, both of which can cause spoilage when fermented in anaerobic conditions (Reddy and Obulam, 2011). To improve fermentation efficiency, additives were already added, such as seedlings for nham (sour pork) fermentation by *Lactobacillus brucei* to enhance its antimicrobial activities. It should also depend on the cause of contamination added to each type for the greatest texture and flavor. In summary, the following were the advantages of lactic acid bacteria in fermented feed (Bintsis, 2018):

1. This improves the nutritional feed. In wheat tempeh, for example, the nutritional value of the fermented product will increase. Fermented feed included more vitamins than non-fermented feed because some microbes synthesize vitamins required for growth.

2. Pathogens were inhibited from growing. Lactic acid bacteria in fermented feed were discovered to inhibit the growth of pathogenic microorganisms, keeping the feed safer and capable of long-term storage.

3. The addition of lactic acid bacteria to fermented feed increased beneficial microorganisms in livestock, allowing them to form pathogenic microbes that lower acidity in the digestive tract.

4. Nutritional protein value was increased because fermented feeds could be stored for longer periods of time, had a lower pH, and broke down lactose well. Thus, yeast from natural sources could be grow and make protein content higher.

Low-energy plasma technique

Plasma was an ionized state of matter made up of electrons and cations, and it was a form of gas. It also contains electrically neutral gaseous particles, such as active molecules or atoms (Harry, 2010). Large quantities of electrical energy can be used to form plasma in a neutral gas. When enough energy was released to the free electrons, they interact with the atom and lose their electrons. It was known as ionization, and it occurs very quickly states (Wagenaars, 2006) that ionization greatly increases the number of electrons released, causing the gas to decay and change into plasma.

The generation of a plasma state at atmospheric pressure was referred to as atmospheric plasma. To ignite the plasma, no vacuum was necessary (Huang, et al., 2020). At atmospheric pressure, many gases were employed to produce plasma; argon or helium was frequently used as the main gas (Hubert, et al., 2015). These matter atoms can disintegrate in a plasma state made up of high-energy particles such as ions, electrons, or protons that can transfer energy to molecules in contact with the plasma. Furthermore, it causes the atoms of a molecule to break their bonds. As a result, they induced molecular breakdown or atom rearrangement, which resulted in new structures

like polymerization or binding. As a result, these compounds' characteristics improved when compared to the control (Huang, et al., 2020).

Because of its low cost, atmospheric pressure plasma technology was a preferred option. There were also some simple components that could be constructed in the lab. In materials science, plasma had been used to treat the surfaces of various items such as metals, plastics, glass, and polymers. At this time, atmospheric pressure plasma technology was being used in medical studies, such as sterilizing surfaces with atmospheric pressure plasma (Laroussi, 2015). The effect of atmospheric pressure plasma on DNA damage was already being investigated in the field of surface sterilization. (Connell 'O, et al., 2011; Lee, et al., 2014). Furthermore, research into DNA mutations caused by the low-energy plasma approach was proceeded. (Yaopromsiri, et al., 2015). Additionally, lactic acid enrichment enhanced *Lactobacillus thermophilus* SRZ50 with heavy-ion mutagenesis (Hu, et al., 2018). As a result, it was chosen for application in the induction of bacterial mutants to enhance lactic acid activity in the production of fermented feeds for cattle.

Research Methodology

Screening and selection of lactic acid bacteria

Preserved bamboo shoots (BB), Pra-ra (EPF), Plasom (NPF), pickled mussels (PM), Nham (SP), marinated lettuce (ML), bio-fermented water (EM), and fermented soybean (SB) were all weighted. First, 1 g of all samples were added to a test tube containing 9 ml of distilled water to form a suspension with a dilution of 10^{-1}, followed by a 10-fold serial dilution to 10^{-2}, 10^{-3}, and 10^{-4} times. Then, the dilutions were cultured on a solid MRS medium containing 1% of $CaCO_3$ (Neti, et al., 2018) using the spreading technique. Lactic acid bacteria were initially incubated for 24 to 48 hours at 37°C. The ratio between hydrolysis halo diameter and quality lactic acid activity was evaluated. The clear zone around the colony was then chosen and purified using the cross-streak method on a solid MRS medium containing $CaCO_3$. The agar plates were incubated for 24-48 hours at 37 °C, repeating at least five times until bacterial purity was reached, and the inoculation was kept at 4°C.

To determine the lactic acid production efficiency, lactic acid bacteria that can grow properly on a solid MRS medium containing $CaCO_3$ were chosen. Bacteria were cultivated in MRS liquid medium for 24 hours at 37 °C. Each isolation was carried out in triplicate. First, 1 ml of the cell suspension was centrifuged at 13,000 rpm to measure the lactic acid concentration. The lactic acid solution (20 µl) was then added to 2 ml of $FeCl_3$ solution for 5 minutes at 390 nm using spectrophotometer (**Appendix A**). (Borshchevskaya, et al., 2016) and pH value was measured.

Identification of bacteria strains

Morphology

Bacteria was smeared on a slide. Gram's staining evaluates their shape and arrangement. The crystal violet dye was dropped on the slide, and then immersed in the iodine solution for 1 minute. The decolorizer was used in 95% of the alcohol. The safranin–O dye was dropped on the bacteria drop area. Then, clean water was rinsed off and the cells were observed under a compound microscope for color, shape, and arrangement (American Public Health Association, 2015).

Identification

Each bacterial strain's genomic DNA was extracted according to (Ifuku, et al., 2007) and used as a template for 16S rDNA gene amplification using the polymerase chain reaction (PCR) method. 16SF: 5' AGTTTGATCCTGGCT C3' and 16SR: 5'GGCTACCTTGTTACG A3' were universal primers. Purified DNA fragments were extracted from agarose gels using the DNA Gel Extraction Kit (Thermo Scientific, Thailand). Using a cloning kit (Thermo Scientific, Thailand), purified DNA fragments were cloned into the pTZ57R/T plasmid (InsTAcloneTM PCR), and the recombinant plasmids were electroporated into E. coli DH5α. Bacteria treated with plasmids were tested on antibiotic–resistant medium. First Base Laboratories, Selangor Darul Ehsan, Malaysia, examined the 16S rDNA gene sequencing using the dideoxy nucleotide sequence termination (Sanger, et al., 1977) and compared to the bacterial plasmids in the GenBank database.

Induction of mutation using atmospheric pressure plasma

One isolated lactic acid bacterium was chosen. Atmospheric pressure plasma was used as the low-energy plasma. The plasma generator power was 100 watts, and the gas flow rate was 2 SCCM with 3 conditions: (1) continue bombard for 1 minutes, (2) bombard for 1.5 minutes then rest 1.5 minutes and continue bombard for 1.5 minutes, and (3) continue bombard for 2 minutes. They were generating plasma with argon gas. That was dropped into MRS liquid medium to see whether it would persist. In addition, the efficiency of lactic acid production of the mutant and control conditions was compared using a method description by (Borshchevskaya, et al., 2016).

Identification of mutant by HAT-RAPD technique (Anuntalabhochai, et al., 2000)

PCR methods were utilized to amplify the DNA profile using six primers: OPC06, OPAG13, OPAO20, OPAW18, OPAA14, and OPX12 for evaluation of genetic variation (Nakkanong, et al., 2008). Electrophoresis was used to detect DNA patterns. The electrophoresis was carried out for 60 minutes at a voltage of 100 V on a 1.2% concentrated agarose gel in a TBE buffer solution. It was analyzed under ultraviolet light using a UV transilluminator. The amplified wild-type and mutant DNA fragments were run on the same gel. By observing band shifts between mutant and wild-type samples, mutations can be detected.

Results

Isolation and selection of lactic acid bacteria

Preserved bamboo shoots (BB), Pra-ra (EPF), Plasom (NPF), pickled mussels (PM), Nham (SP), marinated lettuce (ML), bio-fermented water (EM), and fermented soybean (SB) cultured in MRS with 1% $CaCO_3$ were all used to isolate lactic acid bacteria. Lactic acid bacteria were detected at 21, 17, 23, and 4 isolates from Plasom, Nham, bio-fermented water, and fermented soybean, respectively. Furthermore, no lactic acid bacteria were discovered in preserved bamboo shoots, marinated lettuce, pra-ra, or pickled mussels (PM), as indicated in **Table 1**. Lactic acid bacteria, on the other hand, formed a clear zone around the colony and were grown at 37 °C, as illustrated in **Figure**

4. The goal of this research was to establish the type of lactic acid bacteria and their acid production efficiency.

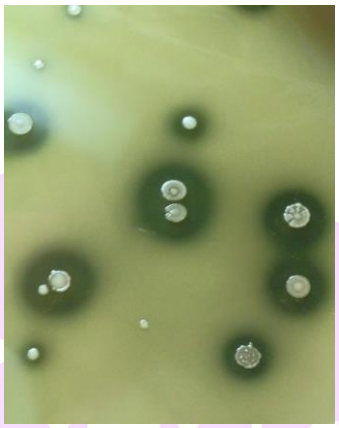

Figure 4 Clear zone of lactic acid bacteria

Table 1 The total number of lactic acid bacteria isolated from various sources

Samples	Number of isolated bacteria
Preserved bamboo shoots (BB)	–
Pra-ra (EPF)	–
Plasom (NPF)	21
Pickled mussels (PM)	–
Marinated lettuce (PL)	–
Nham (SP)	17
Bio-fermented water (EM)	23
Fermented soybean (SB)	4
Total	65

The content of lactic acid was then determined. The bacteria were grown for 24 hours in MRS medium. The amount of lactic acid in the sample was determined. In six isolates, NPF1, NPF8, NPF11, SP2, SB1, and SB4, they were discovered that the bacteria had high lactic acid and a low pH, as shown in **Table 2**.

Table 2 Lactic acid content in MRS liquid medium after 24 hours of culture isolated from various sources, and pH values

Isolated	Lactic acid content (g/L)	pH
NPF1	5.36	4.55
NPF8	5.25	4.56
NPF11	5.39	4.53
SP2	5.30	4.55
SB1	5.60	4.22
SB4	5.45	4.51

Identification of lactic acid bacteria

Six isolates were selected (NPF1, NPF8, NPF11, SP2, SB1, and SB4). They demonstrated that all six isolates were spherical and gram–positive, providing 16s rDNA sequencing to identify the other species. The results were described in **Table 3** after comparing the obtained data to the base sequence in the GenBank database.

Table 3 Identification of lactic acid bacteria by 16s rDNA gene sequencing

Isolates	Species	Identity (%)
NPF1	*Enterococcus faecium* strain DSM 20477	99%
NPF8	*Enterococcus mundtii* strain QU 25	99%
NPF11	*Enterococcus faecium* strain Aus0004	99%
SP2	*Enterococcus durans* strain 98D	94%
SB1	*Enterococcus faecium* strain AT15	99%
SB4	*Enterococcus faecium* strain DSM 20477	99%

Induction mutation using atmospheric pressure plasma

The bacterial isolate SB1 (*Enterococcus faecium*) was chosen for this research for its high lactic acid efficiency. The bacteria were bombarded with low-energy plasma in this method. For 1 minute, 1.5/1.5 minutes (1.5-minute bombardment, 1.5-minute rest, 1.5-minute bombardment), and 2 minutes, argon gas was used to generate plasma. The rate of survival was investigated. Bacterial survival decreased as the time interval increased. As shown in **Figure 5**, a bombardment of 2, 1.5/1.5, and 1 minute, and survival rates were 2%, 13, and 23, respectively.

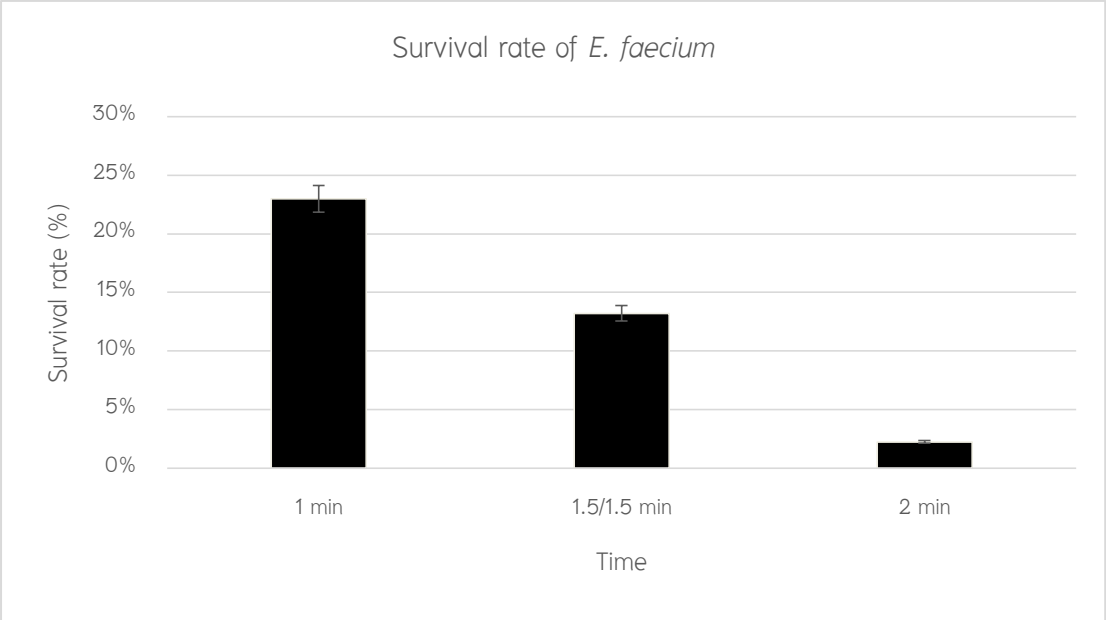

Figure 5 Survival rate of argon-bombarded *Enterococcus faecium*. The power of the plasma was 100 W, and the gas flow rate was 2 SCCM for 1 min, 1.5/1.5 min, and 2 min.

According to this research data, the duration of the bombardment should be 1.5/1.5 minutes. The amount of lactic acid after bombardment in comparison to control. These findings revealed that the bacterial mutant of the MT57 isolate produced lactic acid at a concentration of 5.4 g/L. The ability to produce lactic acid was 12 % better than the control strain (4.9 g/L), as shown in **Figure 6**.

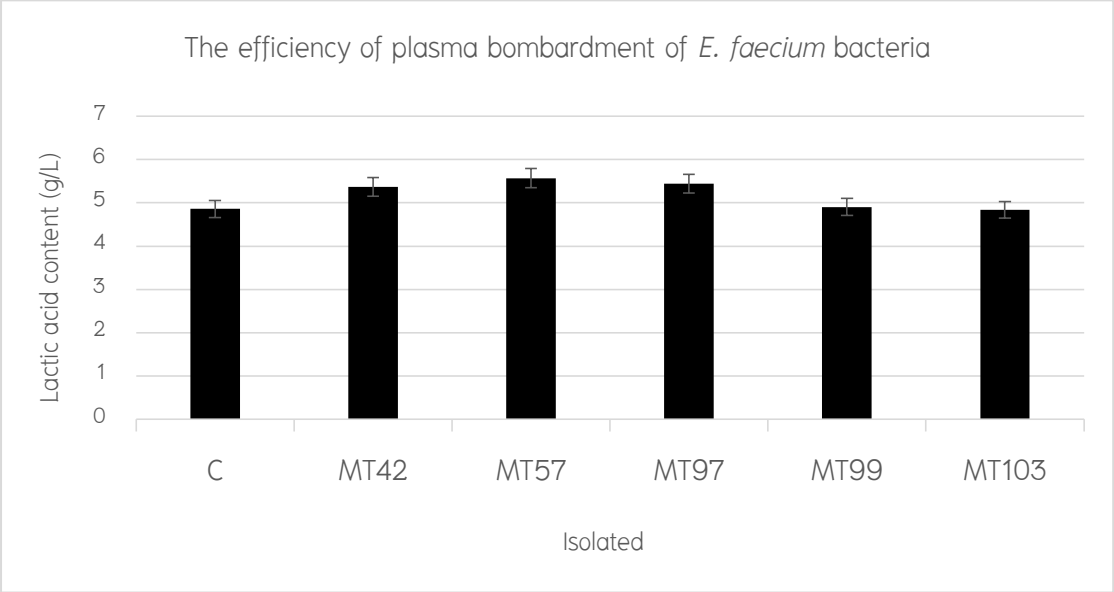

Figure 6 Efficacy of *Enterococcus faecium* on producing lactic acid. It was bombarded with argon ions. The generator power was 100 W, and the gas flow was 2 SCCM for 1.5/1.5 min.

Identification of mutants by the HAT–RAPD technique

HAT–RAPD methods were used to investigate the genetic diversity of bacterial mutant DNA (MT57) in lactic acid bacteria. OPC06, OPAG13, OPAO20, OPAW18, OPAA14, and OPX12 were used as RAPD markers. On an agarose gel, DNA bands were visible after the process. In comparison to the control, the OPAA14 primer exhibited a DNA band at position 1159 base pairs and none at position 514 base pairs. At position 486 base pairs, the OPAG13 primer detected the absence. The OPAO20 and OPAW18 primers revealed the 1093 and 514 base pair, respectively. In numerous sites, including 2838, 1200, 1000, and 339 base pairs, the OPC06 primers revealed the absence. The OPX12 primer, on the other hand, produced DNA bands that were like the control, as seen in **Figure 7**.

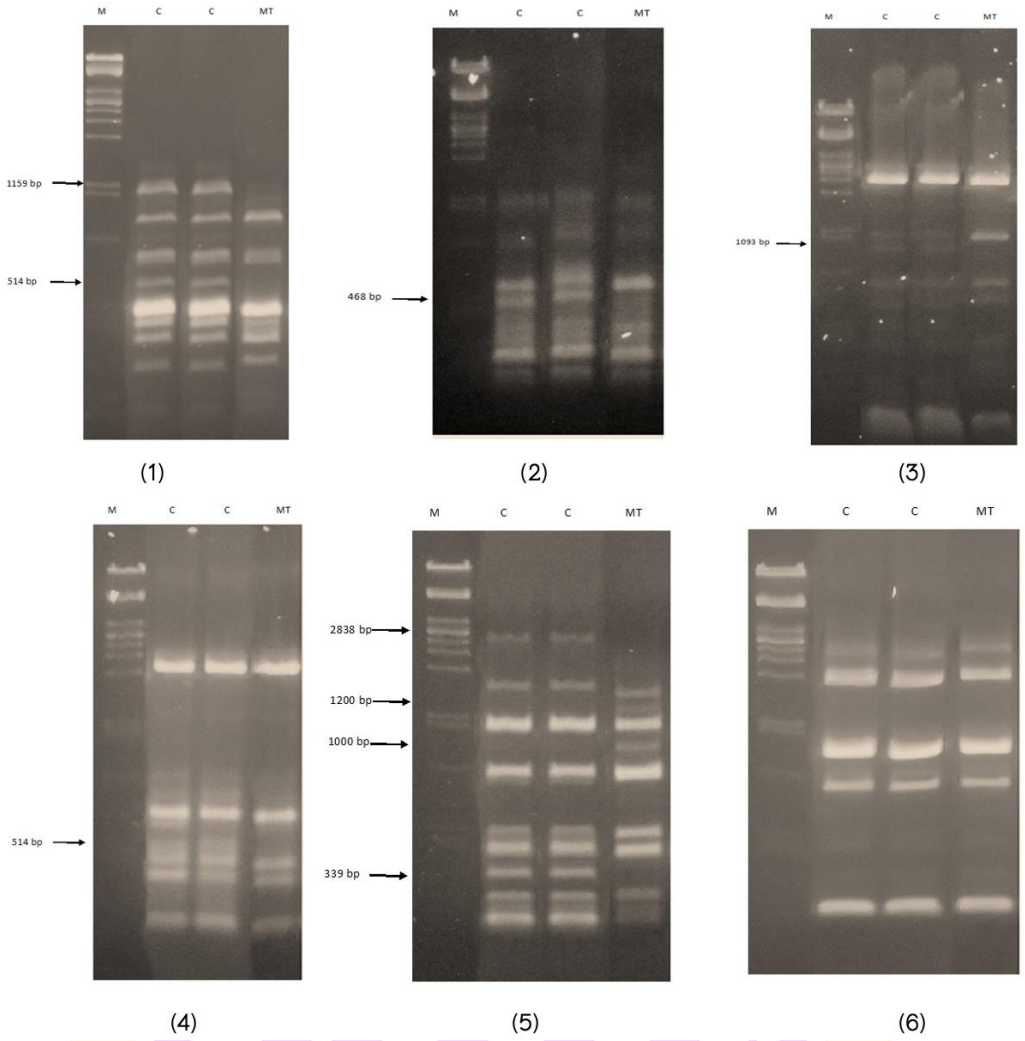

Figure 7 DNA profiles of wild type *Enterococcus faecium* mutant by atmospheric pressure plasma. The HAT-RAPD technique was analyzed using six primers: OPAA14(1), OPAG13(2), OPAO20(3), OPAW18(4), OPC06(5), and OPX12(6). (Molecular weight marker was indicated as M, wild-type were indicated as C and mutant were indicated as MT)

Discussion

This study identified 38 lactic acid bacteria from fermented meat and 27 lactic acid bacteria from fermented vegetable sources. During fermentation, both isolates were spherical (cocci) and did not produce catalase enzymes or carbon dioxide. The result of lactose or 6-carbon sugar fermentation by glycolysis belongs to the homofermentative

type. All isolates produced more than 85% lactic acid (Eiteman and Ramalingam, 2015). In addition, the hydrolysis capacity (H.C.) on solid medium was determined, and the pH of a liquid medium was evaluated (Onda, et al., 2002). Although both isolates had high H.C. values and liquid medium, they had a low pH. Typically, a primary screening method was to examine for a clear zone with a high H.C ratio on solid medium.

According to study on the efficacy of lactic acid bacteria isolated from six isolates, SB1 produces a large amount of lactic acid. Over the duration of 48 hours, the pH was at 4.2. As a result, pH 4.2 might inhibit other pathogenic growth, resulting in long-term silage feed quality preservation (Amaral, et al., 2017). The bacteria most likely to cause silage spoilage, such as *Clostridium*, *Listeria*, and *Bacillus*, as well as the family *Enterobacteriaceae* (Dunière, et al., 2011; Konosonoka, et al., 2012; Rossi and Dellaglio, 2007), were shown to be inhibited by lactic acid with a pH less than 4.20. Furthermore, *Enterococcus* sp., *Leuconostoc* sp., and *Weissella* sp. were lactic acid bacteria with a pH of at least 4.50 in the culture medium (Yang, et al., 2010). Dai, et al. (2020) also stated that good quality tropical grass silage should ferment with bacteria at a pH of less than 4.20. SB1 was identified as *Enterococcus faecium* strain AT15, a spherical, Gram-positive, non-spore forming bacterium, after the 16s rRNA sequence from this research was analyzed with data from the GenBank database (Benson, et al., 2013) at the National Center for Biotechnology Information (NCBI) in the United States of America.

The homofermentative of *Enterococcus* sp. can be used as a pure culture for feed fermentation (Santos, et al., 2013). Various pathogenic microorganisms, including mold and yeast, were inhibited by *Enterococcus* sp. Lactic acid bacteria were generally recognized as safe (GRAS) microorganisms that the Food and Drug Administration (FAD) had authorized for use in foods. As a result, both humans and animals were safe (Gueimonde, et al., 2006).

The isolates NPF1, NPF8, NPF11, SP2, SB1, and SB4 were identified as *Enterococcus faecium* DSM20477, *Enterococcus mundtii* QU25, *Enterococcus faecium* Aus0004, Enterococcus durans 98D, *Enterococcus faecium* AT15, and *Enterococcus faecium* DSM20477, respectively. The 52 isolates from fermented seafood were identified by Nanasombat, et al. (2012). That was largely similar to this study. Induction of mutation by

cold plasma *Enterococcus faecium* mutant resulted in lactic acid with a lower pH than the wild type. Low pH inhibited the growth of fungi or pathogens in the fermented feed during the fermentation process (Puntillo, et al., 2020). Furthermore, the best survival rate condition for the bacterial mutant in this research was bombardment at 1.5/1.5 min, which was the same as Lin, et al. (2012). These results revealed that the MT57 isolated bacterial mutant produced lactic acid at a concentration of 5.4 g/L. Furthermore, the ability to produce lactic acid was 12% higher, as compared to the control strain (4.9 g/L). As a result, such mutants were identified using the HAT–RAPD technique (Anuntalabhochai, et al., 2000). OPC06, OPAG03, OPAO20, OPAW18, and OPAA14 were discovered to differentiate between wild type and mutant. Normally, the primer would bind to DNA at random sites throughout the bacterial genome. A change in the nucleotide sequence, on the other hand, prevents the primer from binding, resulting in an increased or absent DNA band (Ghazi, et al., 2013), which can be used to identify mutations.

Other methods of mutation, such as heavy ion irradiation, were reported for *Lactobacillus thermophilus*. The mutant produced 14.28% more lactic acid than the wild type, according to Hu, et al. (2018). As a result, utilizing lactic acid bacteria in feed fermentation improves feed quality while also inhibiting the growth of a wide range of pathogens. Low–energy plasma techniques can enhance bacterial efficiency while also protecting humans and the environment. As a result, microbial mutation as a method had become an alternative.

Conclusion

Lactic acid bacteria were found to be more abundant in the fermented process that used plants as a raw material than in the fermentation that used meat as a raw material. The lowest value of pH was 4.22. *Enterococcus faecium* was identified as the isolate. Under atmospheric pressure plasma, *E. faecium* was mutated and showed a higher lactic acid concentration than the wild type. To detect mutations, the HAT–RAPD method was performed. Furthermore, since lactic acid bacteria were safe microorganisms that had been approved by the Food and Drug Administration (FAD), they can be controlled to maintain silage quality for a long time.

CHAPTER III

Cellulase–producing bacteria

Literature Review

The composition of agricultural waste

The structures of cellulose, hemicellulose, and lignin in agricultural wastes varies depending on the type of agricultural waste were shown in **Figure 8**. However, cellulose with a composition of 40–60%, hemicellulose with a composition of 20–30%, and lignin with a composition of 15–30% were commonly discovered (Lee, et al., 2008).

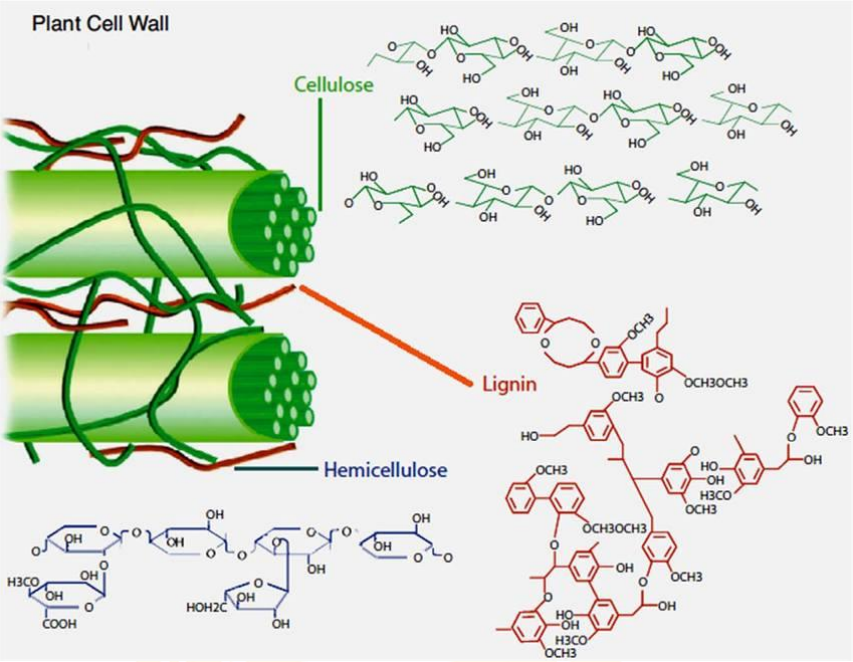

Figure 8 Structure and composition of agricultural waste.

Source: Martin Alonso, et al. (2012)

Cellulose

Cellulose was small fibrous units bound to the cell walls of plants that stick together to form fibers. The basal layer of the cell wall consisted of D-glucose subunits linked by β-1,4 glucosidic bonds (**Figure 9**), including 2000-14,000 units of cellulose. The structure of cellulose is divided into two parts called fibrils:

1. Crystal structure: Atoms were arranged in a specific order. Cellulose contained 30-40% lignocellulose.

2. Amorphous structure: Atoms were disorganized. However, amorphous materials absorb water and biodegrade more readily than crystals (Soonthornchaiboon and Pawongrat, 2012; Tavares, et al., 2014).

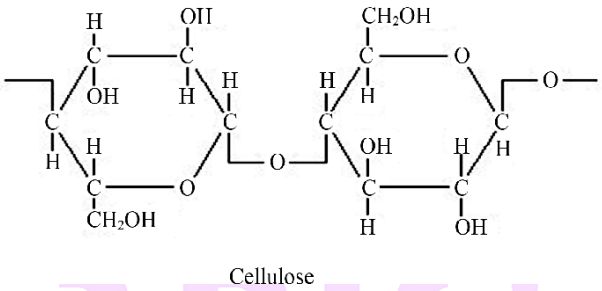

Figure 9 The chemical structure of cellulose.

Source: Richards, et al. (2012)

Hemicellulose

Hemicellulose contains different types of sugars: glucose, mannose, xylose, and arabinose were found in the xylan of polymers: mannan, galactan, and arabinan (Bastawde, 1992). The hemicellulose has an average length of about 200 units, in which the D-xylose polymer was the most abundant at 85-93%. Other components such as glucose, glucuronic acid and galacturonic acid had been found in small amounts (Zhou, et al., 2016). Moreover, xylose forms as β-1,4 glycosidic bonds (Altintas, et al., 2002; Zhou, et al., 2016). The chemical structure of xylan was shown in **Figure 10**.

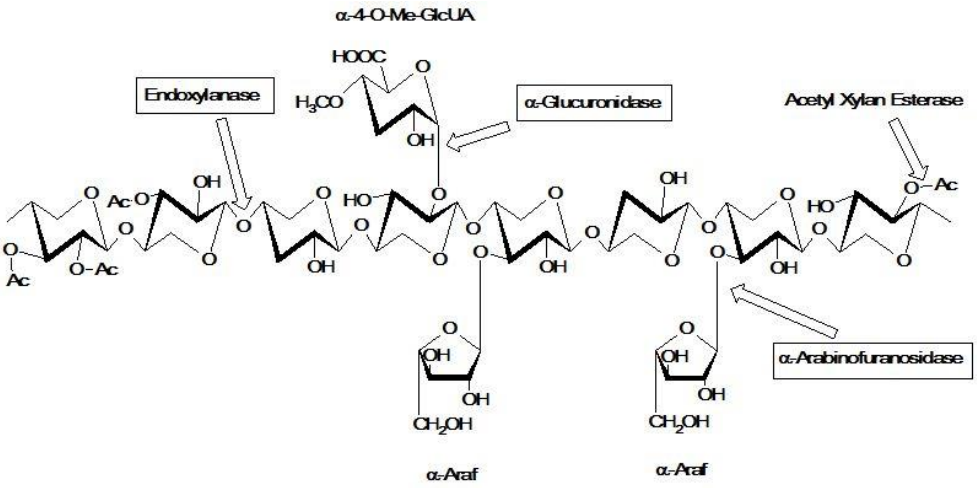

Figure 10 The chemical structure of the polymer consists of hemicelluloses of different sugars.

Source: Sunna and Antranikian (1997)

Lignin structure

Lignin was an aromatic compound found in the cell walls of plants. It was found in varying amounts depending on the type of plant in nature. Lignin prevents cellulose from being easily broken down by microbial enzymes. Lignin was composed of a short-lived non-crystallizing heteropolymer (Cheng, et al., 2008): trans-p-coumaryl alcohol, trans-coniferyl alcohol, and trans-p-sinapyl alcohol (Moore, 2020). In addition, lignin molecules were linked to aromatic substances, such as vanillin and syringaldehyde (Kilby, 1975). The structures of trans-p-coumaryl alcohol, trans-coniferyl alcohool and trans-p-sinapyl alcohol were shown in **Figure 11**.

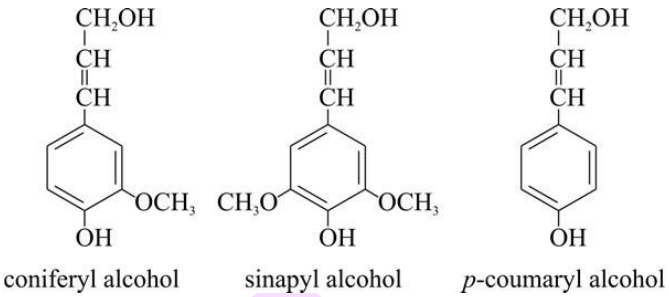

Figure 11 The structure of lignin

Source: Moore (2020).

Cellulase enzymes

Cellulase was an enzyme that breaks the β–1,4 bonds created by fungi, bacteria, protozoa, plants, and animals. The catalytic modules of cellulose were classified into several different groups. It was based on the amino acid sequence and crystal structure (Henrissat, 1991). The carbohydrate–binding module (CBM) and other functional modules were located at the N or C terminal of the catalytic module. Cellulases were a group of enzymes (Percival Zhang, et al., 2006) that include three types of enzymes:

(1) Endoglucanases (EC 3.2.1.4) digest both organized and disorganized cellulose molecules (amorphous) as well as cellooligomer molecules. The cellooligomer at the β–1,4 position was randomly digested. Furthermore, the product was an oligomer and cellobiose.

(2) Exoglucanases (EC 3.2.1.91) consist of cellobiohydrolases (CBHs), which were enzymes that act together with endoglucanase enzymes. Exoglucanase digestion via non–reducing sugar digestion. Therefore, most of the degradation products were cellobiose sugars.

(3) β–glucosidase (BG) (EC 3.2.1.21) digested the molecules of cellobiose and cellooligosaccharides to glucose.

Cellulase enzyme was in high demand in many industries, including textile, fruit, and paper. In addition, the food industry was a supplement to increase digestibility in animal feed. There were two types of cellulose–degrading bacteria: (1) discrete, non–

complexed cellulases (produced by aerobic bacteria and fungi) and (2) complex cellulases (produced on the surface of anaerobic bacteria and fungi). It broke down cellulose, releasing a group of cellulase enzymes (**Figure 12A**), each of which consists of a CBM connected to the catalytic module by a peptide bond. The CBM was located in the N–terminus and C–terminus regions of the catalytic module (Wilson, 2008). **Table 4** illustrated the module structure of heterogeneous bacterial cellulose. In **Figure 12B**, anaerobic microorganisms can form multi–enzyme complexes called cellulosomes, which were vesicled on the surface of microbial cells (Bayer, et al., 2004). Only certain enzymes in cellulosomes were made up of CBM. However, most protein–bound enzymes contribute to CBM. Moreover, the crystal structures of the six endoglucanases and exoglucanase were shown in **Figure 13**. Some anaerobic bacteria can produce cellulosomes and cellulases independently (Berger, et al., 2007; Doi and Kosugi, 2004; Gilad, et al., 2003). Therefore, many specialist researchers had reported the functions of cellulosome (Bayer, et al., 1998; Doi, 2008; Doi, et al., 2003; Doi and Tamaru, 2001; Doi, et al., 1998).

Table 4 Modular structures of cellulase enzymes from various bacteria

Organism	Module structure	Genbank code
Anaerocellum thermophilum	GH9– (CBM3)3 –GH48	ACM60955
A. thermophilum	GH9–(CBM3)3 –GH5	ACM60953
Bacillus subtilis	GH5–CBM3	CAA82317
Clostridium phytofermentans	GH48–Ig–CBM3	ABX43721
C. phytofermentans	GH9–CBM3–(Ig)2 – CBM3	ABX43720
C. thermocellum	GH48–(Doc)2	AAA23226
C. thermocellum	GH26–GH5– CBM11–(Doc)2	AAA23225
C. cellulolyticum	GH48–Doc	ACL75108
Cellulomonas fimi	GH48–Fn3–CBM2	AAB00822
Thermobifi dafusca	CBM2–Fn3–GH48	AAD39947

Note: GH, glycoside hydrolase; CBM, carbohydrate–binding module; Ig, immunoglobulin–like domain; Doc, dockerin; Fn, fibronectin–like domain.

Source: Bayer, et al. (1998)

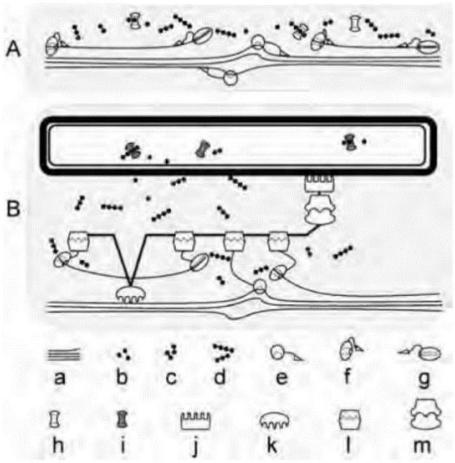

Figure 12 A diagram showing the hydrolysis cellulose of non–complexed (A) and complexed (B) a, cellulose; b, glucose; c, cellobiose; d, oligosaccharides; e, endoglucanase to carbohydrate–binding module (CBM); f, exoglucanase (reducing ends) with CBM; g, exoglucanase (nonreducing ends) with CBM; h, β –glucosidase; i, cellobiose/cellodextrin phosphorylase; j, S–layer homology module; k, CBM; l, type– I dockerin–cohesin pair; m, type–II dockerin–cohesin pair.

Source: Doi (2008)

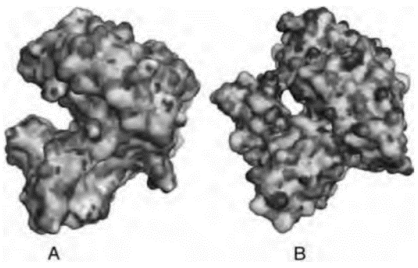

Figure 13 The crystal structure of endoglucanases and exoglucanase from the family six. (A) Active region cleavage in the *Thermobifida fusca* endoglucanase Cel6A construct (PDB code: 1TML). (B) *Humicola insolens* exoglucanase Cel6A construct (PDB code: 1BVW), with a deep circle as the active region. This image was created by the program PyMOL.

Source: Doi (2008)

Industrial use of cellulase enzymes

Cellulase enzymes can be applied in many industries divided by industry type as follows:

(1) The textile industry, starting with fiber manufacture, bring a piece of cloth to weave or knit to spin. After that, the fabric or yarn should be cleaned in preparation for dyeing in the same process. Chemically or mechanically decorated after dyeing, printing, or bleaching. A ready-made finished fabric was manufactured from textiles with specific textures or qualities. Enzymes were utilized in the following steps: reducing fabric weight, polishing the fabric, and cleaning the yarn.

(2) Dirt in clothes contains a variety of biological components, according to the detergent business. It's probable that it was an aqueous solution. Body sweat proteins bind these pollutants, allowing them to be securely absorbed into the tissue. Protease, lipase, and amylase were used in the past, but they were not as clean as they had been. Cellulase enzymes that perform well in alkaline environments were in use. As a result, it made its way into textiles made of clean cotton and blended cotton.

(3) Ethanol can be produced from a variety of raw materials, including sugar, starch, and by-products from various industrial facilities, such as whey manufacturers or canned fruit. These fractions were broken down by enzymes or cellulose acids. Yeast can continue to consume this sugar to make ethanol to get glucose.

(4) The major components of animal feed were various agricultural grains and waste, as well as fiber containing various amounts of cellulose, hemicellulose, and lignin, all of which were difficult for pigs and poultry to digest due to intestinal enzyme catalysis. As a result, the cellulase enzyme was used to produce animal feed from agricultural waste.

Research Methodology

Bacterial strain and vectors

The cellulase–producing bacterium, *B. amyloliquefaciens* (BglC–W), was mutated, and a mutant (BglC–M) was obtained as described in previous work (Sangwijit, et al., 2016). This research used *E. coli* strain DH5α and BL21 (DE3) as hosts for transferring plasmids. All bacterial strains were grown at 37 °C in Luria–Bertani (LB) broth and shaken at 120 rpm. Cloning and expression vectors, pTZ57R/T and pETDuet–1, were purchased from Thermo Fisher Scientific (USA) and Novagen (USA).

Cellulase gene (*BglC*) cloning and vector construction

The genomic DNA of the wild–type strain and the mutant had been extracted and used as a DNA template for cellulase gene cloning. First, the known sequences of the cellulase gene from *B. amyloliquefaciens* registered in GenBank (accession numbers: KY797654.1, MF134665.1, and EU022559.1) have been selected as templates to design primers for amplification the full–length sequence. Both primers, forward primer 5' CCGGCACATATGGCAGGGACAAAAACGCCAGG 3' with *NdeI* restriction site, and reverse primer 5' CTAATGCTCGAGGCCTAAAGCTTAACTAATT 3' with *XhoI* restriction site, were designed. Then, the entire cellulase gene sequences of BglC–W and BglC–M were amplified by PCR. The 1,416 bp of both PCR products were obtained and subcloned into the pTZ57R/T cloning vector. DNA sequencing was performed using an auto sequencer (ABI) by Macrogen, Korea, and nucleotide sequences were determined online with NCBI blast (www.ebi.ac.uk).

Both BglC–W and BglC–M were digested with *NdeI* and *XhoI* and ligated into the corresponding sites of the pETDuet–1 expression vector. The recombinant plasmids of the mutant and control were transformed into *E. coli* BL21(DE3), respectively. The transformed cells were incubated overnight at 37 °C on LB plates with 100 µg/ml ampicillin.

Expression of recombinant BglC–W and BglC–M in *E. coli* BL21 (DE3)

The transformants harboring recombinant BglC–W and BglC–M were cultured in LB–ampicillin (100 µg/ml) medium at 28 °C and shaken at 200 rpm until the OD_{600} reached 0.6 (Polsa, et al., 2020). The recombinant cellulase expression was

induced by isopropyl β-D-1-thiogalactopyranoside (IPTG, 1 mM) for 12 hours at 28 °C. The bacterial cells were harvested by centrifugation, followed by ultrasonication. The measured protein concentration was calculated using the bradford method with bovine serum albumin as a standard.

Temperature and pH effects on BglC-W and BglC-M hydrolysis activity

The hydrolysis activities of BglC-W and BglC-M were assayed using CMC as a substrate. The effect pH was incubated at 50 °C for 30 minutes at pH 2.0-11.0 in a mixture containing 1% (w/v) CMC with each enzyme. Four different buffers were used: citrate buffer (pH 2.0-5.0), potassium phosphate buffer (pH 6.0-7.0), Tris-HCl buffer (pH 8.0-9.0) and CAPS buffer (pH 9.0-11.0). The optimal temperature of each enzyme activity was determined by incubating 1% (w/v) substrate with the enzymes in 50 mM citrate buffer (pH 4.0) for 30 min at various temperatures ranging from 10-100 °C. The amount of reducing sugar was determined by the DNS method (**Appendix B**) (Miller, 1959), and the activity at each pH was calculated. All experiments were carried out in triplicate, and the data was expressed as the mean ± standard deviation. Duncan's multiple range test analyzed the statistical analysis, and the values were considered significant at $P < 0.05$.

Effect of Ca^{2+}, Fe^{2+} and EDTA on cellulase activity

The BglC-W and BglC-M in 50 mM citrate buffer (pH 4.0) with Ca^{2+}, Fe^{2} and EDTA were incubated at room temperature for 30 min. The final concentrations of metals and EDTA were 1, 5, and 10 mM. After incubation, the cellulase activities were measured. All experiments were carried out in triplicate, and the data was expressed as the mean ± standard deviation. Duncan's multiple range test analyzed the statistical analysis, and the values were considered significant at $P < 0.05$.

Structure prediction and molecular docking of BglC

ClustalW (1.83) multiple sequence alignment software (Larkin, et al., 2007). was chosen for amino-acid sequence alignment. After that, ESPript (Robert and Gouet, 2014) was linked to illustrate the secondary structure of the templates selected. The catalytic core of BglC was aligned with that obtained from *B. subtilis* cellulase 5A (PDB

code 3PZT). The carbohydrate–binding module of mutant K370E BglC and *B. subtilis* cellulase 5A (PDB code 2L8A) were aligned.

The structural models of BglC were created using SWISS–MODEL (Waterhouse, et al., 2018). The model of the catalytic domain of BglC was built using the X–ray structure PDB code 3PZT, and the carbohydrate–binding module of BglC–M was built using PDB code 2L8A, which corresponded to a family of 5 catalytic domains and a family of 3 carbohydrate–binding modules (CBM3), respectively.

The coordinates of divalent cations (Ca^{2+} and Fe^{2+}) were simulated within the catalytic core of the model structure. In addition, the coordinates of cellopentaose were docked into the carbohydrate–binding module of the predicted structure of BglC–M. Docking studies in both catalytic and carbohydrate–binding domains were performed by AutoDock Vina (Trott and Olson, 2010). Finally, all structures were displayed with PyMOL (Schrodinger, 2010).

Analysis of the hydrolysis of cellulases against lignocellulosic substrates

The hydrolysis activities of BglC–W and BglC–M were determined using lignocellulosic substrates, including pineapple peel, corncob, and durian peel. The hydrolysis activities were carried out by incubating the enzyme separately for seven days in 5% (w/v) substrates in 50 mM citrate buffer at 50 °C. Then, the reaction mixtures were collected every 24 h. The reducing sugar released from the substrates was measured by the DNS method. All experiments were carried out in triplicate, and the data was expressed as the mean ± standard deviation. Duncan's multiple range test analyzed the statistical analysis, and the values were considered significant at $P < 0.05$.

Results

Cloning and sequence analysis of *BglC*

Sequence comparison between cellulase genes of the wild type (BglC–W) and the mutant (BglC–M) revealed that BglC–W and BglC–M consisted of 1,416 nucleotides, encoding a protein of 471 amino acids. The amino acid sequence alignment of BglC–W and BglC–M was almost identical. However, a single amino acid, lysine, located at position 370, was substituted with glutamic acid (K370E). Analysis of the conserved domain

further confirmed that our cellulase gene was comprised of the catalytic domain (from 1M to 301I), which belongs to family 5 of glycoside hydrolases (GH5), and a family 3 cellulose binding module (CBM3) (from 326I to 471H). In addition, a catalytic domain (CD) and a family of three carbohydrate–binding modules (CBM3) were connected by a short linker sequence (from 302L to 325G). Based on sequence alignment and domain analysis, the mutant residue (K370E) was situated in CBM3, not in the catalytic site.

Characterization of cellulase enzymes

The enzymes with more stable and higher catalytic activity under a broad range of pH and temperature were required for a feed fermentation process. Both cellulase genes (BglC–W and BglC–M) were subcloned and introduced into host cells, then incubated with 1% CMC at pH ranging from 2 to 11. The reducing sugar was liberated from the reaction and measured using the DNS method, and the enzyme activity was also calculated. As shown in **Figure 14**, the cellulase activity of BglC–W and BglC–M attained the highest values at pH 4.0. The effect of temperature on cellulase activities was measured, and the result was shown in **Figure 15**. The highest activity of BglC–M was observed at 50˚C, and the cellulase activity of BglC–M was exhibited 2.5 times higher over a broad range of pH and temperature, which also retained about 80% of the activity at 90˚C after 30 min of incubation (**Figure 15**).

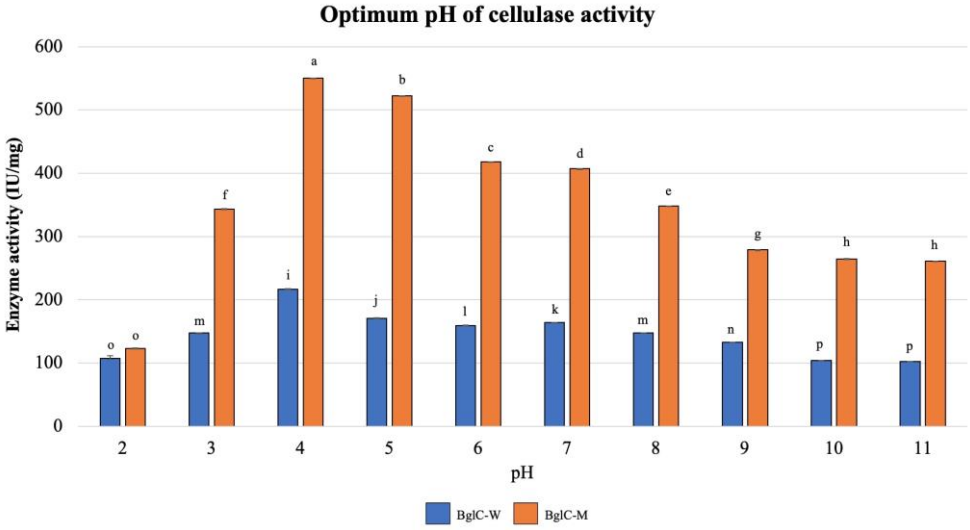

Figure 14 Cellulase activities of BglC–W and BglC–M at various pH levels ranging from 2 to 11 at 50 °C. The letters indicate a significant difference ($P < 0.05$) as determined by Duncan's multiple range test.

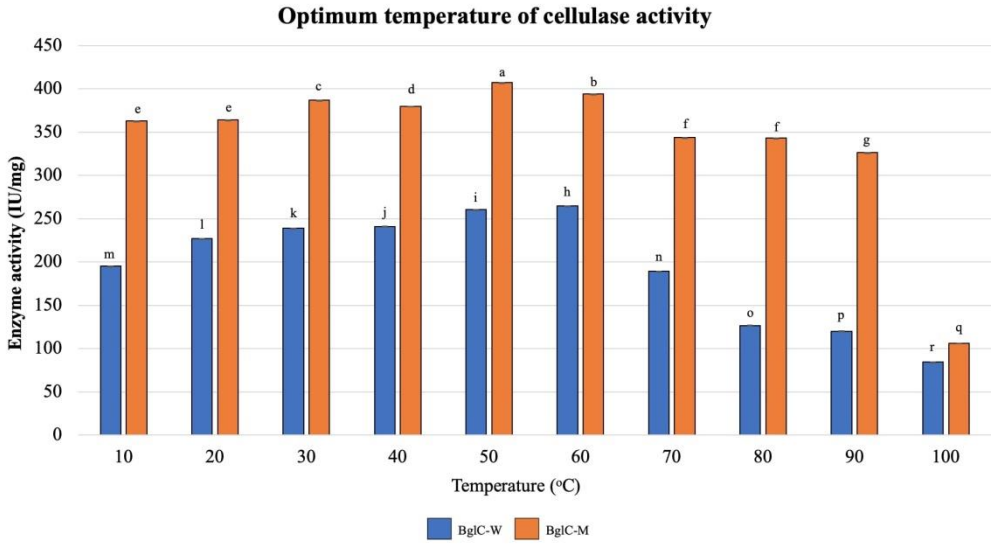

Figure 15 Cellulase activities of BglC–W and BglC–M at various temperature ranging from 10 to 100 °C. The letters indicate a significant difference ($P < 0.05$) as determined by Duncan's multiple range test.

Effects of Ca^{2+}, Fe^{2+} and chelating agents

As shown in **Table 5**, Ca^{2+} and Fe^{2+} on cellulase activity of BglC–W and BglC–M were reported. The effects of these ions were proven to be dependent on their concentration. At the lowest concentration of 1 mM, Ca^{2+} and Fe^{2+} were able to increase cellulolytic activity slightly. The activities of both enzymes slightly increased in the presence of Ca^{2+} and Fe^{2+} at low concentrations, but it decreased when ion concentrations increased. Under the same conditions, increasing the EDTA concentration resulted in a slight decrease in enzyme activity.

Table 5 Effect of ions and chelating agents on cellulase activity

Relative cellulase activity	BglC–W				BglC–M			
	0 mM	1 mM	5 mM	10 mM	0 mM	1 mM	5 mM	10 mM
Ca^{2+}	100.00 ± 0.11[c]	103.57 ± 0.36[b]	94.14 ± 0.11[d]	81.44 ± 0.21[g]	100.00 ± 0.25[c]	115.97 ± 0.47[a]	92.57 ± 0.21[e]	88.66 ± 0.39[f]
Fe^{2+}	100.00 ± 0.28[b]	110.27 ± 0.05[a]	53.14 ± 0.45[e]	45.97 ± 0.01[f]	100.00 ± 0.47[b]	100.10 ± 0.07[b]	80.52 ± 0.24[c]	66.30 ± 0.12[d]
EDTA	100.00 ± 0.34[a]	73.34 ± 0.15[f]	74.20 ± 0.35[e]	64.19 ± 0.22[g]	100.00 ± 0.30[a]	83.29 ± 0.31[c]	86.60 ± 0.30[b]	80.54 ± 0.23[d]

Note: The letters indicate a significant difference ($p < 0.05$) as determined by Duncan's multiple range test.

Structural comparison between BglC–W and BglC–M

Sequence analysis of the cellulase enzyme

The amino acid sequence alignment between the control (BglC–W) and mutant (BglC–M) *B. amyloliquefaciens* cellulases (BaCel5) was shown in **Figure 16**. Analysis of the conserved domain (**Figure 16**) confirmed that the BglC gene belonged to a cellulase superfamily, consisting of a GH5 family catalytic domain (CD ~301 residues) and a family 3 cellulose–binding module (CBM3 ~144 residues), according to the CAZy classification (http://www.cazy.org/). The two domains were joined by a short linker sequence (302LGSKDSTKERPETPAQDNPAQENG327), rich in hydrophobic residues. Based on sequence alignment and domain analysis, the mutant residue (K370E) was suggested to be locate in CBM3, not the catalytic motif.

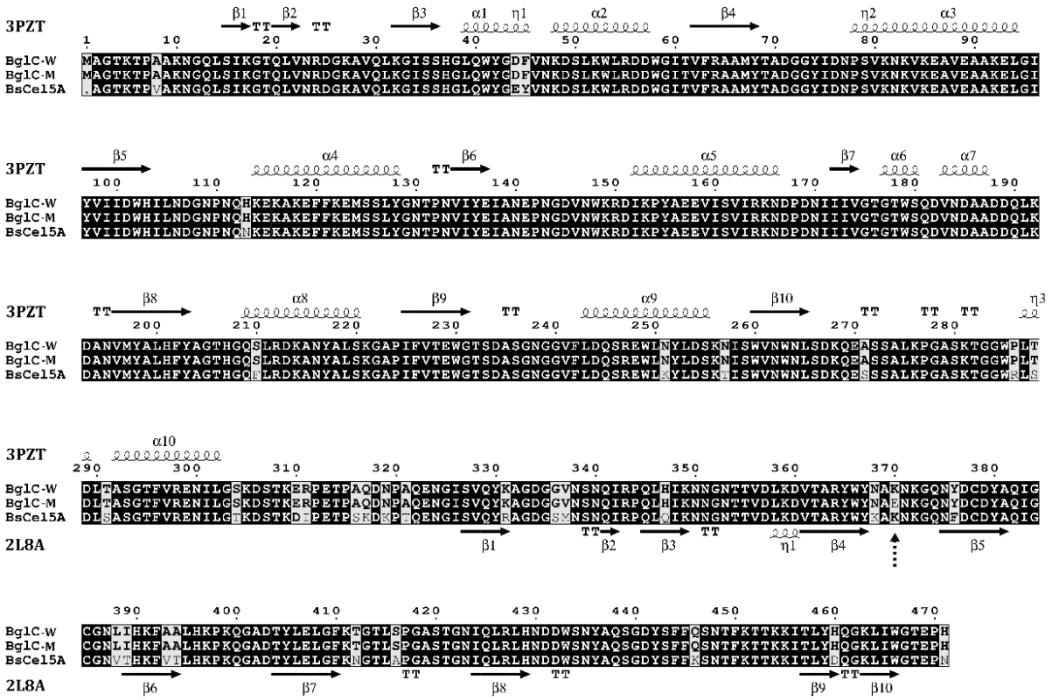

Figure 16 Amino acid sequence alignment of wild type and mutant cellulase from *B. amyloliquefaciens* (BglC–W and BglC–M, respectively) and cellulase from *B. subtilis* 168 (BsCel5A). Secondary structures were predicted using the X–ray structures of the catalytic domain and carbohydrate–binding module of BsCel5A as templates (PDB entries 3PZT and 2L8A, respectively). The catalytic domain was shown above the sequences, but the carbohydrate–binding module was below the sequences. The dashed arrow indicated the mutant residue (K370E). α–helices and β–strands were displayed as squiggles and arrows, respectively. TT indicates turns. Fully conserved residues were printed as white characters on a black background. Similar residues were written in bold black characters and boxed.

Analysis of the BglC catalytic core

The catalytic core of BsCel5A (PDB code 3PZT) was used as a template to compare with that of BglC. The alignment result showed that our cellulase shared 96% amino acid identity with the catalytic core of the structural template. In the previous report, the BsCel5A catalytic core structure was composed of a typical (β/α)8–TIM–barrel

domain with the catalytic residues on β–strands (Santos, et al., 2011). Structural analysis revealed that the model structure of the catalytic core of our cellulase displayed a common TIM barrel fold. In addition, Ca^{2+} and Fe^{2+} were docked in the model structure of the catalytic core, thus having the same binding free energy of –1.4 (in kcal/mol). This study suggests that the docked metals were located at the catalytic core, surrounded by the polar serine and asparagine for their coordination sites.

Analysis of BglC carbohydrate–binding module (CBM3)

The CBM3 amino acid sequence of BglC–W and BglC–M shared 90% and 89% sequence identity, respectively, with BsCel5A (PDB code 2L8A) as a template model. The predicted structure revealed that CBM3 folded into a β–sandwich, a dominant fold among CBMs. It was made up of two β–sheets with four and five antiparallel β–strands, similar to the selected template (**Figure 17**). The predicted structure also had one short α–helix at the C–terminus, which was similar to that of BsCel5A (**Figure 17**). The structure of cellopentaose docked into the structure of BglC–M had a binding free energy of –7.5 kcal/mol.

From the docking study, 376Y was close to the substrate's reducing end terminal residue (~8 Å apart), which may facilitate the substrate's occupancy. 376Y was proposed to lie along with the hydrophobic platform since it may form a hydrophobic stack against the incoming cellulose chain's pyranose rings (**Figure 17**). From the docking study of cellopentaose with the model structure of BglC–M, the residues proposed to form hydrogen bonds with cellopentaose were 370E of BglC–M and 398K of BsCel5A CBM3 (homologous to 370K of BglC–W) (**Figure 17**). The oxygen atom of the sugar residue at the non–reducing end (subsite –3) recognizes the side–chain oxygen of 370E and the amide side chain of 398K with the predicted hydrogen bond distances of 3.8 Å and 3.6 Å, respectively (**Figure 17**). 398K of BsCel5A CBM3 (homologous to 370K of BglC–W) was located on a surface loop, and its amide side chain was far from the hydroxyl side chain 464Y (BsCel5A CBM3) with the distance of 5.4 Å, thus being predicted in BglC–W similarly. The predicted hydrogen bonding with 2.6 Å between 370E (BglC–M) and 436Y linked the flexible loops together, thus making the structure more compact.

The backbone carbonyl of 370E of BglC–M was structurally homologous to 398K of BsCel5A and was proposed to form a hydrogen bond within the sugar ring at subsite –2, with 3.0 Å (**Figure 17**). Similarly, the backbone carbonyl of 373G formed a hydrogen bond with the oxygen atom of the sugar residue (subsite –1) docked at a predicted distance of 3.9 Å (**Figure 17**). The glucosyl substrate at subsite –2 was proposedly to be stacked against the indole ring of 433W (**Figure 17**).

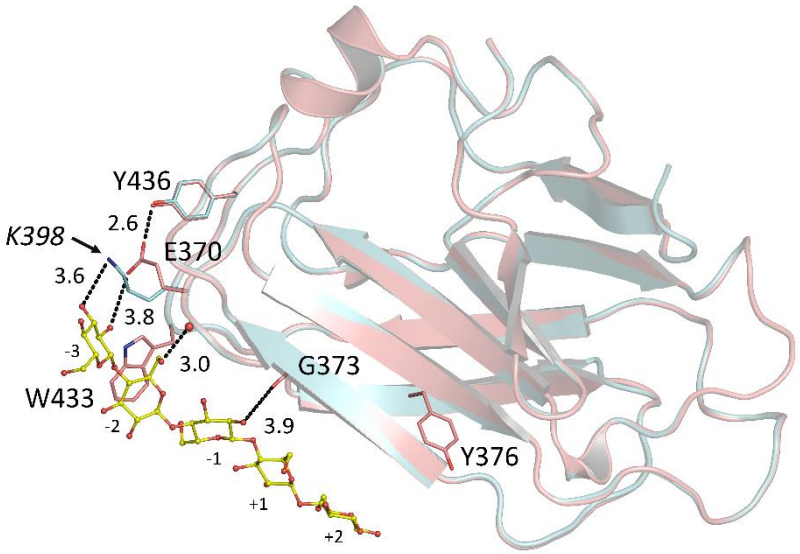

Figure 17 The superposed structures of the cellulose–binding domain were shown. The structure model of BglC–M from *B. amyloliquefaciens* was shown in salmon. The structure of BsCel5A CBM3 from *B. subtilis* 168 (PDB code 2L8A) was shown in cyan. The residues involved in carbohydrate recognition in the structure model of BglC–M K370E was shown as stick models with carbon in salmon, nitrogen in blue, and oxygen in red. K398, labeled in italic, was from the structure of BsCel5A CBM3 shown as a stick model with carbon in cyan. The docked cellopentaose was shown as a ball–and–stick model with carbon in yellow. Sugar–binding subsites were labeled. The black dashed line represented a predicted hydrogen bond formed in the BglC–M structure model between the surrounding residues and the cellopentaose molecule; the distances between them were given in Å.

Hydrolysis activity on lignocellulosic substrates

The hydrolysis activity of cellulases on pineapple peel, corncob, and durian peel was tested. The results showed an increase in hydrolysis activity by measuring the amount of reducing sugar liberated from substrates since the first day of incubation. As shown in **Figure 18**, the results indicated that BglC–M exhibited the highest hydrolysis activity against all substrates. Therefore, the most suitable substrate for this experiment was the corncobs, since it released the highest amount of reducing sugar on the 7th day.

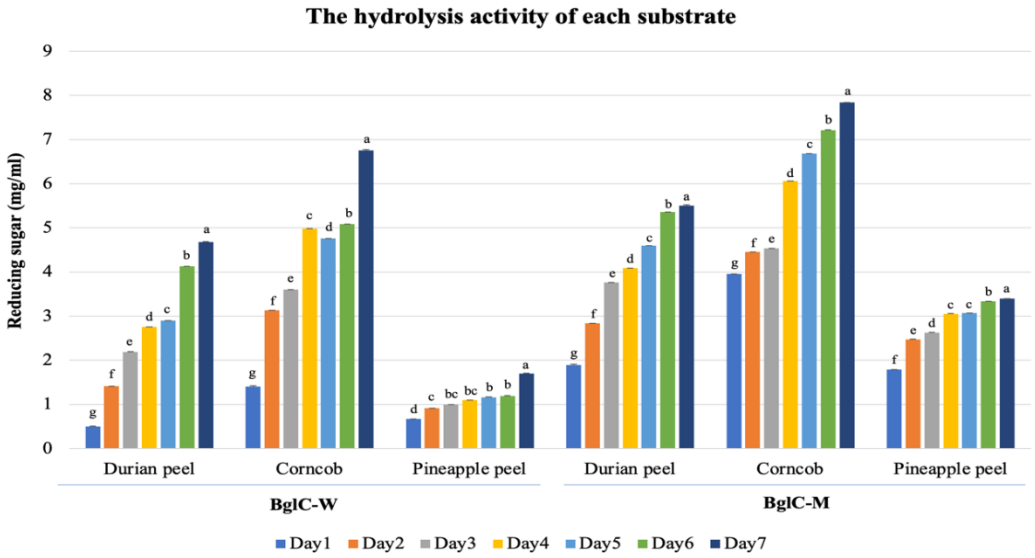

Figure 18 Hydrolysis activities of BglC–W and BglC–M on durian peel, corncob, and pineapple peel. The letters indicate a significant difference ($P < 0.05$) as determined by Duncan's multiple range test.

Discussion

The cellulase–producing bacteria isolated from horse manure was *Bacillus amyloliquefaciens* from previous reports (Sangwijit, et al., 2016). It can degrade lignocellulose, consisting of cellulose (45–55%), hemicellulose (25–35%), and lignin (Xu, et al., 2020). In addition, it produces cellulase and xylanase enzymes to break down plant cell walls into single sugar molecules. The other microorganisms use sugar as their food source to produce organic acids.

To maintain the quality of fermented feed, several groups of cellulase-producing bacteria, such as *Cellulomonas*, *Cellvibrio*, *Pseudomonas* sp., *Bacillus*, and *Micrococcus* (Immanuel, et al., 2006; Nandimath, et al., 2016) were reported. In poultry feed, cellulolytic enzymes had higher total weight and energy values than in animals (Café, et al., 2002). In addition, cellulase and xylanase increased feed intake and milk production (Romero, et al., 2016). Therefore, the cellulase enzyme was very important for animal feed. During feed fermentation, the temperature inside the fermentation chamber increases gradually, up to 42˚C (Dai, et al., 2020). Therefore, our mutant has higher catalytic activity between 40-60˚C, which is suitable for fermentation. Interestingly, the mutant produced cellulase with approximately 2.5-fold higher catalytic activity than the wild type. Sequence analysis determined that the mutant K370E, located in CBM3 at the C-terminus, may be involved in enzyme activity.

The docked metal atoms (Ca^{2+} and Fe^{2+}) can be coordinated by the side chains of the polar residues of serine and asparagine, carbonyl oxygen, and nitrogen amide (**Table 5**). The metal-binding motif with hepta-coordination may contribute to its stability, thus further enhancing cellulase activity. Such a metal binding site had been reported previously for the crystal structure of the catalytic core of *B. subtilis* cellulase 5A (Santos, et al., 2011). Yaniv, et al. (2012) also confirmed that the role of metal ions was to facilitate the maintenance of loops, but not for protein reconformation. Moreover, EDTA was a strong chelator and effectively removes concentrations of divalent cations from the catalytic domain, thereby removing the metal binding motif and suggesting lower stability. Therefore, the 1 mM to 10 mM range of EDTA reduces cations, resulting in decreased enzyme stability and activity.

Docking studies presume that the coordination of metal ions by serine and asparagine can stabilize the structure of the enzyme and increase its cellulolytic activity. Fe^{2+} and Co^{2+} had previously been reported to increase the activity of endocellulase Cel-5A enzyme at concentration as low as 1 mM (Ma, et al., 2020). Moreover, Co^{2+} ion in the endoglucanase CelCM3 can increase enzyme activity (Khalili Ghadikolaei, et al., 2018). Metal ions were proposed lead the enzyme in its stable and optimized conformation

(Santos, et al., 2011; Yan, et al., 2008). The contribution of metal ions in our study could facilitate a more stable enzyme structure, thus increasing its activity.

Usually, the carbohydrate-binding modules (CBMs) were the amino acid sequence that was important in carbohydrate-binding. The alignment results showed that our CBM belongs to CBM 3 family, forming a flat surface for cellulose recognition (Santos, et al., 2011). A specifically shaped substrate was needed to catalyze the catalytic site and optimize the enzymatic reaction (Santos, et al., 2011). The recognition of protein and carbohydrate-binding use the Van der Waals bond. Moreover, the reaction was made from an aromatic ring complex between furanose and pyranose. The hydrogen bonds between the polar saccharide groups and amino acid side chains of Y380 and Y436 were aromatic groups attached to the β-sandwich core, which are hydrophobic, suggesting that most of the interactions of CBM3 with cellulose were due to the polarized side chains. Therefore, the increase in enzyme activity on the K370E mutant was likely a change in the electrostatic cycles around CBM3 causing the positive side chain (K) to change to the negative side chain (E). The predicted hydrogen bonding with 2.6 Å between E370 (BglC-M) and Y436 linked the flexible loops together, thus making the structure more compact. These might increase the stability of the enzyme and collectively contribute to the accommodation of the cellulose chain. Our biochemical assays indicated that K370E mutant exhibited approximately 2.5-fold improvement in activity compared to the wild-type. Docking studies of BglC-M CBM3 with cellopentaose reported that the carbohydrate-binding site involves hydrophobic stacking against the pyranose rings and that hydrogen bonds form between the hydroxyl groups of cellopentaose and the protein structure.

On this face, two aromatic residues were W433 and Y436, while Y376 was buried at β-sandwich core that make hydrophobic contacts. The study showed that aromatic residues and polar side chains contributed to CBM3 BglC with cellulose. Yaniv, et al. (2012) It had been found that the base substitution by site mutagenesis from asparagine to tryptophan (N126W) in the carbohydrate-binding domain enhanced the binding ability of cellulase from *Clostridium thermocellum*, thus proposing its crystalline structure. However, the activity of the cellulase had not been demonstrated.

The distance between K398 and Y464 was 5.4 Å in BsCel5ACBM3 (K370 to Y436 in BglC-W). Therefore, the replacement of E370 by K370 in the model corresponds to reported experiments to increase enzymatic activity in mutants. It refers to the dynamic structure and evolution of the enzyme, which increased the properties of enzymes not only at the catalytic site, but also at the site of the substrate module (Zhang, et al., 2015). Mutations outside the catalytic site enhance the enzymatic activity by changing the protein, reacting with substrates and transition conditions. The amino acids can promote catalysis with groups involved in certain catalytic mechanisms (Suto, et al., 2002), such as structural flexibility, which contributed to forming new catalytic regions by mutation. Thus, the substrate was necessary to catch the transition conditions (Zhang, et al., 2015).

Thermostability and pH stability produced by the mutants are also the keys to improving enzyme properties and activities (Contreras, et al., 2020). Moreover, CBM plays an important role in substrate binding, which further improves the catalytic activity (Badino, et al., 2017) and thermostability (Westh, et al., 2017). Our study indicated that a mutant, which involved the modification of a single residue charged into the CBM3 domain by plasma immersion ion implantation, increased its cellulase activity.

According to the composition of lignocellulosic biomass containing 45–55% cellulose, the reducing sugar released during our experiment could be calculated as 20–40% of total cellulose on each lignocellulosic substrate. This result indicated that the mutant could be used to hydrolyze these lignocellulosic wastes for animal feed. In the future, this mutant cellulase will be applied to hydrolyze lignocellulosic wastes for fermented animal feed, especially corncob and durian peel. This could provide low-cost animal feed and reduce air pollution by avoiding the combustion of lignocellulosic waste.

Furthermore, it was the first evidence showing that a single amino acid substitution in CBM, not in the catalytic domain, increased its enzyme activity. Moreover, it can be applied to animal feed.

Conclusion

B. amyloliquefaciens was mutated by cold plasma implantation to enhance its cellulase activities. The cellulase mutant (BglC–M) showed higher catalytic activity about 2.5–fold than the control under a wide range of temperature and pH. The molecular docking study proposed carbohydrate–aromatic and hydrogen bonding interactions between cellopentaose and BglC. Moreover, the residue that recognized the incoming substrate was predicted. Sequence analysis and structure prediction revealed that a single amino acid residue was substituted from lysine to glutamine at position 370 (K370E) in the cellulose binding module, while not in the catalytic domain. The predicted structure of BglC–M with bound substrate revealed the role of mutant K370E, thus facilitating the attachment of the two loops. This amino acid (K370E) involved a charge residue change on the CBM3, resulting in increased structural stability and enzymatic activity. In addition, the hydrolysis ability of cellulase was investigated on agricultural wastes, including pineapple peel, corncob, and durian peel. A greater released of reducing sugar was detected in the corncob. Although an amino acid mutation in CBM (N126W) increased the binding activity of *C. thermocellum* cellulase had been reported by Yaniv, et al. (2012), its enzyme activity was not demonstrated. This was the first evidence shown that a single amino acid substitution in CBM, not in the catalytic domain, increased its enzyme activity.

CHAPTER IV

Xylanase–producing bacteria

Literature Review

Xylanase enzyme

Xylan is the major polysaccharide in primary cell wall, about 20% and its composition depend on the original. Structurally, xylan is polysaccharide with a backbone composed of β–1,4–linkage between D–xylose residues (Duan, et al., 2021). The digestion of xylan requires enzymes with many different and specific mechanisms. The enzymes involved in the breakdown of hemicellulose was called hemicellulase or glucan hydrolase. They had divided the specific actions of the substance (Suto, et al., 2002):

(1) The substances were only degradable to L–arabinose (1,3) and (1,5)–2–L–arabino–furanosyl. Thus, the arabinose sugar (L–arabinose) was produced.

(2) The enzyme D–galactanase only degraded galactan and produces the sugar, L–arabino–D–galactan.

(3) D–mannanase was an enzyme which can break down β–(1,4)–D–mannanopyranosyl from D–mannan.

(4) β–xylanase cleaved the xylan bond.

The degradation of xylan to obtain small subunits found outside the main xylose related to β–(1,4)–D–xylopyranosyl and many other enzymes also involved in the digestion of the main branches or main strands e.g., β–(1,2), β–(1,3), or β–(1,4). Each enzyme was different and specific to the subunits and linkage bonds that can split the enzyme as the following mode:

1. The branched digestive enzyme (Beg, et al., 2001) indicates that the xylan plant was a polymer consisting of xylose molecules connected by β–(1,4) bonds. It was composed of xylose molecules. Acetyl, arabinofuranosyl, or glucuronic groups of enzymes were responsible for reducing branched subunits. It had been verified that the enzyme that works on the main branch cannot operate without disapproval. Therefore,

digestion begins with trimming by the acetyl esterase, L–arabinofuranosidase, and glucuronidase enzymes.

2. All branches were eliminated by the main digestive enzymes; The main branch was digested by three types of enzymes as follows:

1.Endo–β–1,4–D–xylan xylanohydrolase (E.C.3.2.1.8). It worked by randomly break the β–1,4 bonds in the main chain. These were xylooligosaccharides of different sizes.

2.Exo–β–1,4–D–xylanase. It acted to branch xylan and xylooligosaccharides into subunits from the non–reducing end, then the product was xylose.

3.β–D–xyloside xylohydrolase (E.C.3.2.1.37). It digested disaccharides, a function product of endo–xylanase and exo–xylanase, producing xylose sugar.

Normally, the enzyme xylanase was activated in foods containing xylan (Balakrishnan, et al., 1992). The enzyme xylanase was immobilized, and was useful in studies such as repeated use of the enzymes, easy separation yield, and development of enzyme stability (Beg, et al., 2001).

Source of the enzyme xylanase

Xylanase was produced by bacteria and actinomyces bacteria (*Bacillus* sp., *Pseudomonas* sp., *Streptomyces* sp.). The optimal pH range was 5–9, with an optimum temperature of 35–60 °C (Beg, et al., 2001; Mandal, et al., 2015). The bacteria studied for xylanase production were presented in **Table 6** (Amore, et al., 2015; Dhiman, et al., 2008; Maheswari and Chandra, 2000).

Table 6 The xylanase-producing bacteria.

Microorganism
Bacillus pumilus
Bacillus subtilis
Bacillus amyloliquefaciens
Bacillus cereus
Bacillus circulans
Bacillus megatorium
Bacillus licheniformis
Bacillus stearothermophilus
Streptomyces sp.
Streptomyces roseiscleroticus
Streptomyces cuspidosporus
Streptomyces actuosus
Pseudonomas sp.
Clostridium absonum
Thermoactinomyces thalophilus

Source: (Van Schie and Young, 2000)

This study showed that *Bacillus* sp. exhibited high xylanase at pH, alkali, and high temperatures. As a result of their alkaline and heat resistance, xylan degradation bacteria were used in the industry (Mandal, et al., 2015).

Fungi (*Aspergillus* spp., *Fusarium* spp., *Penicillium* spp.) were essential in the production of xylanase because of its high efficiency and the release of cells (Van Schie and Young, 2000). Fungi had high enzyme activity. However, some limitations were not suitable for industrial applications (Mandal, et al., 2015). Fungal enzymes were effective at temperatures below 50°C and pH values in the range of 4-6 (Balakrishnan, et al., 1992), but they cannot be used in the fruit and paper industries, which require an alkaline pH and

temperatures above 60°C (Mandal, et al., 2015). The fungi were also found in cellulase enzymes. Moreover, very few other reports had found a xylanase enzyme without cellulase (Subramaniyan and Prema, 2002). The strains of fungi that produce xylanase were shown in **Table 7**.

Table 7 Fungi produce the enzyme xylanase.

Microorganism
Aspergillus niger
A. foetidus
A. brasiliensis
A. flavus
A. nidulans
A. terreus
Penicilium sp.
Trichoderma reesei
T. longibrachiatum
T. harzianum
T. viride
T. atroviride
Fusarium oxysporum
Thermomyces lanuginosus
Alternaria sp.
Talaromyces emersonii
Schizophyllum commune
Piromyces sp.

Source: (Van Schie and Young, 2000)

The xylanase enzyme can be produced by solid-state fermentation (SSF) or by submerged fermentation (SMF). However, SSF fermentation enzymes were more abundant than SMFs (Van Schie and Young, 2000). In addition, large-scale production in

fungi was more difficult due to slow growth and reproduction with highly viscous substances that affect oxygen (Mandal, et al., 2015).

Research Methodology

Bacterial strains, growth conditions, and vectors

A xylanase-producing bacteria, *Bacillus subtilis*, was isolated from a termite comb. *Escherichia coli* strain DH5α and BL21 (DE3) were used as hosts for transferring plasmids. All bacterial strains were grown at 37 °C in Luria-Bertani (LB) broth with vigorous shaking at 120 rpm. Cloning and expression vectors, pTZ57R/T and pETDuet-1, were purchased from Thermo Fisher Scientific (USA) and Novagen (USA).

Atmospheric pressure plasma jet bombardment

Plasma bombardment of the bacterial samples was carried out using our in-house developed atmospheric pressure plasma jet (APPJ) at the Biotechnology Unit, University of Phayao. A schematic of the APPJ system, comprised of a high voltage power supply, electrodes, and a dielectric tube, is shown in **Figure 19**.

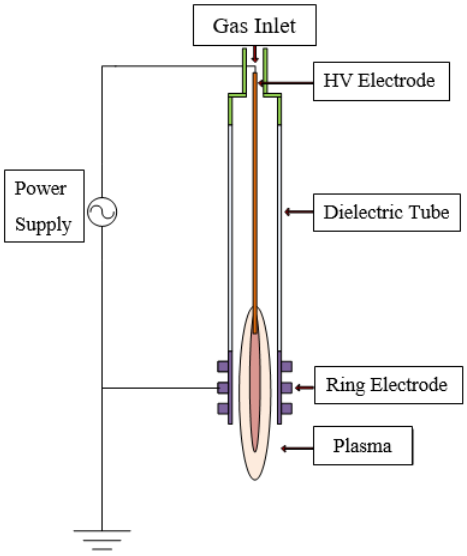

Figure 19 Schematic drawing of the atmospheric pressure plasma jet (APPJ) system.

B. subtilis cells were harvested by centrifugation at 6,000 rpm for 5 min after overnight incubation at 37 °C and resuspended with 100 µl of sterile distilled water. Bacterial suspensions were dropped into holes in a sample holder for plasma bombardment. Both argon and helium plasmas were chosen to generate plasma with an energy input of 120 W and a gas flow rate of 2 SCCM (standard cubic centimeters per minute) at room temperature for all experiments. The bacterial samples were bombarded at time intervals ranging from 1 to 5 min. After plasma bombardment, 1 ml of LB media was added to each bombarded sample and incubated at 37 °C on a rotating shaker for 1 h. Then, 100 µl of each sample was spread on LB agar containing 1 % (w/v) beechwood xylan and incubated overnight at 37 °C.

Bacterial survival comparison

After bombardment, all bacterial samples were recovered by spreading them on LB agar plates and incubating them at 37 °C. The number of colonies was counted to determine the colony–forming units (CFUs). The effectiveness of the bombardment was calculated as the percentage of CFUs observed on treated plates relative to CFUs on untreated plates at the lowest dilution where survival was observed (Humud, 2013). The percentage of bacterial survival was calculated using the following formula:

$$R = \frac{(No-Nt)}{N0} x100\%$$

where: N_0 = C.F.U. of non–treated bacterial control and N_t = C.F.U. of treated bacteria.

Screening for xylanase (*XynA*) gene mutation

After the bacterial cells were bombarded with either argon or helium plasmas, the bombarded bacterial samples were screened for xylanase (*XynA*) gene mutation by spotting on agar plates consisting of 1% (w/v) beechwood xylan and incubated at 37°C for 24 h. Wild type *B. subtilis* was grown on the same agar media as the control. The hydrolysis halos were stained by congo red in order to observe bacterial xylanase activity (Klunk, et al., 1999). The ratio between hydrolysis halo diameter evaluated the qualitative

xylanase activity of each bombarded bacterial to the colony diameter ratio (H.C.). The mutant with the highest H.C. ratio was selected with the xylanase gene MxynA and the control CxynA.

Gene cloning and vectors construction

Xylanase gene cloning

Control and mutant chromosomal DNA were extracted and used as a DNA template for xylanase gene cloning. A known sequence of *B. subtilis* xylanase gene in GenBank (accession no.; WP_038829967.1) was chosen as a template to design primers for amplifying the xylanase gene. Two primers, forward primer 5'CCGGCAGGATCCGCAGGGACAAAAACGCCAG 3' with restriction site *BamHI*, and reverse primer 5' CTAATGAAGCTTGCCTAAAGCTTAACTAATT3' with restriction site *HindIII* were designed. Then entire xylanase gene sequences of CxynA and MxynA were amplified by PCR. The 642 bp PCR products were obtained and subcloned into the corresponding sites of the pTZ57R/T vector. DNA sequencing was performed using an auto sequencer (ABI) by Macrogen, Korea, and the nucleotide sequences were determined online with NCBI blast (www.ebi.ac.uk).

Construction of recombinant expression vectors and transformation of *E. coli* BL21 (DE3)

Both CxynA and MxynA were digested with *BamHI* and *HindIII* and ligated into the corresponding sites of the pETDuet-1 vector. The recombinant plasmids of the mutant and the control, named pMxynA and pCxynA, were transformed into *E. coli* BL21(DE3), respectively. The transformed cells were cultured on LB plates containing 100 µg/ml of ampicillin and incubated overnight at 37 °C.

Expression and purification of recombinant MxynA and CxynA in *E. coli* BL21 (DE3)

The control and the mutant transformants were cultured in LB-ampicillin (100 µg/ml) medium at 28 °C with vigorous shaking at 200 rpm until the OD_{600} reached 0.6. The expression of the recombinant xylanase was induced with isopropyl β-D-1-thiogalactopyranoside (IPTG, 1 mM) for continuous 12 h cultivation at 28 °C. The bacterial cells were harvested by centrifugation followed by ultrasonication. Then both MxynA and

CxynA were purified using Protino, Ni–TED 1000 kit (Mycherey–Nagel, Germany). Protein concentration of the purified xylanase was measured using the bradford method with bovine serum albumin as standard.

Structural analysis between MxynA and CxynA

Three–dimensional (3–D) structures of the MxynA and CxynA were developed by homology modeling, a computational tool that has been widely applied in the field of structural biology. The three–dimensional structure was generated by SWISS–MODEL protein–modeling server (http://swissmodel.expasy.org/).

Characterization of MxynA and CxynA

Xylanase activity of MxynA and CxynA was assayed with 1 % (w/v) of beechwood xylan at various temperatures ranging from 10 to 100 °C for 15 min. The amount of reducing sugar was determined by the DNS method (**Appendix C**) (Miller, 1959). One unit of enzyme activity was defined as the amount of enzyme that liberated one nanomole of reducing sugar per minute. The optimum pH values of MxynA and CxynA were determined, ranging from pH 2.0 – 11.0 at 50 °C for 15 min.

Enzyme kinetic assays

Kinetic parameters were determined using beechwood xylan as substrates at concentrations in the range of 0.1–10 mg/mL. The reaction mix contained 25 μg/mL of the enzyme, 0.5 mM citrate buffer pH 6.0, and was incubated at 50 °C for 15 min. The amount of reducing sugar released was measured using the DNA method. The K_m, k_{cat}, and k_{cat}/K_m were obtained from Lineweaver–Burk plots (Lineweaver and Burk, 1934).

Hydrolysis of xylanase on lignocellulosic raw materials

Xylanase hydrolysis activities of MxynA and CxynA were investigated using lignocellulosic material, including rice straw, corncob, and para grass. The hydrolysis activities were carried out by incubating each material's purified enzyme in 5% (w/v) at 37°C for seven days. The suspension from the reaction was collected every 24 h to measure the reducing sugar released from each material by the DNS method.

Results

Atmospheric pressure plasma jet induced mutation in bacterial cells

B. subtilis was bombarded under various conditions by the plasma jet, then the survival of each treated bacteria was investigated using a plate count method and compared with the bacterial control. Higher survival inactivation efficiencies were observed in helium plasma treatment at 1– and 2–min treatments. The highest survival inactivation was observed at 5 min treatment with argon plasma (**Figure 20**). The bombarded bacteria were spread on media containing 1% (w/v) beechwood xylan to screen for bacterial mutants. The mutant with the most significant xylanase activity showed the highest H.C. ratio on a plate containing beechwood xylan, observed only under argon plasma bombardment at 1 min (**Figure 21**).

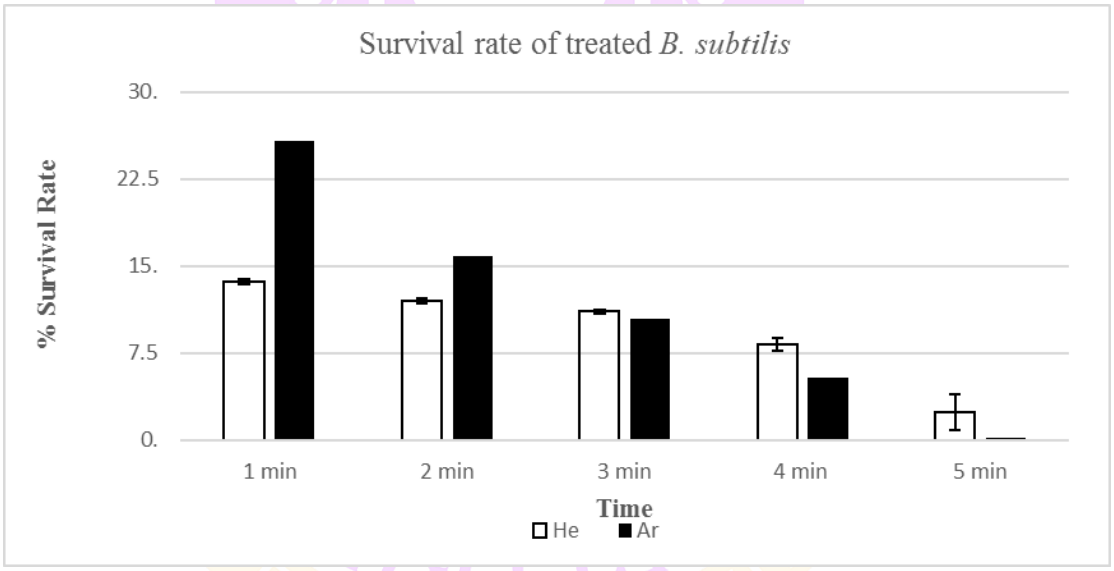

Figure 20 Survival rate comparison of bacteria bombarded by atmospheric pressure plasma jet using helium and argon plasma.

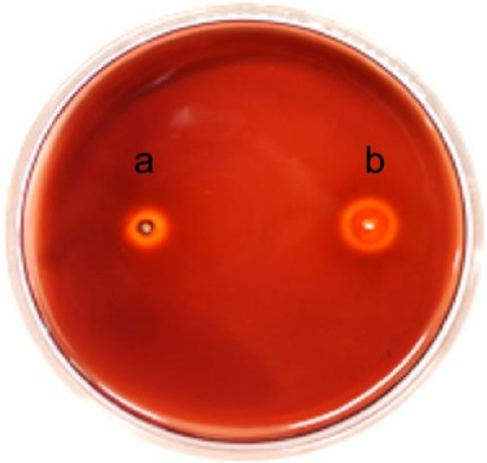

Figure 21 Congo Red staining displayed hydrolysis halo zone of *B. subtilis* (a) control and (b) mutant.

Cloning of the xylanase gene and sequence analysis

The entire CxynA and MxynA were amplified by PCR using the specific primers (as described in materials and methods), subsequently cloned into pTZ57R/vector, and sequenced. Both CxynA and MxynA nucleotide sequences consisted of 642 nucleotides encoding for 213 amino acids. Nucleotide alignment between CxynA and MxynA revealed that five nucleotide substitutions were found in MxynA (data not shown), but only one amino acid residue changed in the MxynA sequence.

The amino acid comparison between CxynA and MxynA showed that these two sequences were almost identical (**Figure 22**), except the threonine residue was substituted into serine residue at position 162 (T162S). Our xylanases belong to the glycosyl hydrolase family 11 (GH11) based on the amino acid sequence homology. Generally, the structure of GH11 xylanases consists of two large β-pleated sheets and a single α-helix that form a structure resembling a partially closed right hand (Törrönen and Rouvinen, 1997). The 3-D structures of MxynA and CxynA were simulated by SWISS-MODEL protein-modeling webserver (http://swissmodel.expasy.org/). The BLAST program performed the template search for homology modeling. From our results, GH11 xylanase from *B. subtilis* with PDB No. 2DCY was chosen as the template for structural analysis. Based on sequence alignment and domain analysis, T162S residue was located at a loop

connecting the β–sheet B7 and A6 exposed to a hydrophilic environment (**Figure 23**). The former β–strand constitutes an active site and carries the conserved residues. For instance, F153 and W157 maintain the substrate during the reaction mechanism (Murakami, et al., 2005).

Figure 22 Sequence comparison of XynA of the wild type (CxynA) and the mutant (MxynA) using the CLUSTAL–W program. The red arrow indicates the mutant residue (T162S).

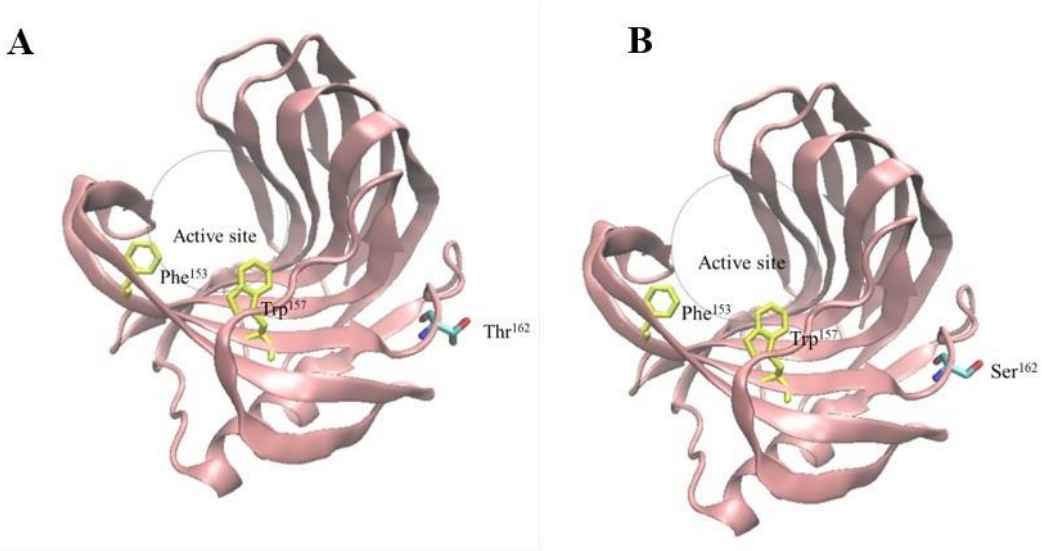

Figure 23 The ribbon representation of the three-dimensional structures of CxynA (A) and MxynA (B) shows the position of the mutation (T162S). In addition, hydrophobic residues located at β-sheet B7 involved in substrate binding are shown as yellow sticks. The model was generated with the SWISS-MODEL server using family 11 xylanase from *Bacillus subtilis* (PDB code: 2DCY).

Characterization comparison between the xylanase enzymes

The effects of pH and temperature on xylanase activity were determined. The purified MxynA and CxynA were incubated with 1% beechwood xylan and a pH ranging from 2.0 to 11.0 at 50 °C for 15 min. The quantity of released reducing sugar was detected and calculated using the DNS method. The catalytic activity of CxynA and MxynA at pH 5.0 were 304.10 IU/mg and 1463.47 IU/mg, respectively (**Figure 24**). Furthermore, both MxynA and CxynA showed their similarity of activities in a wide pH range of 4.0 – 8.0.

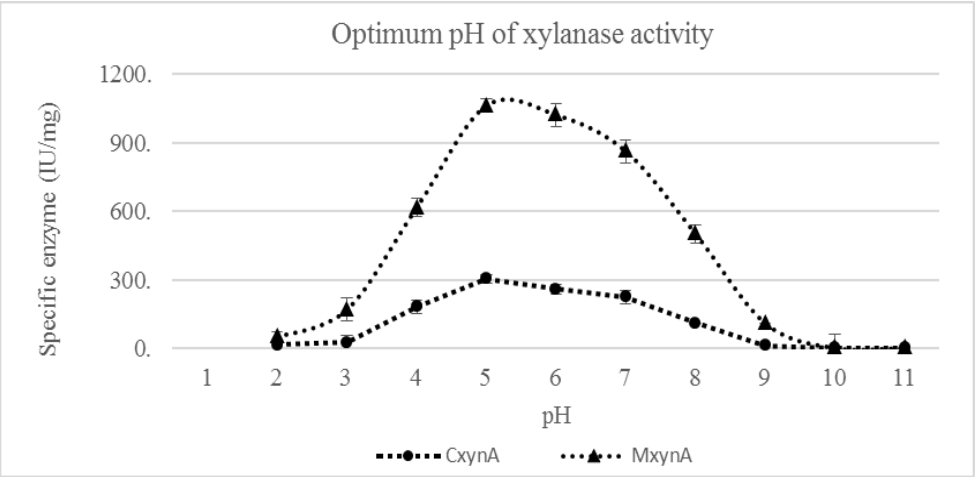

Figure 24 Xylanase activities of MxynA and CxynA at different pH ranging from pH 2.0–11.0 at 50 °C.

For optimal temperature, the catalytic activity of both xylanases was carried at a broad range of temperatures. Both MxynA and CxynA had an optimum temperature of 60˚C. However, the catalytic activity of MxynA was approximately 2–fold that of CxynA over a broad range of temperatures from 10–100 ˚C. Moreover, the catalytic activity of MxynA still retained about 80% activity at 90 ˚C after 15 min of incubation (**Figure 25**).

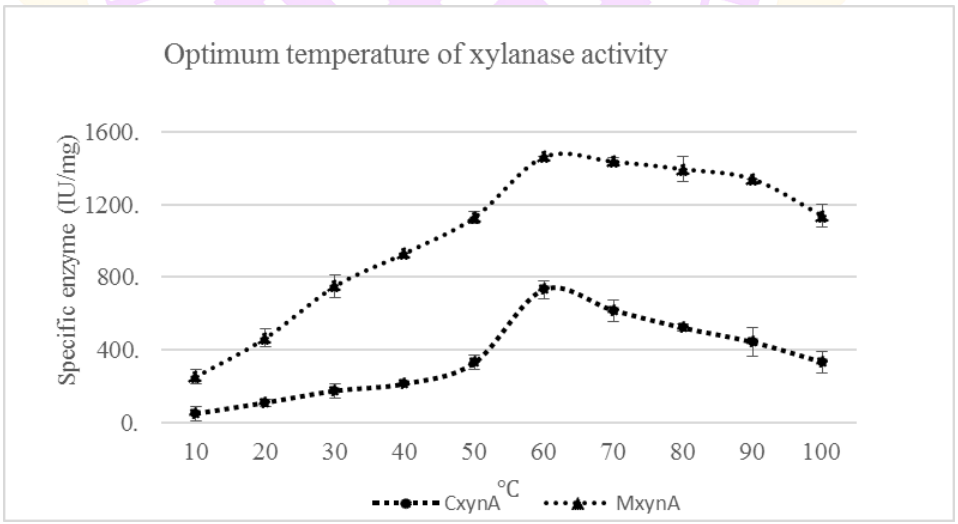

Figure 25 Xylanase activities of MxynA and CxynA at different temperatures ranging from 10–100 °C

The kinetic parameters of the purified enzymes CxynA and MxynA towards xylan were determined to reveal the substitution effects from threonine to serine at position 162 on enzyme activity. As shown in **Table 8**, the K_m value of MxynA was not significantly different from that of CxynA. At the same time, the k_{cat} value and k_{cat}/K_m value of MxynA were approximately 2–fold that of CxynA. These results suggest that mutation leads to a higher turnover number.

Table 8 Kinetic parameters on beechwood xylan of CxynA and MxynA.

Kinetic parameter	**K_m (mg/mL)**	**k_{cat} (sec^{-1})**	**k_{cat}/K_m ($S^{-1}mg^{-1}mL$)**
CxynA[a]	9.11	15.43	1.69
MxynA[a]	10.8	35.19	3.26

Note: [a] Values were the mean of three replicates.

Lignocellulosic biomass hydrolysis by xylanase

Since MxynA exhibited enzyme activity about four times higher than CxynA over a broad range of temperatures and pH, both MxynA and CxynA were applied to hydrolyze lignocellulosic wastes, including rice straw, para grass, and corn cob. The reducing sugars released from each hydrolysis reaction were then measured. Reducing sugars were detected from the first day of incubation, increasing gradually until the end of day 7^{th} (**Figure 26**).

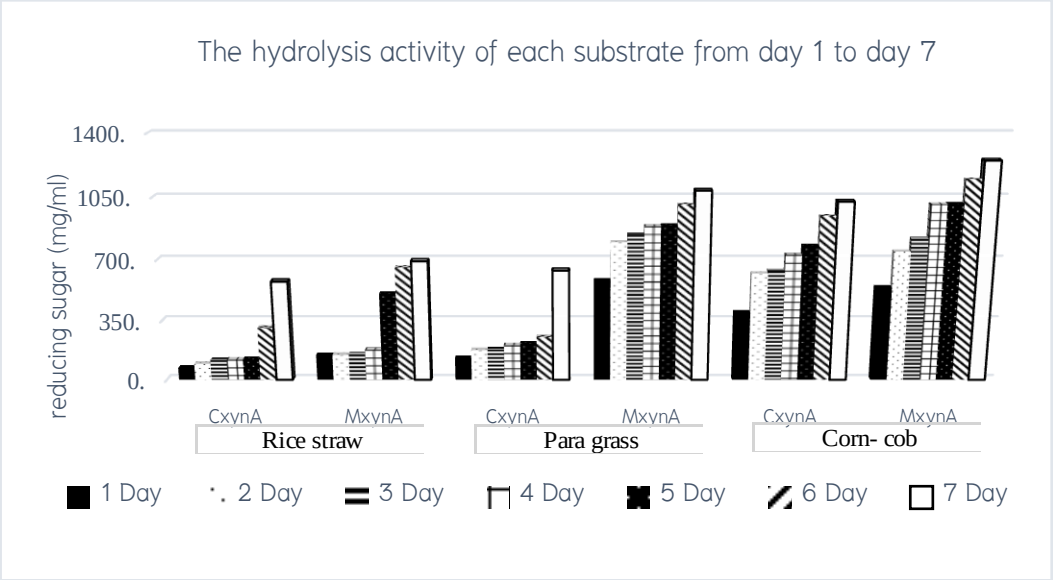

Figure 26 The hydrolysis activity of each substrate from day 1 to day 7

Discussion

The effect of the argon and helium plasma bombardment on *B. subtilis* survival was shown in **Figure 20**. The survival at 1 min of bombardment reveals that helium plasma has a significantly different, greater effect than argon plasma. When exposure times were increased, the effect of argon plasma on survival dramatically decreased while the effect of helium plasma gradually decreased. At 5 min exposure, survival under argon bombardment was barely detected. These results indicate that the longer the exposure to plasma bombardment, the lower the bacterial survival. Previous research has reported argon plasma having a greater effect on inactivating bacterial cells than helium plasma (Chandana, et al., 2018). The different effects on bacteria survival between helium and argon plasma could be due to argon and helium gases physical and chemical characteristics, especially the different ionization energies and molecular weight of ions. The penetration depth of light ions such as helium was higher than that of heavy ions like argon, at low energy levels or shorter exposure times (Cai, et al., 2006) When exposure time was increased, the penetration depth of argon ions into cells was deeper. In addition, heavy ions have higher linear energy transfer (LET) than light ions, which causes a greater relative biological effect (RBE) (Bai, et al., 2016). Heavy ions with a different LET spectrum

killed more cells by inducing DNA double-strand breaks (DSBs) which are more challenging to repair (Aufderheide, et al., 1987; Löbrich, et al., 1994). Therefore, 5 min exposure to argon bombardment led to more cell damage than the light ion, helium.

After plasma bombardment, the mutant, MxynA, with the highest xylanase activity, was screened under argon plasma bombardment. According to the above experimental data, the recombinant MxynA showed a higher xylanase activity, approximately two-fold, under a wide range of temperature conditions. The catalytic activity of MxynA was about 3.5- 3.9-fold higher than that of the control at pH 4 – 6. pH values decreased rapidly during the fermentation process and were usually kept under pH 4-5 (Kim, et al., 2021). Meanwhile, the temperature increased gradually, up to 42˚C (Dai, et al., 2020). Therefore, enzymes that had a high catalytic activity between 40-50˚C were required. Since the xylanase activity of MxynA displayed high hydrolysis characteristics over a wide pH range of 4-8 and a broad temperature range of 20-60 ˚C (**Figure 24** and **Figure 25**), this enzyme is suitable for livestock feed fermentation.

The kinetic parameters analysis of the purified enzymes CxynA and MxynA toward beechwood xylan were determined. It was discovered that mutants had a similar K_m to the control but a significantly increased k_{cat} (**Table 8**). The apparent k_{cat} value and k_{cat}/K_m value of MxynA were 35.19 s^{-1} and 3.26 s^{-1} mg^{-1} ml, respectively, while k_{cat} value and k_{cat}/K_m of CxynA were 15.43 s^{-1} and 1.69 s^{-1} mg^{-1} ml. The higher values of turnover number (k_{cat}) indicated an improved catalytic efficiency. These results suggest that mutation plays a significant role in enzyme action. The homology structure model of MxynA was generated using GH11 xylanase from *B. subtilis* (PDB No. 2DCY) as the template for evaluation serine at position 162 (S162). The structure model reveals that S162 is located on the loop connected to the β-sheet B7 and A6 exposed to a hydrophilic environment (**Figure 23**). To the best of our knowledge, there is no report on the role of an amino acid at this loop in substrate binding and enzyme catalysis. However, we found that the replacement of threonine with serine increased the enzyme's catalytic efficiency (**Table 8**). According to amino acid sequence alignment, shown in **Figure 22**, the amino acid equivalent of S162 can be substituted to threonine, asparagine, and glutamine, which were polar amino acids and usually contribute to the formation of hydrogen bonds with

water molecules (Murakami, et al., 2005). As shown in **Figure 27**, the hydroxyl group of T162 in CxynA and S162 in MxynA were similarly oriented to protein surfaces to form hydrogen bonds with water molecules. However, T162 of CxynA possesses a methyl group with more hydrophobicity, which was also exposed to the protein surface, so it might be less favorable to create an interaction with water than serine MxynA. Therefore, this enhancement of the enzyme catalysis may be explained by the fact that serine substitution conduces more hydrophilic interactions of enzyme and substrate with increased enzyme turnover. Consequently, it might contribute to the enhancement of enzyme catalysis.

Moreover, the substituted position occurred at highly conserved residues QYWSVRXXXR (X corresponds to a non-conserved residue). This phenomenon might indicate that these conserved sequences may play an important role in catalytic activity by supporting or involving the enzyme binding to polymeric xylan. For further characterization, multiple sequence alignment was carried out, and the result informs that our mutation residue belongs to the 'knuckles' of the enzyme, which was reported to be a secondary substrate-binding site (SBS) of *B. circulans* (Cuyvers, et al., 2011)

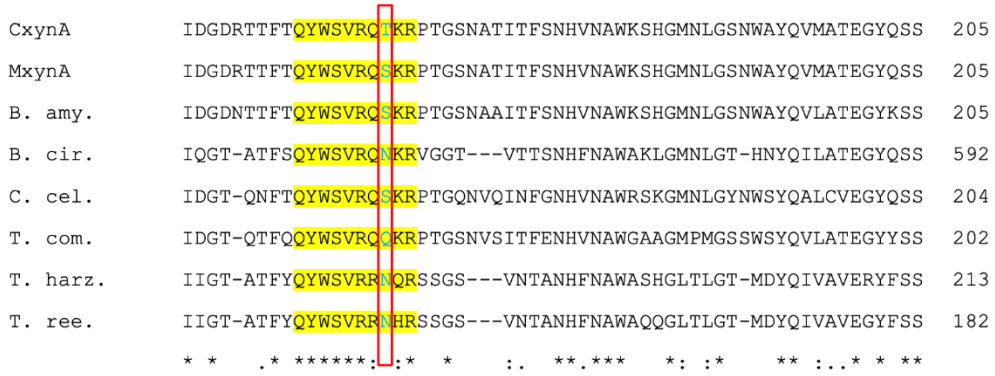

Figure 27 Amino acid sequence alignment of small molecular mass xylanases (generally less than 30 kDa). The sequence alignment is based on structure considerations. The sequences are B. cir = *B. circulans* (accession no.; AYV73613.1); T. com. = *Thermobacillus composti* (accession no.; WP_015253740.1); C. cel. = *Clostridium cellulolyticum* (accession no.; WP_015925319.1); B. amy. = *Bacillus amyloliquefaciens* (accession no.; ADK92885.1); B. kawa. = *Aspergillus kawachii* (accession no.; BAA07264.1); T. harz. = *Trichoderma harzianum* (accession no.; AIK67330.1); T. ree. = *Trichoderma reesei* (accession no.; APU51339.1); The conserved residue QYWSVRXXXR were indicated by yellow highlighting. Residues variable within polar amino acid group are displayed as blue letters on a red box.

For lignocellulosic waste hydrolysis, three kinds of biomass were used as substrates. The highest reducing sugar was liberated from para grass after seven days (62.54 mg/g substrate) of incubation with xylanase produced from MxynA. According to the composition of lignocellulosic biomass, which contains 25–35% of hemicellulose, the reducing sugar released during our experiment can be calculated as 10–25 % of total hemicellulose in each lignocellulosic substrate. This result indicates that the mutant xylanase can be used to hydrolyze these lignocellulosic wastes without a pretreatment process. Therefore, lignocellulosic wastes could be used for cattle feed, particularly corncob and para grass, using MxynA.

Additionally, cattle feed from fermented corncob with the mutant xylanase had been primarily given to dairy cows in Phayao province (unpublished data). These results suggest that the atmospheric pressure plasma jet is a reliable tool for inducing bacteria to increase enzyme activity for animal feed production. These can reduce animal feed costs and air pollution from the burning of lignocellulosic waste.

Conclusion

B. subtilis was bombarded by argon plasma to enhance its xylanase activity. It was found that the bacterial mutant which exhibited the highest xylanase activity was obtained with a 1 min bombardment duration. The mutant named MxynA showed a single amino acid residue substitution from threonine to serine (T162S) at the beta-sheet linker and very close to the C terminal. The recombinant MxynA showed higher catalytic efficiency, approximately 4-fold than the control under a broad range of pH and temperatures. In addition, xylanase's hydrolysis ability on agricultural wastes such as rice straw, corncob, and para grass were also demonstrated, and para grass released the highest amount of reducing sugar. To the best of our knowledge, improving the hydrolysis characteristics of xylanase by plasma mutation at the beta-sheet linker region leading to an increase of enzyme turnover (k_{cat}) had rarely been reported.

CHAPTER V

Feed production

Literature Review

Dairy cattle

The Holstein Friesian cattle known by a different name in Thailand, were the most popular breed. In the United Kingdom, it was known as Friesland. This was known in Denmark as “Black and White Friesland” or “Dutch Friesland”. Israel, sometimes known as Israel Friesland, was one milk cattle breed characterized by a marked contradiction between black and white. A fully developed bull weighs between 800 and 1,000 kg. The female develops faster than the male and weighs around 600–700 kg. Cattles mature sexually at the age of 6–7 years, or approximately 18 months after reproduction, and give birth at the age of 28–30 months. High requirement, around 5,000 kg per year, with 3.5% milk fat (Espe, et al., 1932).

The amount of space required for dairy cattle varies depending on the type of housing, mature body weight, and feed management. Maximize space within a particular range while designing a lot or barn. Calculate the space requirements for animal pens and bunks, making sure to leave enough area for growth without compromising cattle condition or performance. The pen size for cattle was determined based on the work of (Ramos and Barbosa, 2016). The house was east or west. The area covered by the roof should reach as far inside the house as possible. For cattle weighing approximately 300–500 kg, a pen measuring 122 x 175 cm should be used for milking and concentrated feed. The house had a one–story gable roof with excellent drainage and ventilation. The amount of time cattle spend resting was influenced by a variety of factors, including the bedding available. Because straw was soft and provides thermal insulation, it was widely used as bedding; however mastitis–causing bacteria had grown in straw and sawdust, leading to an increase in the use of sand in free–stall housing (Bickert, et al., 2000).

Cattles were milked twice a day in the early morning and late afternoon. Milk obtained in the morning was substantially lower in fat (e.g., 3% fat) than milk collected in

the afternoon (e.g., 5%). The milking procedure had a significant effect on the quality and safety of raw milk and milk products. The primary sources of microbial contamination were the mammary gland, the outside of the udder and teats, and milking equipment. Steps of milking process were as follows:

1. The animals should be evaluated before milking, and the milk from each teat should be tested for visible defects. Diseased animals (such as those with clinical mastitis) should be separated or milked last, or milked using different milking equipment or by hand, and should not be consumed by humans.

2. Always wipe the udder and teats with potable water and one disposable towel per cow.

3. The initial amount of milk from each teat should be discarded into specialized containers and not consumed by humans.

4. To avoid teat infection, the udder should be cleaned again after milking and preferably disinfected with a teat dip. Precautions should also be taken throughout the process to avoid infection.

5. To significantly increase the bacteria populations per milliliter of milk passing through it, milking equipment, utensils, and storage containers must be severely contaminated. However, it must be carefully cleaned and disinfected both before and after usage (Lal, 2020).

6. After milking, clean the equipment with warm water (between 38 – 55°C) and detergent to remove minerals, fat, and protein from the milk (Reinemann, et al., 2000).

Today, the cattle industry was quickly expanding to satisfy increasing consumer demand. Cattle, buffalo, pigs, poultry, milk, and other meat consumption had increased every year (Lal, 2020). According to a Department of Livestock Development data, there were 1,774 dairy farmers in the northern region in 2016, with that number increasing to 1,865 in 2017. Furthermore, the number of dairy cattle increased by 14.06% in 2017. In the province of Phayao Thailand, these were 16 dairy farmers, ranking the province 40th in the country (Information and Statistical Data Group, 2017).

Cattle feed

Roughage, such as grass, legumes, and straw, was the cattle's primary source of nutrition. Roughage can be fed fresh as pasture or in a cut–and–carry system, or it can be stored as hay or silage. Roughage was frequently supplemented with cereals, concentrates, and agricultural byproducts such as oil–seed cakes, sugar cane tops, and so on. Roughage should be the basis of the feed ration and should contribute to fulfilling (at least) the entire maintenance requirements. Grains and concentrates should only be offered to fulfill extra requirements like growth, pregnancy, and milk production. A high intake of non–fibrous feed will affect the rumen ecology.

The protein and sugar (energy) content of the grass were high during the beginning of the growing season, while the lignin level was low. The protein and sugar content of the cell walls decreases as they mature, and the cell walls become lignified. As a result, it was critical to collect roughage at the ideal time and store it for use during dry seasons. Fresh grass, maize, straw, and agricultural waste such as sugarcane shoots, banana trees, cassava leaves, and water hyacinths were all used in rough feeding. As a result, concentrated feed must be added to rough feed in Thailand.

The term "concentrate" refers to a small amount of dry feed containing many nutrients. Animals received energy from the concentrated feed, which contains protein, carbohydrates, vitamins, and minerals. It was a diet that was low in fiber. Bean meal, rice bran, and concentrated by the company had a high nutritional value (Voigt, et al., 1978).

Fermented feed

Fermented feed was one term used to describe a variety of forage plants which were stored in anaerobic conditions, away from outside air, until fermentation developed. Fermented feed helps these plants maintain their nutritional content and can be stored during periods when fresh harvests were unavailable. During the rainy season, the forage crops required for fermentation were harvested from a variety of forage crops, and their growth were adequate to feed the animals. Furthermore, fermented feed generated from agricultural waste was high in nutrients. To increase nutritional value, microbes such as cellulolytic bacteria or yeast can be applied.

The preserving of animal feed in an anaerobic condition for the fermentation process was known as fermented feed. Fermented feed had the advantage of preserving raw material nutritional content. It can also be kept for a long time, although fermented feed had disadvantages: it lost some minerals, such as vitamin D, and it quickly degrades if exposed to air. As a result, professional expertise in practice was required (Dai, et al., 2020). Bacteria break down cellulose and xylan to generate water-soluble carbohydrates in the fermentation process.

Lactic acid bacteria convert it to lactate by maintaining a low pH (4.0), which inhibits the growth of anaerobic and aerobic pathogens, thereby preserving the fermented feed's quality (Kim, et al., 2021). *Bacillus amyloliquefaciens* (Ye, et al., 2017), *Bacillus macernas* SM (Ali, 2003) and *Bacillus megaterium* MYB3 (Bai, et al., 2017) were the most common bacteria found in fermented feed. Also used for fermented feed were *Lactobacillus plantarum*, *Lactobacillus casei* (Li, et al., 2016), and *Enterococcus faecium* NCIMB 11181 (Jatkauskas, et al., 2013).

Research Methodology

Comparison of small-scale and large-scale fermentation of feed by mutant bacteria

A mill would be used to chop agricultural wastes such as durian peels, corncobs, pineapple peels, and pineapple cork to a size of 3-5 cm. Fermentation by three microorganisms; *Bacillus amyloliquefaciens*, *B. subtilis*, and *Enterococcus faecium* was fermented in a tank compared to the uninoculated control. After one month of fermentation, the protein content and pH values were measured. The following was the compositions (**Table 9**)

Table 9 The composition of fermented feed for small–scale and large–scale fermentation

Material	Small–scale	Large–scale
1.Agricultural wastes: durian peels, corncobs, pineapple peels, pineapple cork	1.5 kg	150 kg
2.Mutant microorganisms	45 ml	4.5 L
3.Molasses	15 ml	1.5 L
4.Water	1.4 L	140 L

Note: Compared with the fermented feed in the uninoculated control.

Animals and experimental design

This research utilized four healthy, vaccinated, 87.5 % multiparous Holstein Friesian lactating dairy cattle in mid–lactation. All the cattle were 4–6 years old and weighed an average of 416.03 ± 34.66 kg. Before the data was collected, all cattle were randomly divided into 2 groups: treatments and allowed 3 weeks to adjust. Cattles were housed in individual pens and fed roughage ad libitum. Cattle in Treatment 1 received fresh grass + concentrated feed (C) as a control, while cattle in Treatment 2 received fresh grass + concentrated feed 50% + fermented feed from agricultural wastes 50% (C+F). The feed consumed by all dairy cattle in each group was determined using the nutrient requirements for maintenance and production (Council, 2001), with feeding twice daily at 7:00 a.m. and 3:00 p.m. before milking. All animals had access to fresh, clean water and a mineral block always.

Sampling and analysis

All samples were collected weekly for 7,14 ,21, and 28 days. The samples were analyzed for dry matter (DM) and crude protein (CP) using the proximate standard (A.O.A.C., 1990; Lynch and Barbano, 1999). In addition, the pH value was determined using (Bernardes, et al., 2019) and the lactic acid content was determined using (Borshchevskaya, et al., 2016). At every milking time, the milk production of individual cattle was measured on a daily. A lactoscan was used to analyze fat, protein, lactose, and solids–not–fat (SNF) in milk weekly (up to a month) using a mixed sample containing 15 ml

of morning milk and 15 ml of afternoon milk. According to (Harding, 1995), the SNF content was determined. The fat collected milk (FCM) of 4 % was calculated using the method described by (Walker, et al., 2001).

Analytical statistics

All the data were analyzed for variance (analysis of variance, ANOVA) and compared for differences. Between the mean of each trial using Duncan's New Multiple Range Test (DMRT) (Steel and Torrie, 1980) at a 95% confidence level.

Results

Comparison of small-scale and large-scale fermentation of feed by mutant bacteria

There was no significant difference between small-scale and large-scale fermentation. **Figure 28** reveals that corncobs had the highest protein content after 7 days, compared to about 10% uninoculated, while other agricultural wastes had 8–9% protein content. **Figure 29** indicated that the average pH of fermented feed was increased by 20–40% as compared to uninoculated agricultural waste. The pH ranged from 3.5 to 5.0, with the uninoculated pineapple peel maintaining a consistent pH of 3.8 and the inoculated pineapple peel maintaining a constant pH of 3.6. Furthermore, the concentration of lactic acid increases in the reverse at different pH levels. In this case, the lactic acid concentration was high while the pH was low. Furthermore, after 35 days, each agricultural waste had a high lactic acid level of roughly 6 g/L (**Figure 30**).

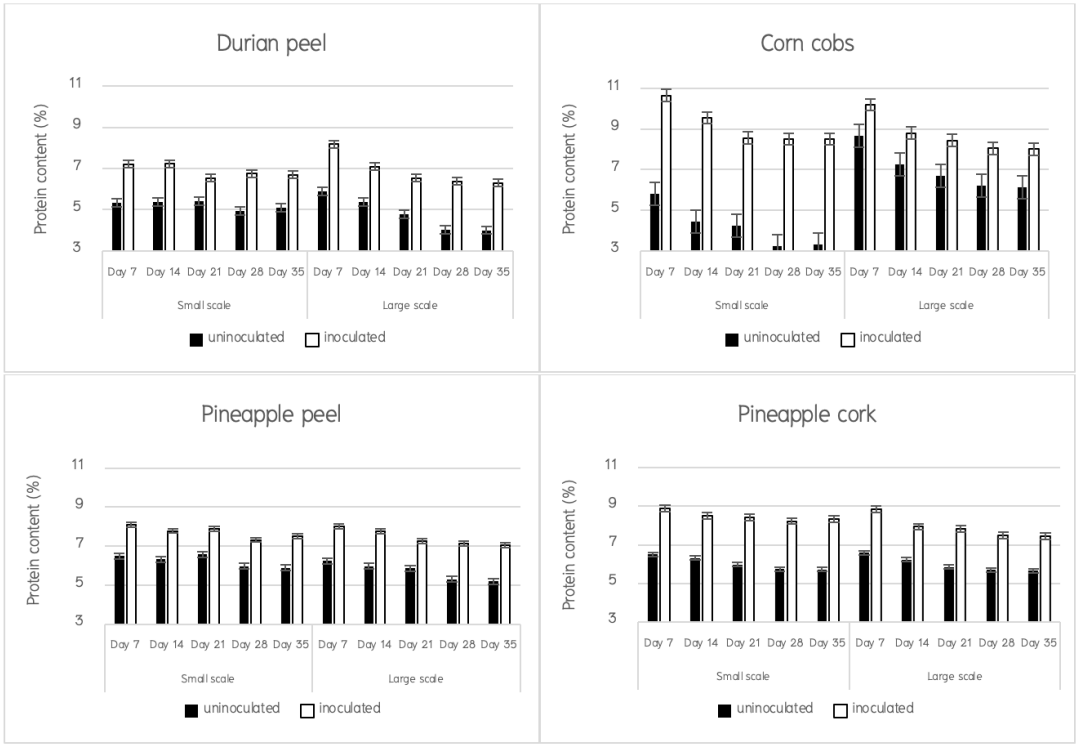

Figure 28 The protein content of agricultural waste was fermented for one month

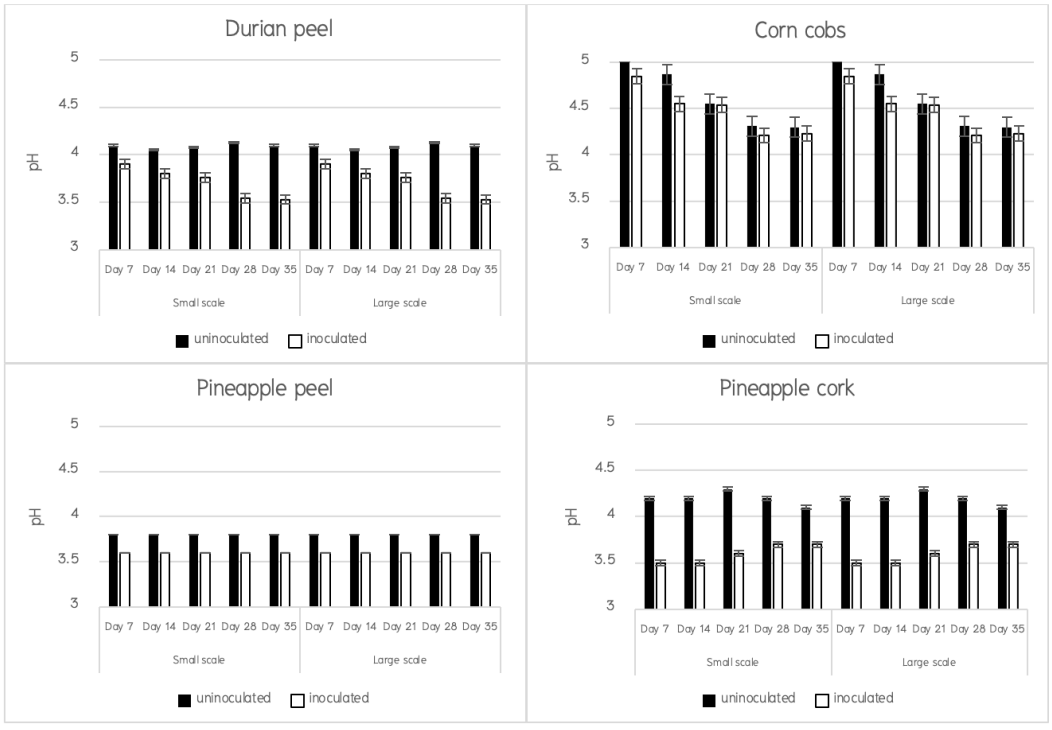

Figure 29 The pH value of agricultural waste was fermented for one month

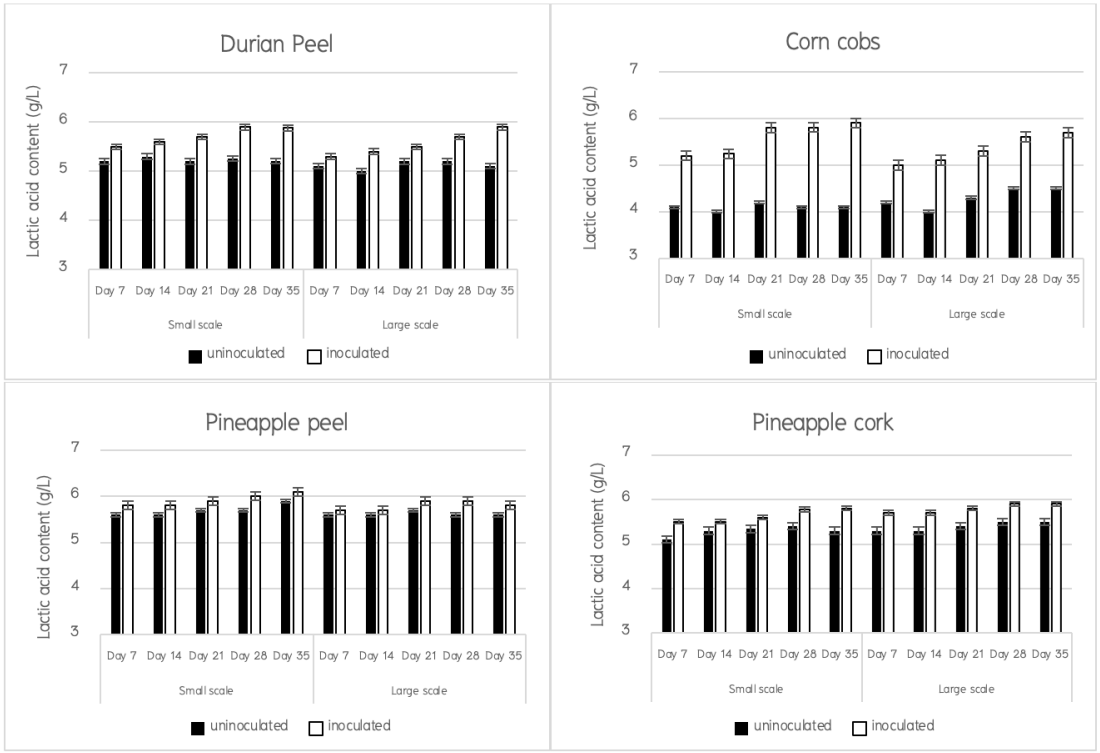

Figure 30 The lactic acid content of agricultural waste was fermented for one month

The fermentation quality of feed

According to this research, corncobs had a significant protein content. In addition, corncobs were abundant in Phayao. Corncobs were used in the dairy cattle experiment, consequently. Corncobs were fermented using mutant bacteria to compare protein content to the concentrated feed produced by the company. The protein content of the corncobs in the fermenter (150-liter) was determined. The protein content of corncobs fermented with corn dust was tested for seven days in a 150-liter fermenter and found to be 11.75 %. Corncobs fermented with corn dust and combined 50:50 with concentrated feed (used as cattle feed in the experiment) had a protein level of 15.75 % as concentrated feed, as shown in **Table 10**.

Table 10 The protein content in the feed.

Feed	Protein content (%)
1.Fermented corncobs mixed with mutant microorganisms	10.65%
2.Fermented corncobs mixed with mutant microorganisms, mixed corn dust	11.75%
3.Fermented corncobs mixed with corn dust, mixed with concentrated feed (ratio 50:50)	15.75%
4.Concentrated feed from the company	16%

Production and composition of milk

Cattle in formula 2 (C+F) had the same milk content as cattle in the control group in dairy cattle (C). **Figure 31** revealed that there was no significant difference between the dairy cattle in the control group ($P<0.05$).

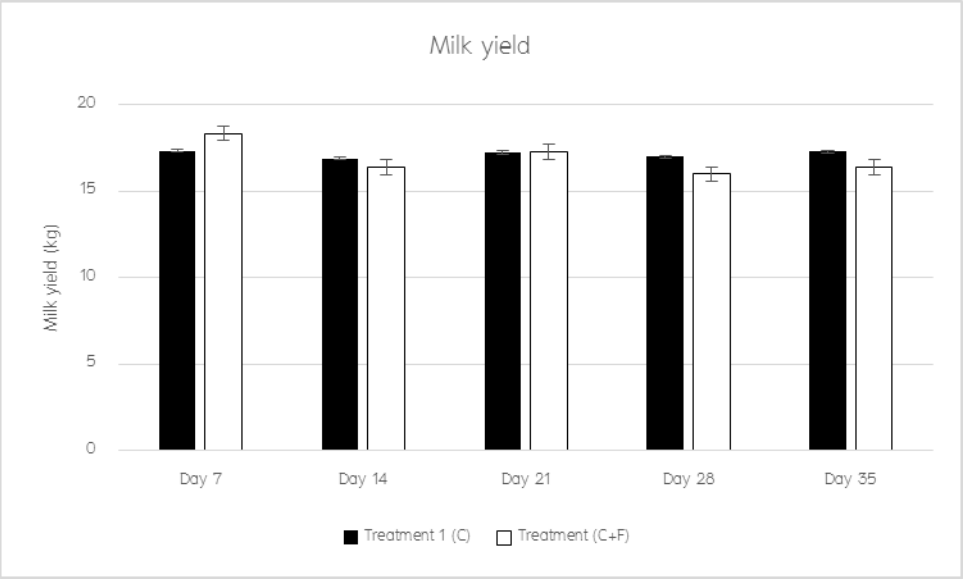

Figure 31 The amount of dairy milk on a weekly basis.

In addition, the fat, protein, lactose, and ash content of milk were investigated. The milk composition of formula 2 (C+F) was not significantly different from the control ($P<0.05$). Protein and fat content were 3.3% and 4.2%, respectively. The average lactose and ash content of milk were 4.9% and 12.75%, respectively, as shown in **Figure 32**.

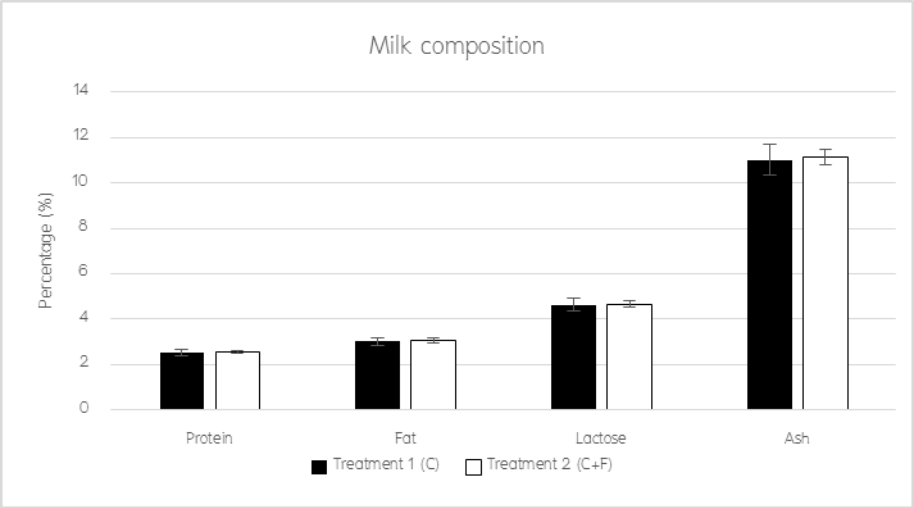

Figure 32 The average milk composition over a one-month period

The cost of dairy cattle feed was also described in **Table 11**. By dividing the quantity of concentrated feed (C) and the amount of fermented feed (C+F), the volume of feed was calculated. The cost of concentrated feed (C) was 7.2 baht/kg, according to the data. Treatment 2 (C+F), on the other hand, had the cost 4.5 baht/kg. Therefore, the cost of concentrated feed can be reduced by 40%. All 1 % molasses, mutant microorganisms, transportation, and concentrated additives in the formula were factored into the cost of fermented feed.

Table 11 The cost of feeding dairy cattle

Ingredient	Amount (Kg)		Cost (Baht)	
	Formula 1	Formula 2	Formula 1	Formula 2
Fresh grass (Napier grass)	225	225	450	450
Corn cobs		36.75		36.75
Molasses		0.375		3.75
Corn dust		37.5		75
Concentrated feed (Company)	150	75	2,250	1,125
Bacterial mutant		0.375		0.375
Total	375	375	2,700	1,690.88
per Kg	1	1	7.2	4.5

Note: The costs shown in the table were the prices during the trial period, which ended in December 2017.

Furthermore, cattle feces from this research were excessively liquid and odorous before consuming corncobs fermented feed, which might be due to overfeeding and low-quality feed, negatively impacting the cattle's health. When feed corncob fermented feed containing mutant bacteria, however, cattle feces appear lumpier, not filthy, and has a little odor, as seen in **Figure 33**.

(1) (2)

Figure 33 Cattle feces before to the use of fermented feed (1), Cattle feces immediately after the use of fermented feed (2).

Dissemination activities

Farmers typically discarded agricultural waste. Instead of being disposed of by burning, it may be utilized as animal feed, saving money. Agriculture waste had two drawbacks: it was unstable and had a low value. As a result, the fermentation process was necessary. For the fermentation process, knowledge and experience were required. The utilization of naturally occurring mutant microorganisms that take a long time to ferment. As a result, the goal of this research used to utilize what was learned and spread it to farmers. Starting with the growth of microorganisms and proceeding through the storage, fermentation, and usage of animal feed.

Discussion

According to the data, the feed without corn dust supplementation had the highest protein content of 10.65 %, whereas the feed with corn dust had the highest protein content of 11.75 %. As a consequence, corn dust supplementation was observed to increase protein content, and was comparable to a research (Jala and Srichana, 2011) that found that using corn dust as an additive in silage corn increased protein content. The silage containing 10% corn dust had a protein content of 9.32%. Corn silage treated with 0%,2.5%, and 5% corn dust had protein level of 8.60 – 8.88%. In addition, (Thavorn, et

al., 2017) investigated at the use of Thai sweet, fermented rice balls to make corn husk for fermented feed in beef cattle.

According to the research, the corn husk had a protein content of 1.81% of dry matter. As a result, the protein content of the fermented corn husk increased by twice to 6.85%. The corn husk had been fermented with molasses, which costs about 1.4 baht per kilogram. Corn dust, the residue, had 89.52% dry matter, 7.08% protein, 2.18% fat, 17.04% fiber, 3.93% ash, and 66.77% digestible carbohydrates (Department of Livestock, 2001). It was also determined that adding 5–10% corn dust to corn silage produced the highest quality corn silage in terms of dry matter and protein content (Jala and Srichana, 2011).

The protein content of corncob fermented feed was determined using the Kjeldahl technique (Lynch and Barbano, 1999), and the protein content was determined to be 15.75%, and was comparable with (Wachirapakorn, et al., 2014). Therefore, the researchers examined the effects of concentrated feed protein content, as well as the use of corncobs and rice straw as roughages, on cattle digestibility and milk production. The roughages were prepared in a 1:1 ratio from rice straw and corn cobs, with protein levels of 12%, 14%, 16%, and 18%, respectively. As a result, dairy cattle's protein level was sufficient at 14–16%, at milk production of 11–13 kg/day. Furthermore, after 30 days of feeding, the average milk yield was 16.89 ± 2.69 kg, with a fat content of 3.06 ± 0.27%, a protein content of 2.56 ± 0.14%, a lactose content of 4.67 ± 0.22%, and an ash content of 11.14 ± 0.45%.

Similarly, the researchers examined the effect of concentrated feed on different protein levels. As a result, dairy cattle's protein levels were adequate at 14.1%, and milk production of 26–28 kg/day. Furthermore, the milk composition was 4.18% fat, 3.64% protein, 4.5% lactose, and 12.9% ash, which was similar to this study (Wachirapakorn, et al., 2014). Cornmeal (100%) was also used as a dairy cattle feed, with a protein content of 13.2%, which was sufficient for dairy cattle producing 13.2 kg of milk per day. In addition, the milk had 4.1% fat, 3.4% protein, 4.6% lactose, and 12.9% ash (Ferraretto and Shaver, 2012). Furthermore, even though use of corn silage increased protein content by 16.7%, the milk composition remained unchanged at 3.58% fat and 3.05% protein. As

a result, milk composition was unaffected by protein quantity, although cattle digestibility increased. The protein content of palm pulp in concentrated feed formulation was 16–18%, according to (Lunsin, 2018). Consequently, they had no obvious effect on the composition of milk. The large number of microbes used for fermentation, resulted in a considerable increase in milk yield. Similarly, yeast (*Saccharomyces cerevisiae*) included a significant number of enzymes, according to (Denev, et al., 2007). It assisted in the complementation of enzymes already present in the digestive tract, resulting in improved digestibility. The supplement enzymes increase feed intake, resulting in increased weight and yield in cattle (Chung, et al., 2012).

Additionally, before and after the feeding of fermented feed, cattle feces were examined. The only concentrated feed produced was liquid and odorous cattle feces. The cattle were also fed highly concentrated feed, which influenced the digestive tract (Hubbard and Lowrance, 1998). The concentrated feed was also low in fiber, rich in nutrients, and easy to digest. On the other hand, the dairy was given at a high concentration, which had an effect on the digestive system, reducing the capacity to chew the cud, decreasing dry matter digestion, and causing hoof difficulties (Li, et al., 2012). After feeding, the cattle feces were lumpier, cleaner, and had a slight odor. Fermented feed was thought to include mutant bacteria and were beneficial to animal health. Health and disease resistance had improved. In a similar study, yeast fermented cassava pulp was utilized to partially replace soybean meal in concentrated feed. The results showed that native beef had better rumen efficiency and growth rate, as well as an improved immune system (Khampa, et al., 2010).

Conclusion

Because the production cost was low, cheap, and simple, the bacterial mutant for agricultural applications can be considered for supplementation. The efficiency of the bacteria might also increase the quality of cattle feed, resulting in a higher-grade fermented feed. The bacteria-fermented cattle feed provided normal cattle growth while reducing farmer costs by up to 40%, reducing production costs for dairy and beef cattle,

and reducing burning by using agricultural waste to generate fermented feed. It also reduced smoke dust pollution from PM 2.5.

BIBLIOGRAPHY

A.O.A.C. (1990). **Official Methods of Analysis** (15 ed.). Washington, D.C.: Association of Official Analytical Chemist.

Ajila, C. M., et al. (2012). Bio-processing of agro-byproducts to animal feed. **Critical Reviews in Biotechnology**, 32(4), 382-400.

Ali, S. G. (2003). Biotechnological application of alkaline cellulase in food technology. **Media used: Bacterium used: Methods**, 6(2), 117-124.

Altintas, M., Ulgen, K., Kirdar, B., Önsan, Z., andOliver, S. (2002). Improvement of ethanol production from starch by recombinant yeast through manipulation of environmental factors. **Enzyme and Microbial Technology**, 31, 640-647.

Amaral, D. M. F., Silva, L. F., Casarotti, S. N., Nascimento, L. C. S., andPenna, A. L. B. (2017). *Enterococcus faecium* and *Enterococcus durans* isolated from cheese: Survival in the presence of medications under simulated gastrointestinal conditions and adhesion properties. **Journal of Dairy Science**, 100(2), 933-949.

American Public Health Association. (2015). **Compendium for the Microbiological Examination of Foods**. Washington, DC: American Public Health.

Amore, A., et al. (2015). Application of a new xylanase activity from *Bacillus amyloliquefaciens* XR44A in Brewer's Spent Grain saccharification. **Journal of Chemical Technology and Biotechnology**, 90.

Anuntalabhochai, S., Chundet, R., Chiangda, J., andApavatjrut, P. (2000). Genetic diversity within Lychee (*litchi chinensis* Sonn.) based on RAPD analysis. **International Society for Horticultural Science**, 5751.

Aufderheide, E., Rink, H., Hieber, L., andKraft, G. (1987). Heavy ion effects on cellular DNA: strand break induction and repair in cultured diploid lens epithelial cells. **International Journal of Radiation Biology and Related Studies in Physics, Chemistry and Medicine**, 51(5), 779–790.

Axelsson, L. (2004). **Lactic Acid Bacteria: Classification and Physiology** (Vol. 3). Marcel Dekker, New York: CRC Press.

Badino, S., et al. (2017). Exo–exo synergy between Cel6A and Cel7A from *Hypocrea jecorina*: Role of carbohydrate binding module and the endo–lytic character of the enzymes. **Biotechnology and Bioengineering**, 114.

Bai, B., Yan, C., andLi, G. (2017). Study on the characteristics of straw fermentation by *Bacillus megaterium* MYB3. **IOP Conference Series: Earth and Environmental Science**, 8, 1–7.

Bai, W., Cao, Y., Liu, J., Wang, Q., andJia, Z. (2016). Improvement of alkalophilicity of an alkaline xylanase Xyn11A–LC from *Bacillus* sp. SN5 by random mutation and Glu135 saturation mutagenesis. **BMC biotechnology**, 16(1), 77–77.

Balakrishnan, H., Dutta–Choudhury, M., Srinivasan, M., andRele, M. (1992). Cellulase–free xylanase production from an alkalophilic *Bacillus* species. **World Journal of Microbiology and Biotechnology**, 8, 627–631.

Bastawde, K. B. (1992). Xylan structure, microbial xylanases, and their mode of action. **World Journal of Microbiology and Biotechnology**, 8(4), 353–368.

Bayer, E. A., Belaich, J.–P., Shoham, Y., andLamed, R. (2004). The cellulosomes: multienzyme machines for degradation of plant cell wall polysaccharides. **Annual Review of Microbiology**, 58(1), 521–554.

Bayer, E. A., Chanzy, H., Lamed, R., andShoham, Y. (1998). Cellulose, cellulases and cellulosomes. **Current Opinion in Structural Biology**, 8(5), 548–557.

Beg, Q., Kapoor, M., Mahajan, L., andHoondal, G. S. (2001). Microbial xylanases and their industrial applications: A review. **Applied microbiology and biotechnology**, 56, 326–338.

Benson, D. A., et al. (2013). GenBank. **Nucleic acids research**, 41(Database issue), D36–D42.

Berger, S., Sinha, A. K., andRoitsch, T. (2007). Plant physiology meets phytopathology: plant primary metabolism and plant–pathogen interactions. **Journal of Experimental Botany**, 58(15–16), 4019–4026.

Bernardes, T. F., Gervásio, J. R. S., De Morais, G., andCasagrande, D. R. (2019). Technical note: A comparison of methods to determine pH in silages. **Journal of Dairy Science**, 102(10), 9039–9042.

Bickert, W. G., et al. (2000). **Dairy freestall housing and equipment** (7 ed.): Iowa State

University.

Bintsis, T. (2018). Lactic acid bacteria: their applications in foods. **Journal of Bacteriology and Mycology: Open Access**, 6.

Borshchevskaya, L. N., Gordeeva, T. L., Kalinina, A. N., andSineokii, S. P. (2016). Spectrophotometric determination of lactic acid. **Journal of Analytical Chemistry**, 71(8), 755–758.

Bureenok, S., Suksombat, W., andKawamoto, Y. (2011). Effects of the fermented juice of epiphytic lactic acid bacteria (FJLB) and molasses on digestibility and rumen fermentation characteristics of ruzigrass (*Brachiaria ruziziensis*) silages. **Livestock Science** 138, 266–271.

Burgé, G., et al. (2015). Relationships between the use of Embden Meyerhof pathway (EMP) or Phosphoketolase pathway (PKP) and lactate production capabilities of diverse *Lactobacillus reuteri* strains. **Journal of Microbiology**, 53(10), 702–710.

Café, M., Borges, C. A., Fritts, C. A., andWaldroup, P. (2002). Avizyme improves performance of broilers fed corn–soybean meal–based diets1. **The Journal of Applied Poultry Research**, 11(1), 29–33.

Cai, Q., Ledden, B., Krueger, E., Golovchenko, J. A., andLi, J. (2006). Nanopore sculpting with noble gas ions. **Journal of Applied Physics**, 100(2), 24914–249146.

Chalantom, V., Mathana, S., andPongtep, W. (2008). The use of selected lactic acid bacteria isolates for acceleration of fermented fish (Pla–ra) process. **Journal of Fisheries**

and Environment, 32(3), 17–25.

Chandana, L., Sangeetha, C. J., Shashidhar, T., andSubrahmanyam, C. (2018). Non–thermal atmospheric pressure plasma jet for the bacterial inactivation in an aqueous medium. **Science of The Total Environment**, 640–641, 493–500.

Chen, Y. S., Yanagida, F., andShinohara, T. (2005). Isolation and identification of lactic acid bacteria from soil using an enrichment procedure. **Letters in Applied Microbiology**, 40, 195–200.

Cheng, K.–K., et al. (2008). Sugarcane bagasse mild alkaline/oxidative pretreatment for ethanol production by alkaline recycle process. **Applied Biochemistry and Biotechnology**, 151, 43–50.

Chung, Y. H., et al. (2012). A fibrolytic enzyme additive for lactating Holstein cow diets: Ruminal fermentation, rumen microbial populations, and enteric methane emissions. **Journal of Dairy Science**, 95, 1419–1427.

Connell 'O, D., et al. (2011). Cold atmospheric pressure plasma jet interactions with plasmid DNA. **Applied Physics Letters**, 98(4).

Contreras, F., et al. (2020). Engineering robust cellulases for tailored lignocellulosic degradation cocktails. **International Journal of Molecular Sciences**, 21(5), 1589.

Council, N. R. (2001). **Nutrient requirements of dairy cattle**. Washington, DC: The National Academies Press.

Cuyvers, S., et al. (2011). Secondary substrate binding strongly affects activity and binding affinity of *Bacillus subtilis* and *Aspergillus niger* GH11 xylanases. **The FEBS Journal**, 278(7), 1098–1111.

Dai, Z., et al. (2020). Fermentation techniques in feed production. In **Animal Agricultural** (pp. 407–429).

Denev, S. A., et al. (2007). Yeast cultures in ruminant nutrition. **Bulgarian Journal of Agricultural Science**, 13, 357–374.

Department of Livestock. (2001). **Instruction sheet for silage** (Vol. 1). Nonthaburi: The Agricultural Cooperative Federation of Thailand.

Dhiman, S., Sharma, J., andBindu, B. (2008). Industrial applications and future prospects of microbial xylanases: A review. **BioResources**, 3(4), 1377–1402.

Doi, R. (2008). Cellulases of mesophilic microorganisms: cellulosome and noncellulosome producers. **Annals of the New York Academy of Sciences**, 1125, 267–279.

Doi, R., andKosugi, A. (2004). Cellulosomes: Plant–cell–wall–degrading enzyme complexes. **Nature Reviews Microbiology**, 2, 541–551.

Doi, R., Kosugi, A., Murashima, K., Tamaru, Y., andHan, S. (2003). Cellulosomes from mesophilic bacteria. **Journal of Bacteriology**, 185, 5907–5914.

Doi, R., andTamaru, Y. (2001). The *Clostridium cellulovorans* cellulosome: An enzyme

complex with plant cell wall degrading activity. **The Chemical Record** 1(1), 24–32.

Doi, R. H., et al. (1998). Cellulosome and noncellulosomal cellulases of *Clostridium cellulovorans*. **Extremophiles**, 2(2), 53–60.

Duan, P., et al. (2021). Xylan structure and dynamics in native brachypodium grass cell walls investigated by solid–state NMR spectroscopy. **ACS Omega**, 6(23), 15460–15471.

Dunière, L., Gleizal, A., Chaucheyras–Durand, F., Chevallier, I., andSergentet, D. (2011). Fate of *Escherichia coli* O26 in corn silage experimentally contaminated at ensiling, at silo opening, or after aerobic exposure, and protective effect of various bacterial inoculants. **Applied and Environmental Microbiology**, 77, 8696–8704.

Eiteman, M. A., andRamalingam, S. (2015). Microbial production of lactic acid. **Biotechnology Letters**, 37(5), 955–972.

Espe, D. L., Cannon, C. Y., andHansen, E. N. (1932). Normal growth in dairy cattle. **Iowa Agriculture and Home Economics Experiment Station Research Bulletin**, 12(154).

Ferraretto, L. F., andShaver, R. D. (2012). Effect of corn shredlage on lactation performance and total tract starch digestibility by dairy cows. **The Professional Animal Scientist**, 28(6), 639–647.

Ghazi, F., Benmechernene, Z., Mebrouk, K., andGurakan, C. (2013). The reproducibility of random amplified polymorphic DNA (RAPD) profiles of *Streptococcus thermophilus* strains with XD9, M13 and OPI–02 MOD primers. **African Journal of**

Biotechnology, 12(44), 6245–6252.

Gilad, R., et al. (2003). CelI, a noncellulosomal family 9 enzyme from *Clostridium thermocellum*, is a processive endoglucanase that degrades crystalline cellulose. **Journal of Bacteriology**, 185(2), 391–398.

Greenwood, P. L. (2021). Review: An overview of beef production from pasture and feedlot globally, as demand for beef and the need for sustainable practices increase. **Animal**, 15, 1–16.

Gueimonde, M., Frias, R., andOuwehand, A. C. (2006). Assuring the continued safety of lactic acid bacteria used as probiotics. **Biologia**, 61(6), 755–760.

Hammes, W. P., andVogel, R. F. (1995). **The genus *Lactobacillus*. The genera of lactic acid bacteria** (Vol. 2). Glasgow, UK: Blackie Academic and Professional.

Harding, F. (1995). **Milk Quality** (1 ed.). Boston, MA: Springer.

Harry, J. (2010). **Introduction to plasma technology: science, engineering and applications**. New Jerssey, New York: Wiley–VCH.

Henrissat, B. (1991). A classification of glycosyl hydrolases based on amino acid sequence similarities. **The Biochemical Journal**, 280 (Pt 2), 309–316.

Hong, Z., et al. (2011). A new mutation breeding method for *Streptomyces albulus* by an atmospheric and room temperature plasma. **Journal of Microbiology Research**,

6(13), 3154–3158.

Hu, W., et al. (2018). The mutagenesis of *Lactobacillus thermophilus* for enhanced L–(+)–lactic acid accumulation induced by heavy ion irradiation. **Brazilian Archives of Biology and Technology**, 60, 1–12.

Huang, Y.–W., et al. (2020). An overview of low–temperature plasma surface modification of carbon materials for removal of pollutants from liquid and gas phases. **Plasma Processes and Polymers**, 18(3), 1–23.

Hubbard, R., andLowrance, R. (1998). Management of dairy cattle manure. **Agricultural Uses of Municipal Animal, and Industrial Byproducts**, 91–102.

Hubert, J., et al. (2015). Chemical and physical effects of the carrier gas on the atmospheric pressure PECVD of fluorinated precursors. **Plasma Processes and Polymers**, 12(10), 1174–1185.

Humud, H. (2013). Deactivation of *Staphylococcus aureus* and *Escherichia coli* using plasma needle at atmospheric pressure. **International Journal of Current Engineering and Technology** 3(5), 1848–1851.

Hwanhlem, N., et al. (2011). Isolation and screening of lactic acid bacteria from Thai traditional fermented fish (Plasom) and production of Plasom from selected strains. **Food Control**, 22(3–4), 401–407.

Ifuku, S., et al. (2007). Surface modification of bacterial cellulose nanofibers for property enhancement of optically transparent composites: dependence on acetyl–group DS.

Biomacromolecules, 8(6), 1973–1978.

Immanuel, G., Dhanusha, R., Prema, P., andPalavesam, A. (2006). Effect of different growth parameters on endoglucanase enzyme activity by bacteria isolated from coir retting effluents of estuarine environment. **International Journal of Environmental Science and Technology**, 3(1), 25–34.

Information and Statistical Data Group. (2017). Information on the number of livestock in Thailand in 2018. Retrieved from http://ict.dld.go.th/th2/images/stories/stat_web/monthly/2560/T1-1.pdf

Jala, A., andSrichana, D. (2011). Utilization of corn dust as additive of corn silage. **Thai Science and Technology Journal**, 19(3), 13–28.

Jatkauskas, J., Vrotniakiene, V., Ohlsson, C., andLund, B. (2013). The effects of three silage inoculants on aerobic stability in grass, clover–grass, lucerne and maize silages. **Agrilcultural and Food Science**, 22(1), 137–144.

Jirapornvaree, I., Suppadit, T., andPopan, A. (2017). Use of pineapple waste for production of decomposable pots. **International Journal of Recycling of Organic Waste in Agriculture**, 6(4), 345–350.

Khalili Ghadikolaei, K., et al. (2018). A cold–adapted endoglucanase from camel rumen with high catalytic activity at moderate and low temperatures: an anomaly of truly cold–adapted evolution in a mesophilic environment. **Extremophiles**, 22(2), 315–326.

Khampa, S., Chuelong, S., Siriutane, T., andIttharat, S. (2010). Using of cassava root raw

fermented yeast products as diet on crossbred native cattle fattening for economic of small holder farmers. **Khon-Kaen Agricultural Journal**, 38 (1), 20-23.

Kilby, B. A. (1975). Comprehensible biochemistry: By Michael Yudkin and Robin Offord. Pp 576. Longman Group Limited, U.K. (1973) £5.95. Published in the U.S.A. by Houghton Mifflin Company of Boston under the title Biochemistry. **Biochemical Education**, 3(4), 76.

Kim, D., Lee, K., andChoi, K. (2021). Role of LAB in silage fermentation: effect on nutritional quality and organic acid production—An overview. **AIMS Agriculture and Food**, 6, 216-234.

Klunk, W. E., Jacob, R. F., andMason, R. P. (1999). Quantifying amyloid beta-peptide (Abeta) aggregation using the congo red-abeta (CR-abeta) spectrophotometric assay. **Analytical Biochemistry**, 266(1), 66-76.

Konosonoka, I. H., Jemeljanovs, A., Osmane, B., Ikauniece, D., andGulbe, G. (2012). Incidence of *Listeria* spp. in dairy cows feed and raw milk in Latvia. **International Scholarly Research Network Veterinary Science**, 2012, 1-5.

Lal, R. (2020). Integrating animal husbandry with crops and trees. **Frontiers in Sustainable Food Systems**, 4(113), 1-12.

Larkin, M. A., et al. (2007). Clustal W and Clustal X version 2.0. **Bioinformatics**, 23(21), 2947-2948.

Laroussi, M. (2015). Low-temperature plasma jet for biomedical applications: A review. **IEEE**

Transactions on Plasma Science, 43(3), 703–712.

Lee, J.–S., Parameswaran, B., Lee, J.–P., andPark, S.–C. (2008). Recent developments of key technologies on cellulosic ethanol production. **Journal of Scientific and Industrial Research**, 67, 865–873.

Lee, J. K., et al. (2009). Growth inhibitory effect of fermented Kimchi on food–borne pathogens. **Food Science and Biotechnology**, 18, 12–17.

Lee, Y., et al. (2014). Atmospheric–pressure plasma jet induces DNA double–strand breaks that require a Rad51–mediated homologous recombination for repair in *Saccharomyces cerevisiae*. **Archives of Biochemistry and Biophysics**, 560, 1–9.

Li, S., et al. (2012). Effects of subacute ruminal acidosis challenges on fermentation and endotoxins in the rumen and hindgut of dairy cows. **Journal of Dairy Science**, 95(1), 294–303.

Li, X., et al. (2016). Effects of applying lactic acid bacteria to the fermentation on a mixture of corn steep liquor and air–dried rice straw. **Animal Nutrition**, 2(3), 229–233.

Lin, H., et al. (2012). Screening of *Lactobacillus rhamnosus* strains mutated by microwave irradiation for increased lactic acid production. **African Journal of Microbiology Research**, 6(31), 6055–6065.

Lineweaver, H., andBurk, D. (1934). The determination of enzyme dissociation constants. **Journal of the American Chemical Society**, 56(3), 658–666.

Löbrich, M., Rydberg, B., andCooper, P. K. (1994). DNA double-strand breaks induced by high-energy neon and iron ions in human fibroblasts. II. Probing individual notI fragments by hybridization. **Radiation Research**, 139(2), 142-151.

Lunsin, R. (2018). Effect of oil palm meal on nutrient utilization and milk production in lactating dairy cows fed with urea-treated rice straw. **Agriculture and Natural Resources**, 52(3), 285-289.

Lynch, J. M., andBarbano, D. M. (1999). Kjeldahl nitrogen analysis as a reference method for protein determination in dairy products. **Journal of AOAC International**, 82(6), 1389-1392.

Ma, L., et al. (2020). Cloning and characterization of low-temperature adapted GH5-CBM3 endo-cellulase from *Bacillus subtilis* 1AJ3 and their application in the saccharification of switchgrass and coffee grounds. **AMB Express**, 10(42), 1-11.

Maheswari, M., andChandra, T. S. (2000). Production and potential applications of a xylanase from a new strain of *Streptomyces cuspidosporus*. **World Journal of Microbiology and Biotechnology**, 16, 257-263.

Mandal, A., et al. (2015). Parametric optimization of submerged fermentation conditions for xylanase production by *Bacillus cereus* BSA1 through Taguchi methodology. **Acta Biologica Szegediensis**, 59(2), 189-195.

Martin Alonso, D., Wettstein, S., andDumesic, J. (2012). Bimetallic catalysts for upgrading of biomass to fuels and chemicals. **Chemical Society reviews**, 41.

Miller, G. C. (1959). Use of dinitrosalicylic acid reagent for determination of reducing sugar. **Analytical Chemistry**, 31(3), 426–428.

Mokoena, M. P. (2017). Lactic acid bacteria and their bacteriocins: classification, biosynthesis and applications against uropathogens: a mini–review. **Molecules**, 22(8).

Moore, D. (2020). **21st Century Guidebook to Fungi– reviews and contents** (2 ed.). United Kingdom: Cambridge University

Murakami, M. T., et al. (2005). Correlation of temperature induced conformation change with optimum catalytic activity in the recombinant G/11 xylanase A from *Bacillus subtilis* strain 168 (1A1). **FEBS Letters**, 579(28), 6505–6510.

Nakkanong, K., Charassri, N., andSayan, S. (2008). Analysis of genetic diversity in early introduced clones of rubber tree (*Hevea brasiliensis*) using RAPD and microsatellite markers. **Songklanakarin Journal of Science and Technology**, 30.

Nanasombat, S., Phunpruch, S., andJaichalad, T. (2012). Screening and identification of lactic acid bacteria from raw seafoods and Thai fermented seafood products for their potential use as starter cultures. **Songklanakarin Journal of Science and Technology**, 34, 255–262.

Nandimath, A., Kharat, K., Gupta, S., andKharat, A. (2016). Optimization of cellulase production for *Bacillus* sp. and *Pseudomonas* sp. soil isolates. **African Journal of Microbiology Research**, 10, 410–419.

Neti, Y., Dyah, K., Susilawaty, andYessy, K. (2018). Lactic acid bacteria during fish

fermentation (rusip). **MOJ Food Processing and Technology**, 6(2), 211–216.

Office of Agricultural Economics. (2017). Agricultural economic data maize. Retrieved from http://www.oae.go.th

Onda, T., et al. (2002). Widespread distri–bution of the bacteriocin–producing lactic acid cocci in Miso–paste products. **Journal of Applied Microbiology**, 92, 695–705.

Percival Zhang, Y. H., Himmel, M. E., andMielenz, J. R. (2006). Outlook for cellulase improvement: screening and selection strategies. **Biotechnology Advances**, 24(5), 452–481.

Polsa, N., Suyotha, W., Suebsan, S., Anuntalabhochai, S., andSangwijit, K. (2020). Increasing xylanase activity of *Bacillus subtilis* by atmospheric pressure plasma jet for biomass hydrolysis. **3 Biotech**, 10(1), 22.

Puntillo, M., et al. (2020). Potential of lactic acid bacteria isolated from different forages as silage inoculants for improving fermentation quality and aerobic stability. **Frontiers in Microbiology**, 11, 1–17.

Rakhmanova, A., Khan, Z., andShah, K. (2018). A mini review fermentation and preservation: role of lactic acid bacteria. **MOJ Food Processing and Technology**, 6.

Ramos, M., andBarbosa, J. (2016). Basic unit cost simulation from free–stall design to dairy cattle confinement using different construction techniques. **Engenharia Agrícola**, 36, 972–983.

Reddy, L., andObulam, V. S. (2011). Effect of fermentation conditions on yeast growth and volatile composition of wine produced from mango (*Mangifera indica* L.). **Food and Bioproducts Processing**, 89, 487–491.

Reinemann, D. J., Wolters, G., andRasmussen, M. D. (2000). Review of practices for cleaning and sanitation of milking machines. Retrieved from www.uwex.edu/uwmril/pdf/milkmachines/cleaning/00_nagano_cip.pdf

Reis, J. A., Paula, A. T., Casarotti, S., andPenna, A. (2012). Lactic acid bacteria antimicrobial compounds: characteristics and applications. **Food Engineering Reviews**, 4, 124–140.

Richards, H., Baker, P., andIwuoha, E. (2012). Metal nanoparticle modified polysulfone membranes for use in wastewater treatment: A critical review. **Journal of Surface Engineered Materials and Advanced Technology**, 2(3A), 183–193.

Robert, X., andGouet, P. (2014). Deciphering key features in protein structures with the new ENDscript server. **Nucleic Acids Research**, 42(W1), W320–W324.

Romero, J., et al. (2016). Improving the performance of dairy cattle with a xylanase–rich exogenous enzyme preparation. **Journal of Dairy Science**, 99(5), 3486–3496.

Rossi, F., andDellaglio, F. (2007). Quality of silages from Italian farms as attested by number and identity of microbial indicators. **Journal of Applied Microbiology**, 103(5), 1707–1715.

Sanger, F., Nicklen, S., andCoulson, A. R. (1977). DNA sequencing with chain-terminating inhibitors. **Proceedings of the National Academy of Sciences of the United States of America**, 74(12), 5463-5467.

Sangwijit, K., Jitonnom, J., Pitakrattananukool, S., Yu, L. D., andAnuntalabhochai, S. (2016). Low-energy plasma immersion ion implantation modification of bacteria to enhance hydrolysis of biomass materials. **Surface and Coatings Technology**, 306, 336-340.

Santos, A. O., Ávila, C. L. S., andSchwan, R. F. (2013). Selection of tropical lactic acid bacteria for enhancing the quality of maize silage. **Journal of Dairy Science**, 96(12), 7777-7789.

Santos, C., et al. (2011). Dissecting structure-function-stability relationships of a thermostable GH5-CBM3 cellulase from *Bacillus subtilis* 168. **The Biochemical journal**, 441, 95-104.

Schrodinger, L. (2010). The PyMOL molecular graphics system, Version 1.3r1. Retrieved from http://pymol.sourceforge.net/overview/index.html

Soonthornchaiboon, W., andPawongrat, R. (2012). Utilization of natural wastes as supporting materials for cell immobilization and Its application for ethanol production. **Veridian E-Journal SU**, 6(1), 795-807.

Steel, R. G. D., andTorrie, J. H. (1980). **Principles and Procedures of Statistics** (Vol. 2). USA: McGraw-Hill.

Subramaniyan, S., andPrema, P. (2002). Biotechnology of microbial xylanases: enzymology, molecular biology, and application. **Critical Reviews in Biotechnology**, 22(1), 33–64.

Sunna, A., andAntranikian, G. (1997). Xylanolytic enzymes from fungi and bacteria. **Critical Reviews in Biotechnology**, 17, 39–67.

Suree, N., Saranya, P., andNatthaneewan, C. (2016). Bacteriocins from *Lactobacillus* strains and their anti–*Listeria monocytogenes* in Nham, Thai fermented pork. **KMITL Science and Technology Journal**, 16(2), 43–48.

Suto, M., et al. (2002). Endophytes as producers of xylanase. **Journal of Bioscience and Bioengineering**, 93, 88–90.

Tavares, A., Xavier, A., andEvtuguin, D. (2014). Biotechnology applications in pulp and paper industry. In (pp. 561–581).

Tengkaew, S., andWiwattanadate, D. (2014). Study if source and potential of biomass from field corn in Thailand. **Prince of Naradhiwas University Journal**, 6(3), 103–111.

Thavorn, E., Thana, S., Sorachakula, C., Dongpaleedham, C., andDanmek, K. (2017). Development of maize husk silage for native beef cattle using design of experiment. **Naraesuan University Engineering Journal**, 12(1), 107–114.

Törrönen, A., andRouvinen, J. (1997). Structural and functional properties of low molecular weight endo–1,4–beta–xylanases. **Journal of Biotechnology**, 57(1–3), 137–149.

Trott, O., andOlson, A. J. (2010). AutoDock Vina: Improving the speed and accuracy of docking with a new scoring function, efficient optimization, and multithreading. **Journal of Computational Chemistry**, 31(2), 455–461.

Tserovska, L. (2002). Identification of lactic acid bacteria isolated from Katyk, goat's milk and cheese. **Journal of Culture Collections**, 3, 48–52.

United Nations. (2019). World Population Prospects Retrieved from https://population.un.org/wpp/Publications/Files/WPP2019_Highlights.pdf

Van Schie, P. M., andYoung, L. Y. (2000). Biodegradation of phenol: mechanisms and applications. **Bioremediation Journal**, 4(1), 1–18.

Velho, J., et al. (2018). Roughage sources for Holstein cows under experimental feeding conditions in Brazil – a meta-analysis. **Semina:Ciencias Agrarias**, 39, 2749–2760.

Voigt, J., Piatkowski, B., andKrawielitzki, R. (1978). Effect of the roughage sequence and concentrates in animal feed on carbohydrate digestion and bacterial protein synthesis in the rumen of dairy cows. **Arch Tierernahr**, 28(1), 67–76.

Wachirapakorn, C., Parmaluk, Wanapat, M., Pakdee, andCherdthong, A. (2014). Effects of levels of crude protein and ground corn cobs in total mixed ration on intake, rumen fermentation and milk production in crossbred Holstein Friesian lactating dairy cows. **Journal of Applied Animal Research**, 42(3), 263–268.

Wagenaars, E. (2006). **Plasma breakdown of low-pressure gas discharges**. Ph.D.

Dissertation, Eindhoven University of Technology, Netherlands.

Wagner, N., Tran, Q. H., Richter, H., Selzer, P. M., andUnden, G. (2005). Pyruvate fermentation by *Oenococcus oeni* and *Leuconostoc mesenteroides* and role of pyruvate dehydrogenase in anaerobic fermentation. **Applied and Environmental Microbiology**, 71(9), 4966–4971.

Walker, G. P., Stockdale, C. R., Wales, W. J., Doyle, P. T., andDellow, D. W. (2001). Effect of level of grain supplementation on milk production responses of dairy cows in mid–late lactation when grazing irrigated pastures high in paspalum (*Paspalum dilatatum* Poir.). **Animal Production Science**, 41(1), 1–11.

Walsham, A. D. S., et al. (2016). *Lactobacillus reuteri* inhibition of enteropathogenic *Escherichia coli* adherence human intestinal epithelium. **Frontiers in Microbiology**, 7, 244–244.

Waterhouse, A., et al. (2018). SWISS–MODEL: homology modelling of protein structures and complexes. **Nucleic Acids Research**, 46(W1), W296–W303.

Westh, P., et al. (2017). Thermoactivation of a cellobiohydrolase. **Biotechnology and Bioengineering**, 115(4), 831–838.

Wilson, D. (2008). Three microbial strategies for plant cell wall degradation. **Annals of the New York Academy of Sciences**, 1125, 289–297.

Xu, P., et al. (2020). Natural variation of lignocellulosic components in miscanthus biomass in China. **Frontiers in Chemistry**, 8, 1–12.

Yan, X. X., An, X. M., Gui, L. L., andLiang, D. C. (2008). From structure to function: insights into the catalytic substrate specificity and thermostability displayed by *Bacillus subtilis* mannanase BCman. **Journal of Molecular Biology**, 379(3), 535–544.

Yang, J., Cao, Y., Cai, Y., andTerada, F. (2010). Natural populations of lactic acid bacteria isolated from vegetable residues and silage fermentation. **Journal of Dairy Science**, 93(7), 3136–3145.

Yang, S. C., Lin, C. H., Sung, C. T., andFang, J. Y. (2014). Antibacterial activities of bacteriocins: application in foods and pharmaceuticals. **Frontiers in Microbiology**, 5, 241.

Yaniv, O., et al. (2012). A single mutation reforms the binding activity of an adhesion-deficient family 3 carbohydrate-binding module. **Acta Crystallographica Section D**, 68(Pt 7), 819–828.

Yaopromsiri, C., Yu, L. D., Sarapirom, S., Thopan, P., andBoonyawan, D. (2015). Effect of cold atmospheric pressure He-plasma jet on DNA change and mutation. **Nuclear Instruments and Methods in Physics Research Section B**, 36(5), 399–403.

Ye, M., Sun, L., Yang, R., Wang, Z., andQi, K. (2017). The optimization of fermentation conditions for producing cellulase of *Bacillus amyloliquefaciens* and its application to goose feed. **Royal Society Open Science**, 4, 1–12.

Zhang, H., et al. (2015). Structural insight of a trimodular halophilic cellulase with a family 46 carbohydrate-binding module. **PloS one**, 10(11), 1–18.

Zhou, X., Li, W., Mabon, R., andBroadbelt, L. (2016). A critical review on hemicellulose pyrolysis. **Energy Technology**, 5(1), 216.

APPENDIX

Appendix A

Quantitative analysis of lactic acid

Equipment

1. Micro pipettes of size 10–200 and 20–1000 µL.
2. Test tube
3. UV–Vis spectrophotometer
4. Volumetric flasks of 10 and 100 ml.

Materials, reagents, and solutions

1. $FeCl_3 \cdot 6H_2O$, reagent grade (Khimmed, Russia)
2. DL–lactic acid, cp grade (89%, VAG Chemie, Germany)

Methods

1. Lactic acid (1.2 g) with the know concentration (89%, ρ = 1.2 g/mL) was placed in a 10–mL volumetric flask and diluted with water
2. A stock solution with the x concentration of lactic acid 89 g/L was obtained
3. A solution of iron(III) chloride (0.2%) was prepared. Iron(III) chloride (0.3 g) was placed in a 100–mL volumetric flask, diluted to the mark with water and stirred to the complete dissolution of the salt. The solution must be of room temperature 25 ± 5°C.
4. A solution of lactic acid (50 µL) of a corresponding concentration was added to 2 mL of a 0.2% solution of iron(III) chloride and stirred.
5. The absorbance of the obtained colored solutions was measured at 390 nm.
6. The reference solution contained 2 mL of a 0.2% solution of iron(III) chloride.
7. Calculation

7.1 The measured OD was plotted on the standard graph of the lactic acid standard solution and determined to be linear regression

7.2. Determine the concentration of the sample solution from the lactic acid standard curve.

The relationship between reducing sugar and absorbance at 390 nm is illustrated in **Figure A–1**

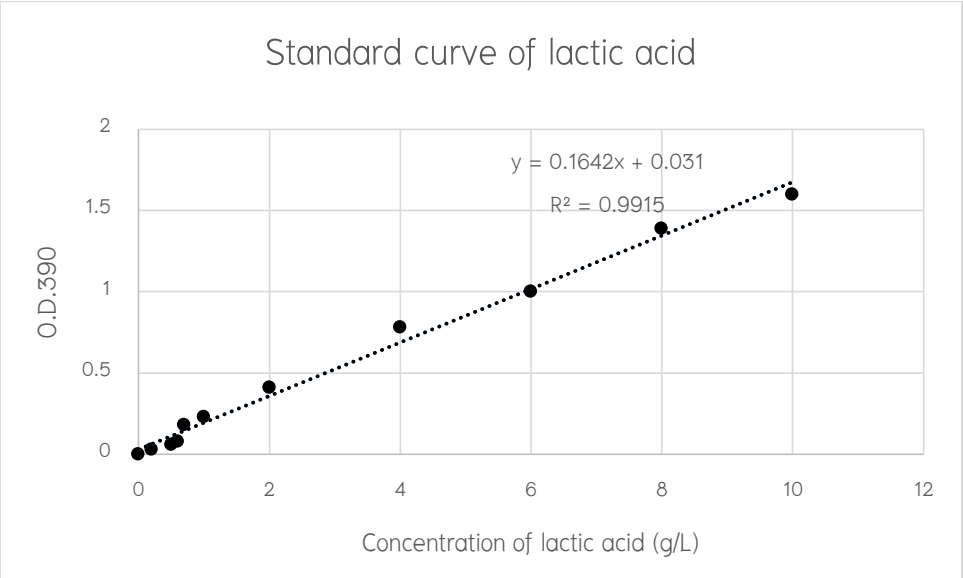

Figure A–1 Standard curve of lactic acid

This, therefore, provides the equation below for the calculation of lactic acid concentration from the absorbance at 390 nm.

$$\text{Lactic acid concentration (g/L)} = \frac{\mathbf{O.D.390\ (nm) - 0.031}}{\mathbf{0.1642}}$$

Appendix B

Reducing sugar determination of glucose

Equipment

1. Micro pipettes of size 10–200 and 20–1000 µL.
2. Test tube
3. UV–Vis spectrophotometer
4. Volumetric flasks of 100 and 1000 ml.

Materials, reagents, and solutions

1. 3, 5–dinitrosalicylic acid (Aldrich) 10.0 g
2. Na_2SO_3 (Ajax Finechem) 0.5 g
3. Na–K tartrate (APS Finechem) 182.0 g
4. NaOH (Merck) 10.0 g
5. Phenol (Merck) 2.0 g
6. Deionized water 1000 ml

Methods

1. NaOH 10 g are added into 700 ml of deionized water and mixed in order to add the 300 g Na–K tartrate.
2. When the solution dissolved, 3, 5–dinitrosalicylic acid 10 g is then added and continuously stirred.
3. The 0.5 g of Na_2SO_3 and 2.0 g of phenol are dissolved, respectively.
4. The volume is adjusted to 1000 ml by deionized water and kept away from light.
5. Reducing sugar determination procedure:

5.1 The samples 0.5 ml are mixed with 0.5 ml of DNS solution. The mixture is boiled for 10 min.

5.2 The sample is cooled down by immersing the sample tube into cold water immediately. Five ml of water is added. The mixture was mixed well and measured at absorbance 540 nm.

5.3 Absorbance 540 nm is converted to glucose concentration with standard curve.

The relationship between reducing sugar and absorbance at 540 nm is illustrated in **Figure B–1**

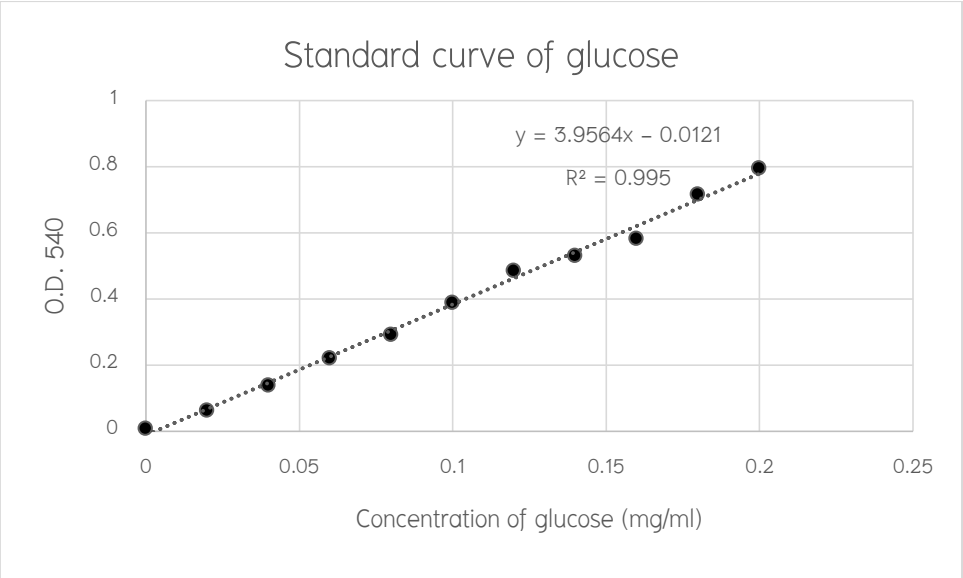

Figure B–1 Standard curve of glucose

This, therefore, provides the equation below for the calculation of sugar concentration from the absorbance at 540 nm.

$$\text{Reducing sugar concentration (mg/ml)} = \frac{\text{O.D.540 (nm)} + 0.0121}{3.956}$$

Appendix C

Reducing sugar determination of xylose

Equipment

1. Micro pipettes of size 10–200 and 20–1000 µL.
2. Test tube
3. UV–Vis spectrophotometer
4. Volumetric flasks of 100 and 1000 ml.

Materials, reagents, and solutions

1. 3, 5–dinitrosalicylic acid (Aldrich) 10.0 g
2. Na_2SO_3 (Ajax Finechem) 0.5 g
3. Na–K tartrate (APS Finechem) 182.0 g
4. NaOH (Merck) 10.0 g
5. Phenol (Merck) 2.0 g
6. Deionized water 1000 ml

Methods

1. NaOH 10 g are added into 700 ml of deionized water and mixed in order to add the 300 g Na–K tartrate.
2. When the solution dissolved, 3, 5–dinitrosalicylic acid 10 g is then added and continuously stirred.
3. The 0.5 g of Na_2SO_3 and 2.0 g of phenol are dissolved, respectively.
4. The volume is adjusted to 1000 ml by deionized water and kept away from light.
5. Reducing sugar determination procedure:

5.1 The samples 0.5 ml are mixed with 0.5 ml of DNS solution. The mixture is boiled for 10 min.

5.2 The sample is cooled down by immersing the sample tube into cold water immediately. Five ml of water is added. The mixture was mixed well and measured at absorbance 540 nm.

5.3 Absorbance 540 nm is converted to xylose concentration with standard curve.

The relationship between reducing sugar and absorbance at 540 nm is illustrated in Figure C–1

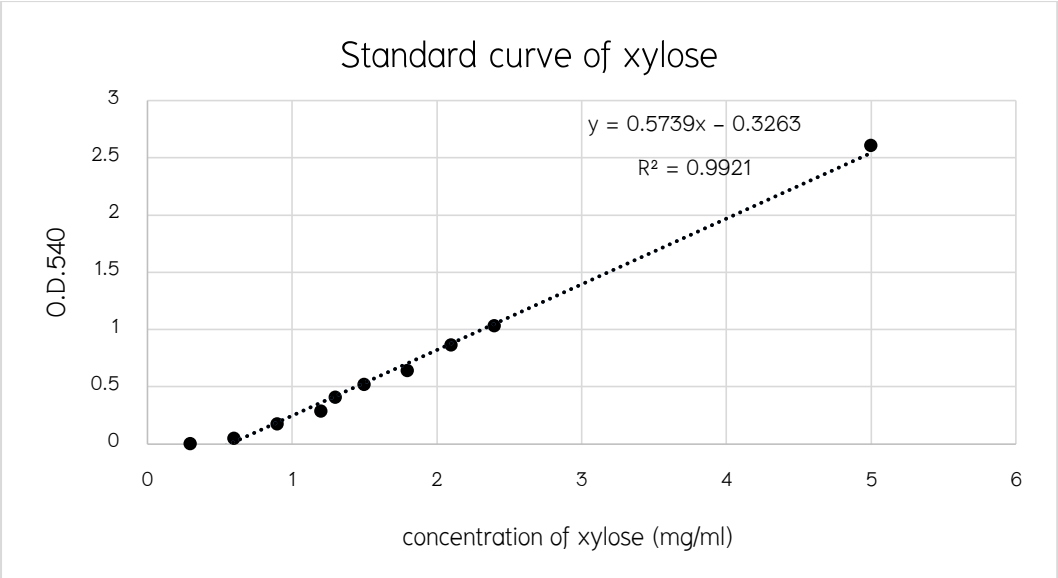

Figure C–1 Standard curve of xylose

This, therefore, provides the equation below for the calculation of sugar concentration from the absorbance at 540 nm.

$$\text{Reducing sugar concentration (mg/ml)} = \frac{\mathbf{O.D.540\ (nm) + 0.326}}{\mathbf{0.574}}$$

BIOGRAPHY

NAME	Nitipol Polsa
DATE OF BIRTH	21 November 1993
PLACE OF BIRTH	Nakhonsawan
INSTITUTIONS ATTENDED	2016, B.S. (Biology). University of Phayao. Phayao.
HOME ADDRESS	95 Moo.4 Mae-Ka, Phayao, Province
PUBLICATION	Polsa, N., Chaweewan, K., Sangwijit, K., Suebsan, S. and Anuntalabhochai, S. (2021). Effect of fermented durian peel by modified bacteria on growth performance and carcass quality of growing-finishing pigs. KhonKaen Agricultural Journal, 49(6). Polsa, N., Songsiriritthigul, C., Suyotha, W., Suebsan S., Anuntalabhochai, S. and Sangwijit, K. (2021). A single mutation in the carbohydrate-binding module enhances cellulase activity in Bacillus Amyloliquefaciens mutant. Walailak Journal of Science and Technology, 18(18). Polsa, N., Suyotha, W., Suebsan S., Anuntalabhochai, S. and Sangwijit, K. (2020). Increasing xylanase activity of Bacillus subtilis by atmospheric pressure plasma jet for biomass hydrolysis. 3Biotech, 10(1).